Skutterudites
Recent Progress

Professor Ctirad Uher
University of Michigan

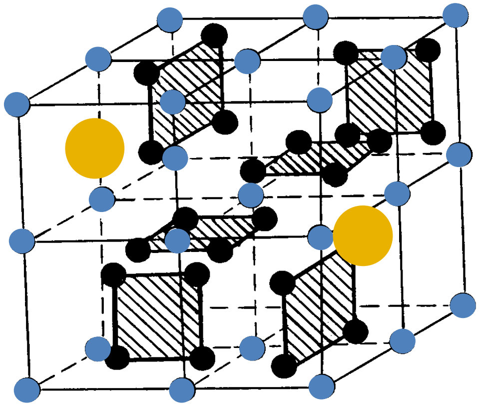

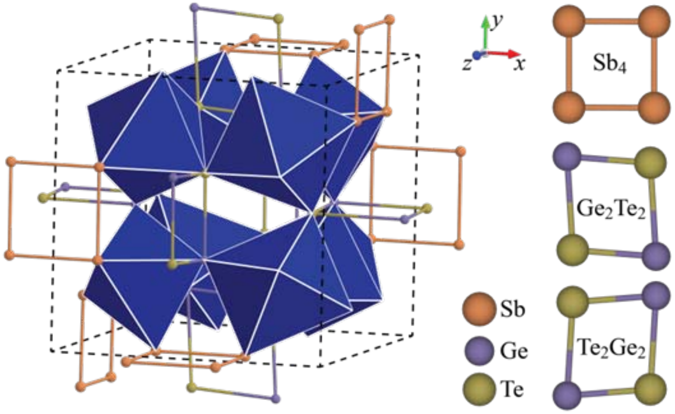

College de France
May 15, 2013

Today, we live in a 16 TW world

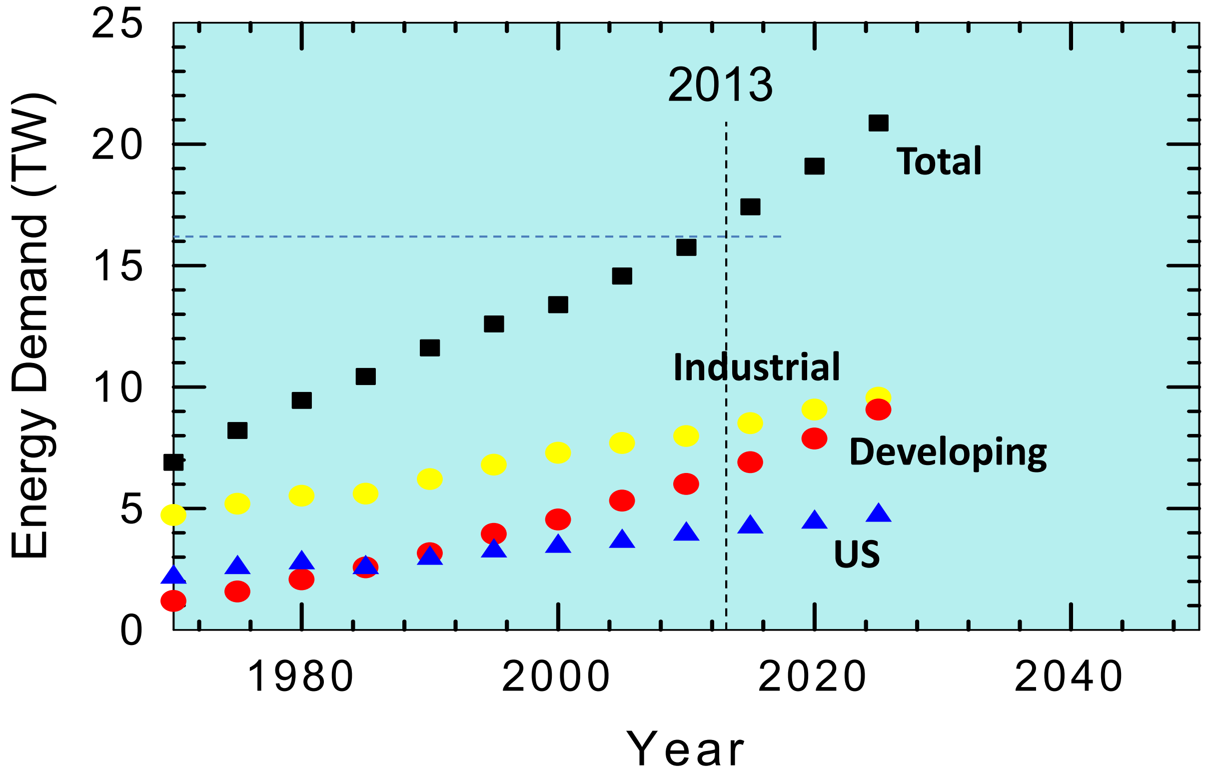

- The demand will double by 2050. (Hoffert et al. (1998))
- Countries with the least per capita energy use are undergoing a rapid industrial development.
- **Enormous pressure on the energy resources.**
- **Cut-throat competition to secure energy supplies.**

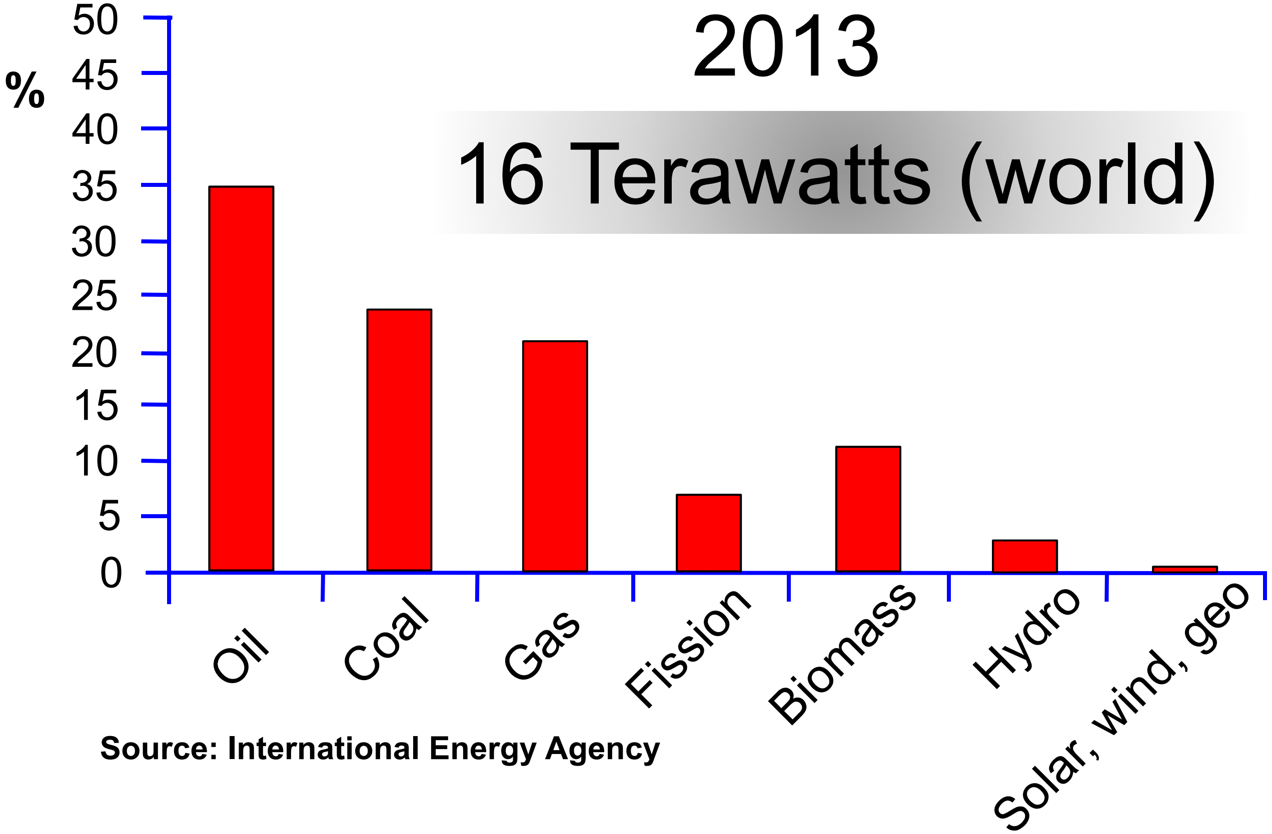

2013

16 Terawatts (world)

Source: International Energy Agency

- Some **80%** of energy is derived from fossil fuels.
- Oil represents the largest (35%) component of the total energy use.
- Easily accessible oil reserves are gradually being depleted.
- New sources of oil are limited and extraction is expensive.
- Moreover, burning fossil fuels presents a serious ecological problem.
- The situation is unsustainable in the long run!

There is no simple solution and no single technology that alone can solve the energy problem!

- Several possibilities exist: (fission, fusion, solar, wind, hydrogen) but none at a stage to fully replace fossil fuels.
- Many decades of intensive technological development in front of us.
- A combination of technologies will be needed to make an impact.

- Thermoelectricity can make meaningful contributions!

Thermoelectricity

A direct conversion of:

Heat into electrical energy (thermoelectric generator)

Electrical energy into heat pump (thermoelectric cooler)

Thermoelectricity

Based on three effects discovered a long time ago:

Seebeck effect (1821)

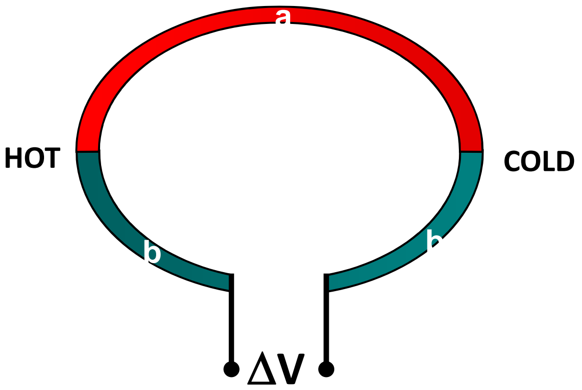

$$\Delta V = S\Delta T$$

- Thermocouples
- Power generation

Peltier effect (1834)

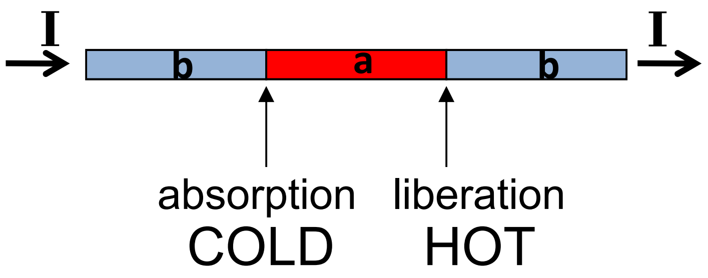

$$Q_{\Pi} = \Pi I$$

- Thermoelectric cooling

Thomson effect (1854)

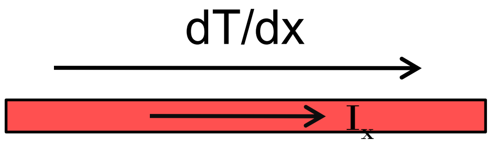

evolution or absorption of heat in a body of a conductor

$$Q_T = \tau I \frac{dT}{dx}$$

- Kelvin relations

$$\Pi = TS$$

$$\tau = T\frac{dS}{dT}$$

Practical realization of thermoelectricity requires both n- and p-type semiconductors

Peltier cooler

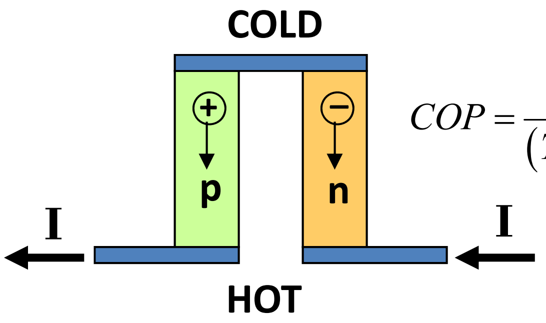

$$COP = \frac{T_c}{(T_h - T_c)} \frac{\sqrt{1 + Z\frac{T_c + T_h}{2}} - \frac{T_h}{T_c}}{\sqrt{1 + Z\frac{T_c + T_h}{2}} + 1}$$

Power generator

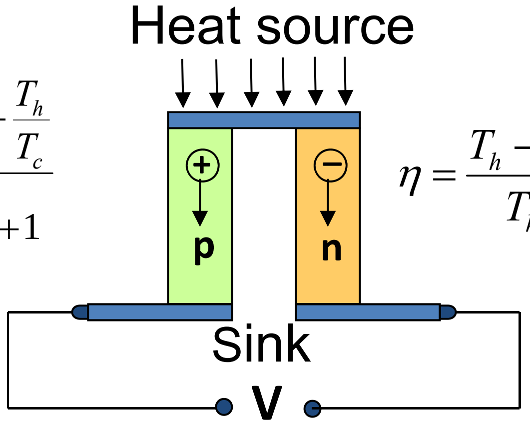

$$\eta = \frac{T_h - T_c}{T_h} \frac{\sqrt{1 + Z\frac{T_c + T_h}{2}} - 1}{\sqrt{1 + Z\frac{T_h + T_c}{2}} + \frac{T_c}{T_h}}$$

The key parameter is **Z (thermoelectric figure of merit)**

$$\mathbf{ZT = S^2\sigma T/\kappa = PT/\kappa}$$

S = Seebeck coefficient
σ = electrical conductivity
κ = thermal conductivity
P = power factor (= $S^2\sigma$)
T = absolute temperature

We aim for as high Z as possible!

Thermoelectric modules

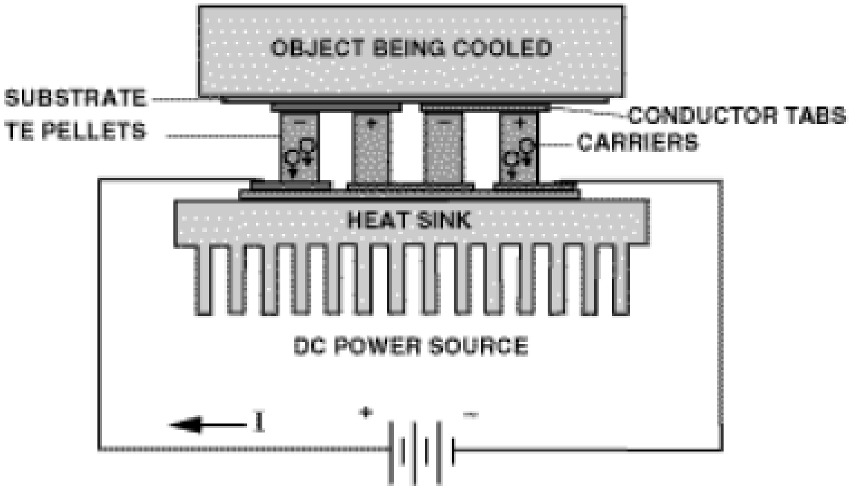

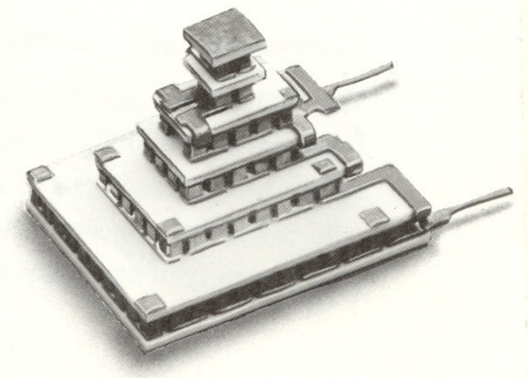

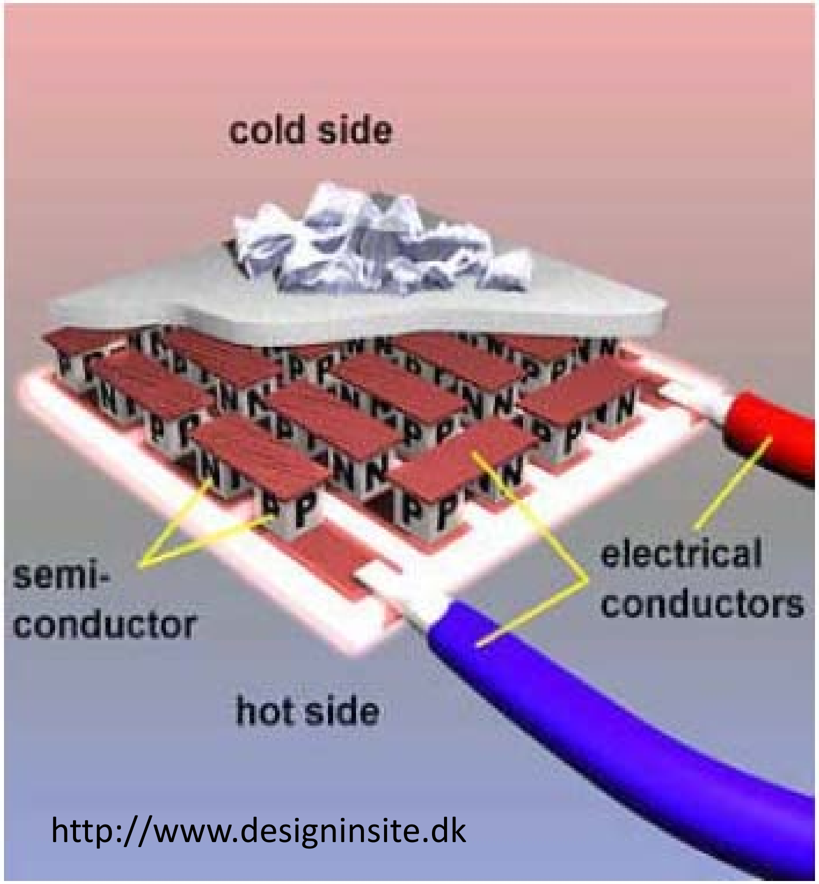

http://www.designinsite.dk

No moving parts, no noise, and exceptionally reliable!

Classical thermoelectric materials

Bi_2Te_3/Sb_2Te_3, (1955) **PbTe,** (1950's) **TAGS** (1961) **Si-Ge** (1964)

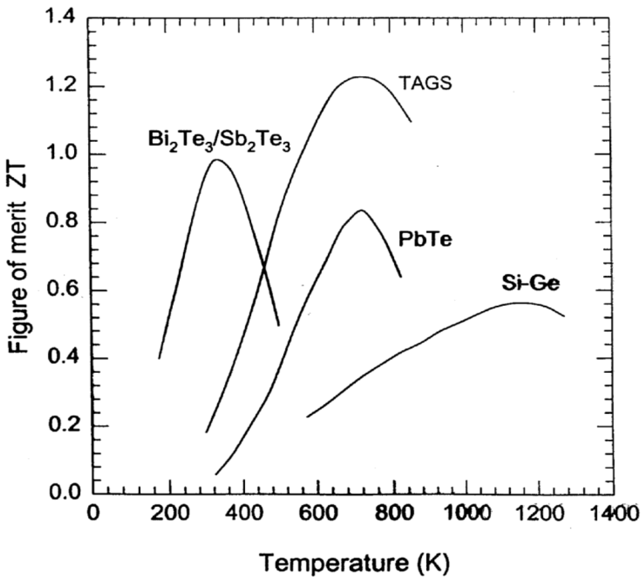

- Current thermoelectric technology based on the above materials.
- ZT ≤ 1 in spite of nearly a half-century research effort.
- Concerns about the toxicity of Pb and rising cost of Te.
- Only niche areas of technology benefiting from thermoelectricity.

Re-emergence of interest in thermoelectricity since mid-1990’s

- Realization that fossil fuel resources are finite.
- Combustion processes are a major source of greenhouse gases.
- Fluids used in refrigeration/air conditioning affect the ozone layer.

- Progress in modeling, design and fabrication of novel materials.
- Better understanding of transport in lower dimensional structures.
- Interest in nanostructured materials.

Willingness of funding agencies to invest in TE research.

Intensive, worldwide search for novel, efficient TE materials.

Novel Bulk Thermoelectrics

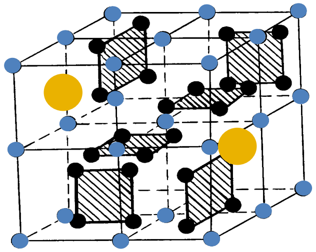

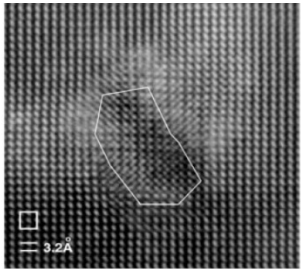

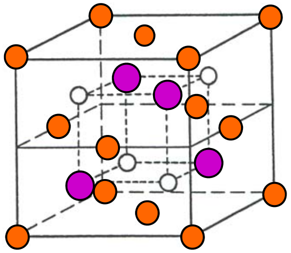

Skutterudites

Clathrates

Complex Chalcogenides

Oxides

Half-Heusler Alloys

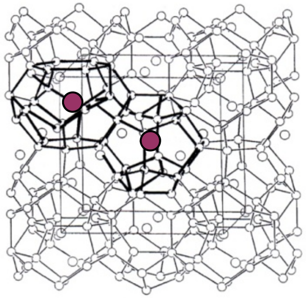

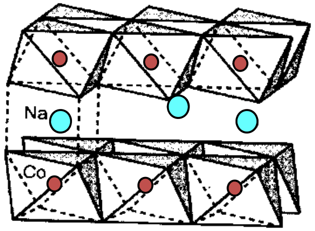

Open crystalline environment

Nanometer-size structural features

Skutterudite compounds

Chemical formula MX_3 M = Co, Rh, Ir X = P, As, Sb

Structure identified by Oftedal in 1928

Cubic structure, space group Im3

Eight MX_3 groups in the unit cell ⇒ 32 atoms/unit cell

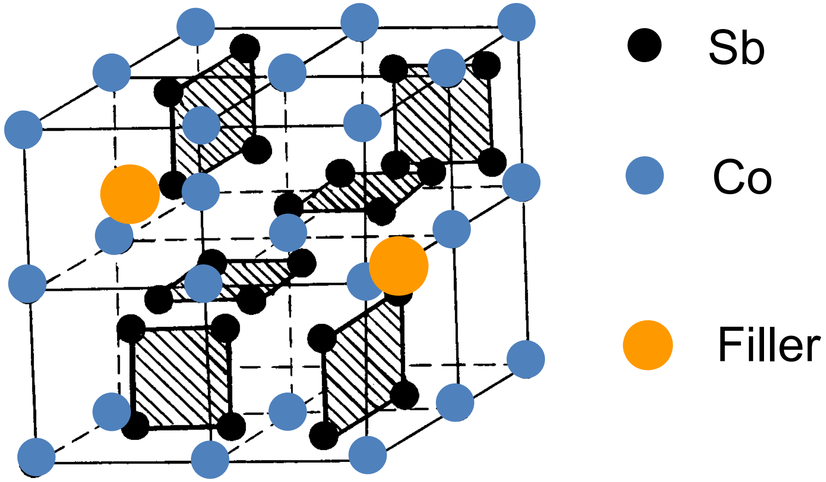

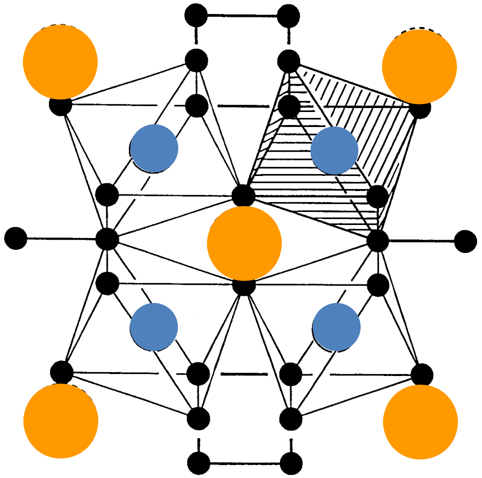

$CoSb_3 \Leftrightarrow \square_2Co_8Sb_{24} \Leftrightarrow \square\, Co_4Sb_{12}$

Cages can be filled with foreign ions ⇔ **Filled skutterudites** Jeitschko (1977)

1995 – Slack suggested that "rattling" of the fillers might lower thermal conductivity.

1995 – Morelli and Meisner proved that it is indeed so.

1996 – Sales et al. demonstrated large atomic displacements of fillers

Since then, filled skutterudites attracted major interest as novel thermoelectrics.

C. Uher, *in Semiconductors & Semimetals,*
Vol.69, 139-253 (2001)

Skutterudites completely specified by:

1. The lattice parameter a
2. The positional parameters y and z

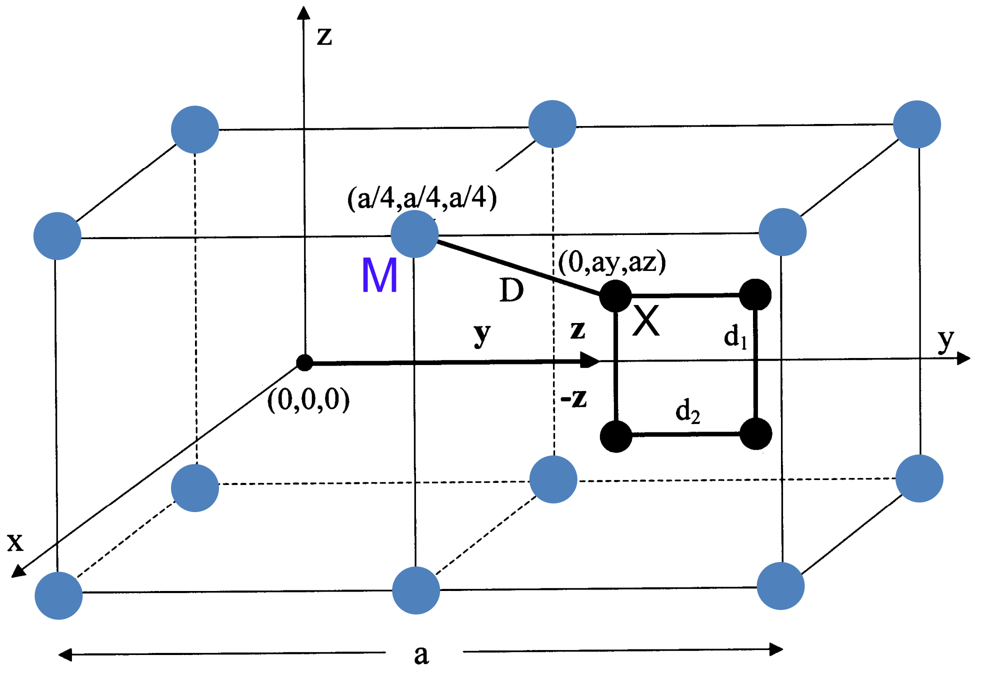

$\frac{1}{4} \leq y < \frac{1}{2}$

$0 < z \leq \frac{1}{4}$

$$D(M\text{-}X) = a[(\tfrac{1}{4})^2 + (y-\tfrac{1}{4})^2 + (z-\tfrac{1}{4})^2]^{\frac{1}{2}}$$

$$d_1(X\text{-}X) = 2az$$

$$d_2(X\text{-}X) = a(1-2y)$$

Original assumption of Oftedal: $d_1 = d_2 \Leftrightarrow$ square X_4 rings

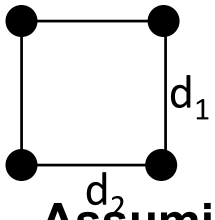

$$2(y + z) = 1$$

Oftedal's relation

Assuming regular octahedral positions for pnicogen atoms

$$y(2z - 1) = z - 3/8$$

Simultaneous solution yields $y = z = 1/4 \Leftrightarrow$ collapse to ReO!

Either the octahedrons are distorted, or pnicogen rings are not exactly square.

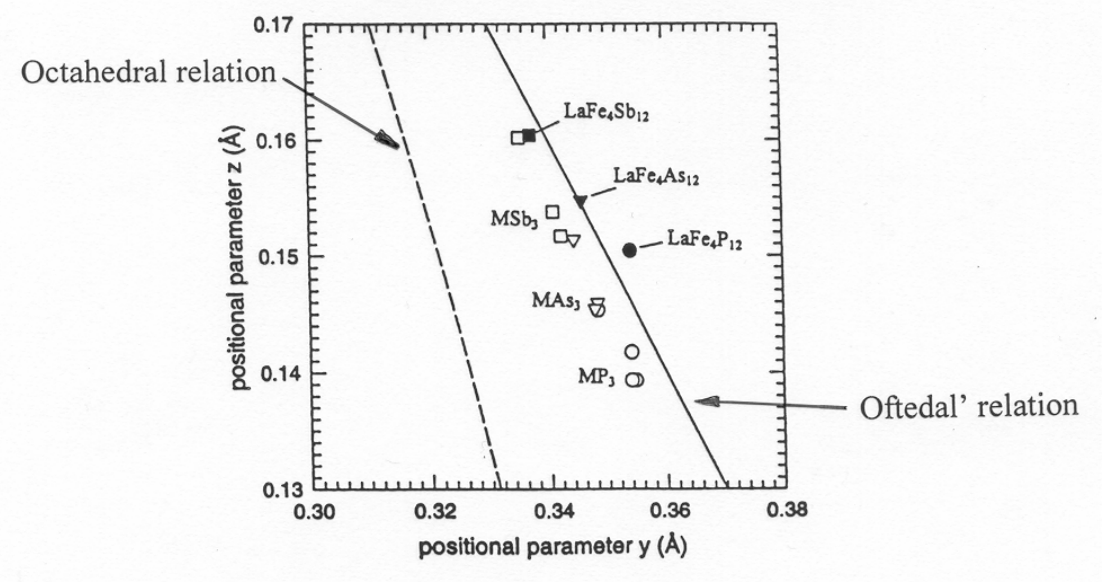

Octahedrons distorted and the Oftedal's relation somewhat violated.

MX_6 cluster

Not a regular octahedron, trigonal prismatic distortion present.

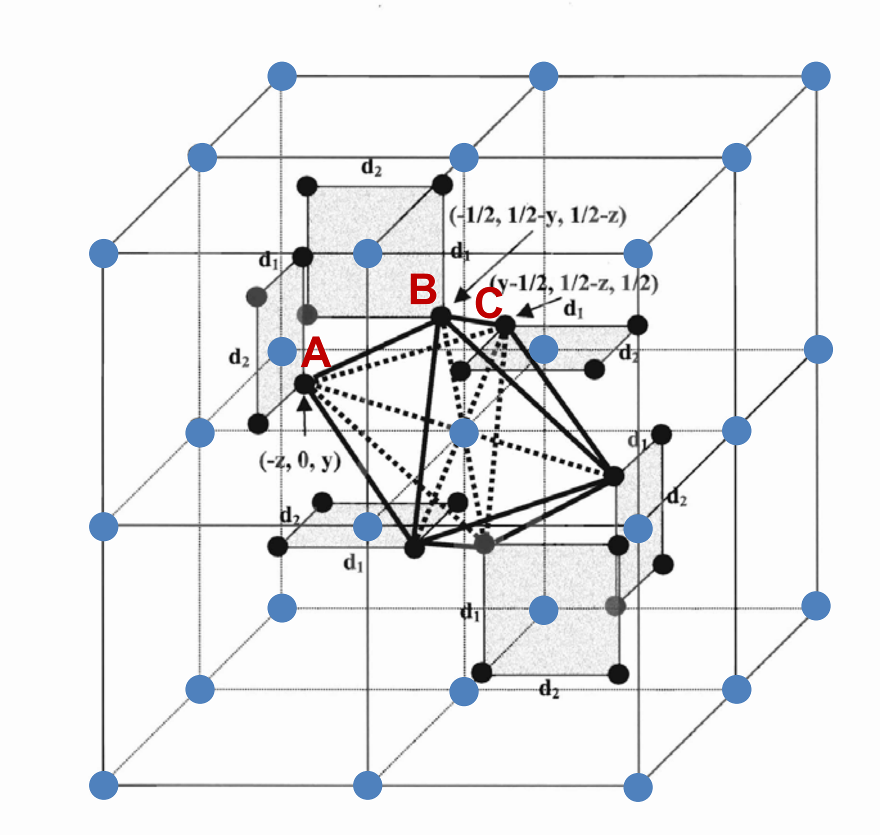

Comparing distances (edge lengths) of the octahedron:

A$(-z,0,y)$ to B$(-\frac{1}{2}, \frac{1}{2}-y, \frac{1}{2}-z)$ = $[(z-\frac{1}{2})^2 + (y-\frac{1}{2})^2 + (y + z -\frac{1}{2})^2]^{\frac{1}{2}}$

B$(-\frac{1}{2}, \frac{1}{2}-y, \frac{1}{2}-z)$ to C$(y-\frac{1}{2}, \frac{1}{2}-z, \frac{1}{2})$ = $[(y^2 + (z-y)^2 + z^2]^{\frac{1}{2}}$

AB ≠ BC

Might possibly be healed by a small amount of Ni.

Evolution of the Pnicogen Ring Structure from the ReO structure

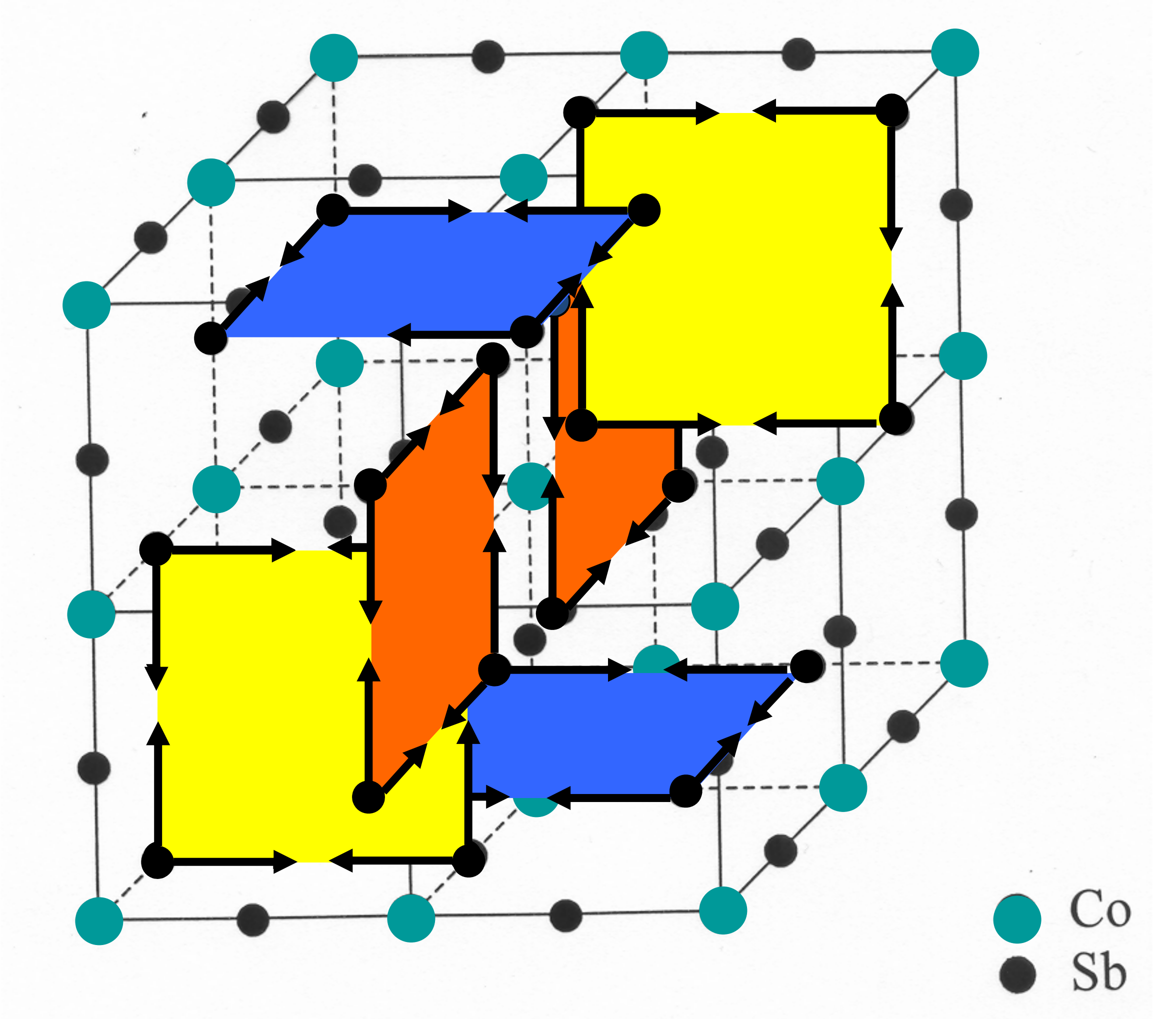

Rings form linear arrays along the (100), (010), and (001).

Bonding

Experimental fact: diamagnetic semiconductor ⇔ no unpaired electrons present

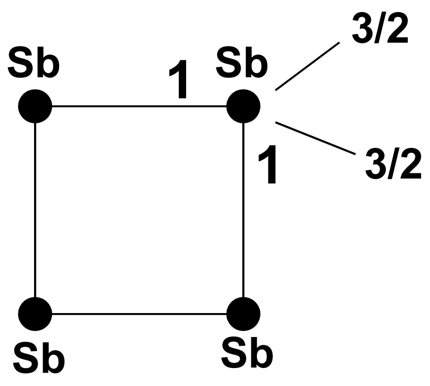

X-atoms: form planar rectangular rings X_4, ns^2np^3 (5 valence electrons), bond with its two X neighbors & with its two M neighbors.

Coordination of X-atoms increases from MP_3 to MAs_3 to MSb_3. This results in a shift from more localized (P) to more delocalized (Sb) bonding.

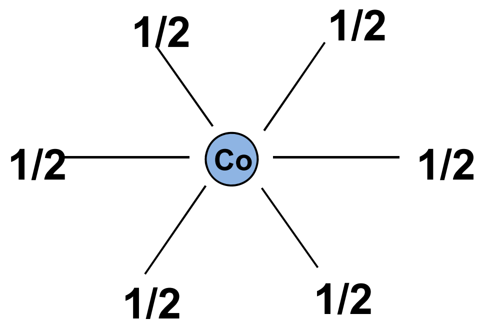

M-atoms: d^7s^2 (9 valence electrons)
3 of them (6 ×½) bond with 6 X-neighbors ⇒ hybrid d^2sp^3 orbitals.
M^{3+} state with 6 nonbonding electrons,
Maximum spin-pairing ⇒ low-spin d^6 state.

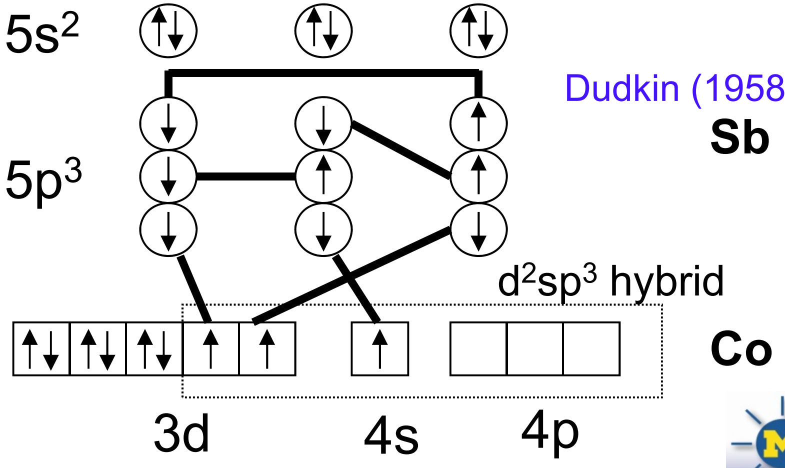

Dudkin (1958)

Band Structure

$CoSb_3$

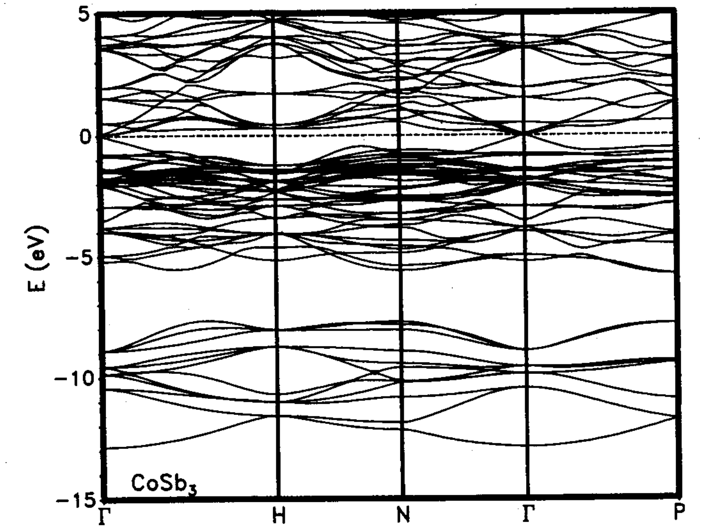

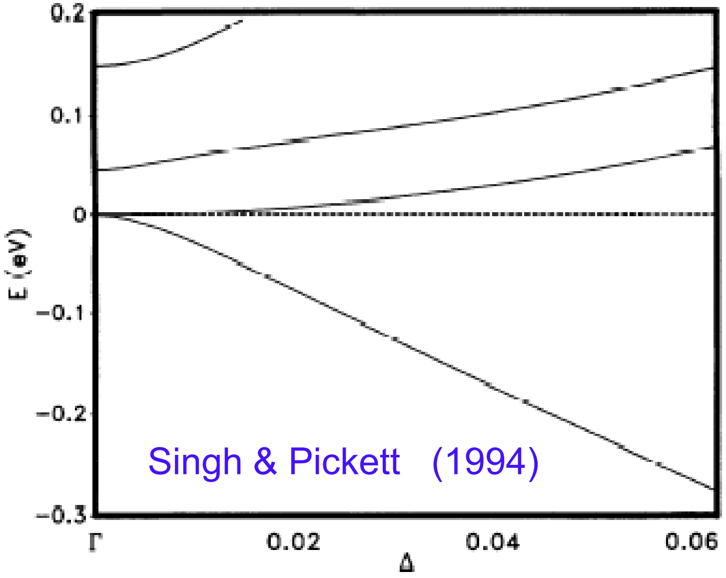

Singh & Pickett (1994)

Pseudogap around the Fermi level.

Linear dispersion ⇒ Kane model

A single gap-crossing band $E_g \approx 50$ meV.

$$\hbar^2 k^2 \Big/ 2m^* = \varepsilon_k \left(1 + \varepsilon_k \Big/ E_g \right)$$

Large effective masses!

Band Structure

Filled skutterudite - $CeFe_4Sb_{12}$

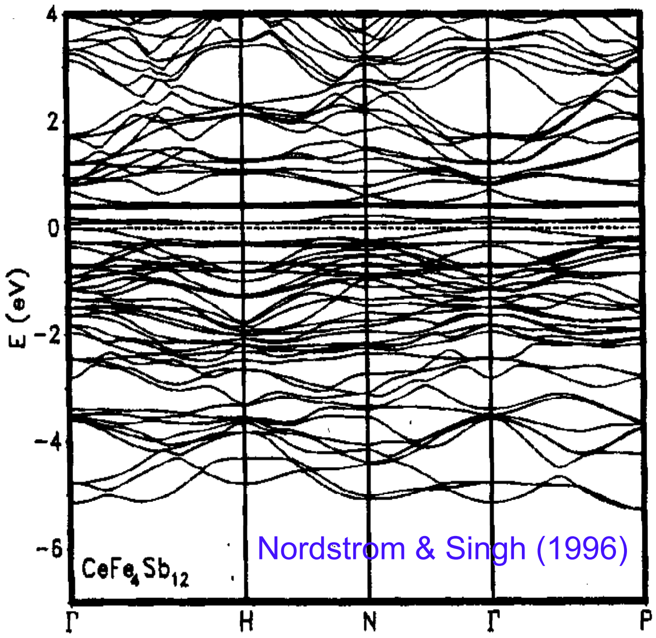

Nordstrom & Singh (1996)

- Similar separation into manifolds of conduction and valence bands as in $CoSb_3$.
- The major difference is the presence of the flat Ce 4f-bands at the bottom of conduction band.
- Via hybridization, Ce 4f states exert strong influence on both conduction and valence bands.
- The flatness of the Ce 4f conduction bands implies large effective mass (~ 10 m_e)
- Narrow -gap semiconductors (Eg ~ 0.1 eV).

An unusual combination of very small bandgaps with large effective masses ⇒

Excellent prospect for large thermoelectric power!

Glen Slack in 1994 – PGEC Paradigm

Filled skutterudites should be interesting because:

- Fillers should be loosely bonded to the cage atoms.
- Fillers should have large atomic displacements.
- They should act as independent oscillators (“rattlers”).
- Interaction of rattlers with the normal modes should lower κ_L.
- Rattlers should not greatly affect excellent electronic properties.

Vibrational Properties of Skuterudites

Symmetry of the structure ($Im3\text{-}T_h^5$) implies the existence of 19 distinct zone center phonon modes:

$$\Gamma = 2A_g + 2E_g + 4F_g + 2A_u + 2E_u + 7F_u$$

(Feldman and Singh 1996)

Phonon density of states obtained from this model is shown

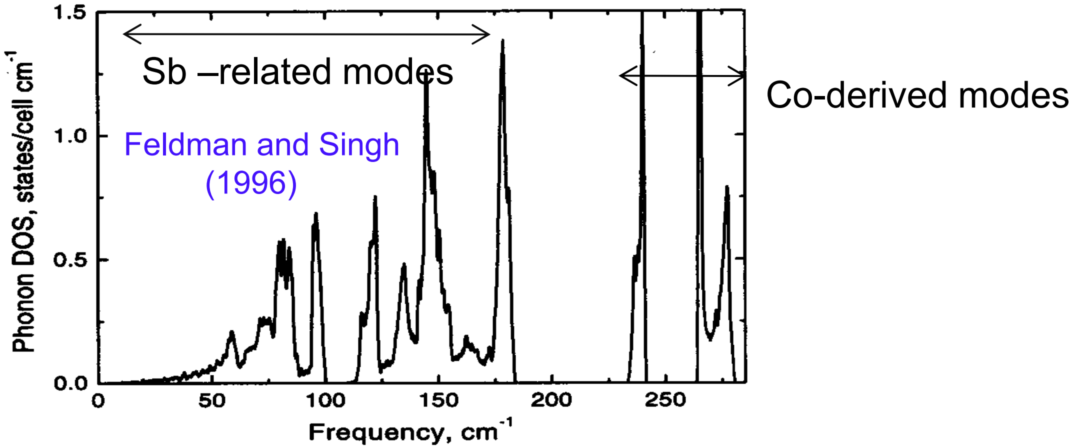

Frequencies below 170 cm^{-1} are due to vibrational modes of antimony.
Co modes (f > 230 cm^{-1}) are well separated from the antimony modes.
It follows that Co modes are irrelevant to the heat transport.
Acoustic modes dominate, optic branches cause breaks in parabolic f-dependence.
Bulk of heat is carried by acoustic modes of Sb with a contribution of optic Sb modes.

Singh et al. (1999): Calculations of the total energy of $CeFe_4Sb_{12}$ as a function of the filler position yielded “bare” Einstein frequency of 68 cm^{-1} for Ce, right in the range of Sb motions governing heat conduction. This suggested “rattling” behavior of the filler species.

Strong experimental support for the ideas of Slack

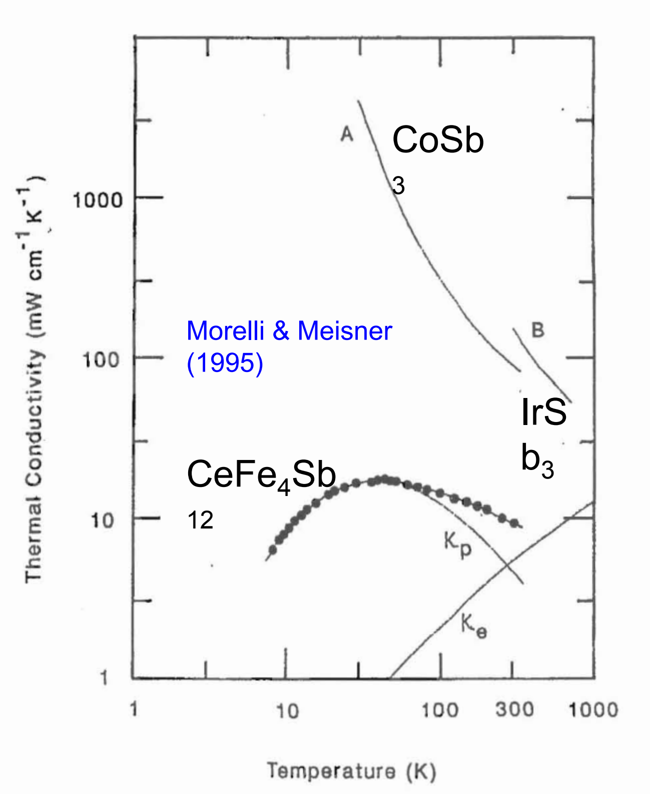

Filled skutterudites have an order of magnitude lower thermal conductivity!

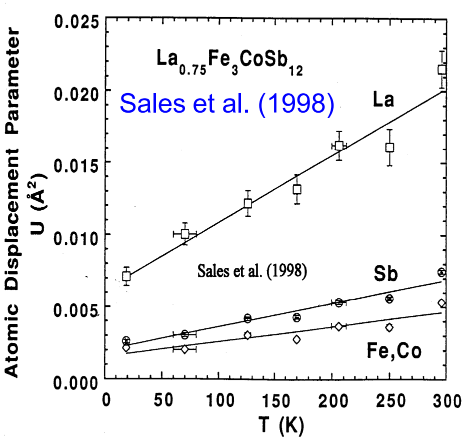

Indeed, atomic parameters of "rattlers" are much larger than of other atoms.

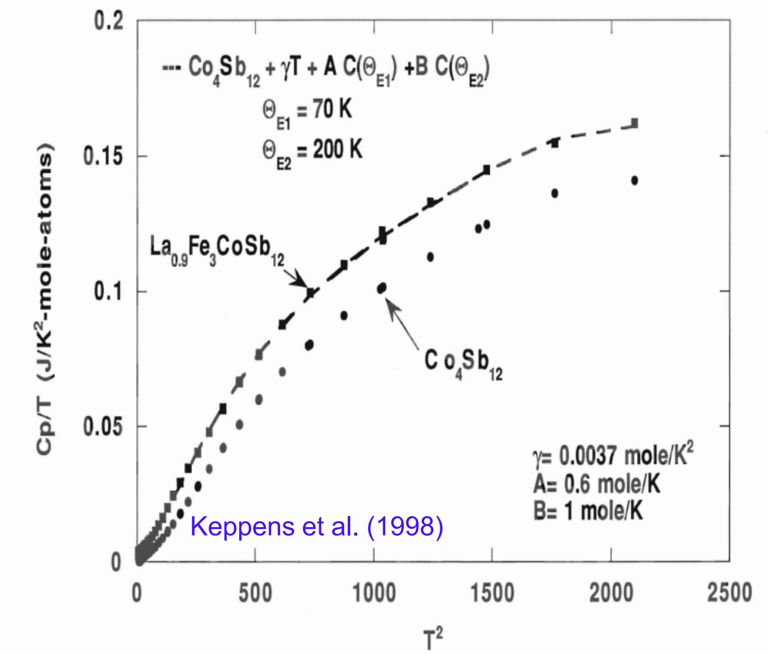

Perhaps the most convincing evidence for "rattling" of fillers comes from the two Einstein oscillator model of Keppens et al. (1998) based on: inelastic neutron scattering and low temperature specific heat.

Resent Challenges to the “Rattling” Theory

Koza et al. (2006)-invited presentation at ICT2006, Vienna

“Rattling” hypothesis lacks any evidence of phase coherence, collectivity or coupling!
Classical “rattler” should have the following properties:

- With T increasing, frequency of the rattler should be blue-shifted and *vice-versa.*
- Independence of the vibrational energy from the wave-vector transfer ($d\omega_q/dq=0$).
- Lack of phase coherence of the vibrational motion.

None of these criteria tested so far.
Only techniques probing simultaneously energy and momentum can provide answer.
High resolution time-of-flight neutron scattering can simultaneously supply $\hbar\omega(Q)$ & $\hbar Q$.
Inelastic neutron scatt. source at Laue Langevin Inst. in Grenoble used on $CeFe_4Sb_{12}$
An order of magnitude improved energy resolution ⇒finer details of guest-host coupling.

- Vibrational modes of Ce fillers are coherently coupled with atoms of the host.
- Presence of van Hove singularities in the phonon spectrum giving $v_g=d\omega_q/dq=0$.
- Phonon transport hindered by Umklapp processes.

The work has stirred a big controversy.
Recent simulation/modelling by Kaviany et al. support Koza’s view.

Sample preparation

Constituents with vastly different melting point and vapor pressures.
Three stable compounds: CoSb (γ-phase); $CoSb_2$ (δ-phase); $CoSb_3$ (ε-phase).
Skutterudites form via a peritectic reaction:

ε-phase $\leftrightarrow$ δ-phase + Liquid at $T_p = 873^oC$

Very slow kinetics$\Rightarrow$ peritectic reaction not completed, $\Rightarrow$ long-term annealing needed.

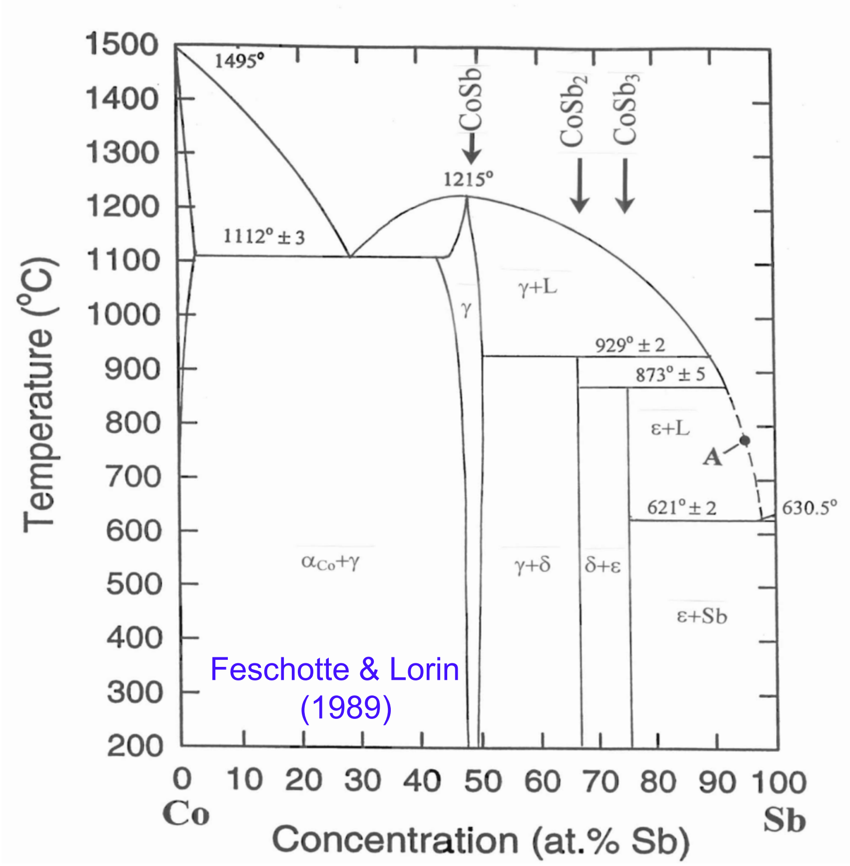

Feschotte & Lorin (1989)

Usual strategies for growth:

- Solid-liquid phase sintering, grinding, hot-pressing.
- From non-stoichiometric melts, e.g., point A shown.
- Flux-assisted growth (small crystals).
- Chemical vapor transport (small crystals).

A new growth prospect:

- Melt spinning

Physical Properties of Skutterudites

Rich variety of physical properties – gold mine for solid state physics

- Binary skutterudites are diamagnetic semiconductors.
- Interesting open structure environment ⇒ filler species modify properties.
- Ternary skutterudites ⇔ isoelectronic substitution, e.g., Fe^{2+} and Ni^{4+} for Co^{3+}
- Superconductivity ⇒phosphite skutterudites, e.g., La Fe_4P_{12}, new $BaPt_4Ge_{12}$.
- Magnetism ⇔ majority of rare-earth fillers have magnetic moment.
- Heavy fermion behavior, e.g., UFe_4P_{12}.
- Most spectacular are the thermoelectric properties!

Why are skutterudites prospective as thermoelectrics?

- Large unit cell
- Reasonably large atomic masses
- Exceptionally high mobilities (~4000 cm^2/V-s)
- Large κ_P can hopefully be reduced

$$P = S^2\sigma \sim \mu\ (m^*)^{3/2}$$

$$\kappa_p \sim M^{-1/2}N^{-2/3}$$

Primary focus on $CoSb_3$

- $M_{Sb} > M_{As} > M_P \Rightarrow$ antimonides have the lowest κ_p.
- Antimonide skutterudites have the largest cage.
- Cobalt and antimony are inexpensive.
- Easy to synthesize via solid or liquid diffusion.
- Minimal hazard to people or environment.
- Other skutterudites, e.g., $IrSb_3$ special advantages

Electronic properties of $CoSb_3$

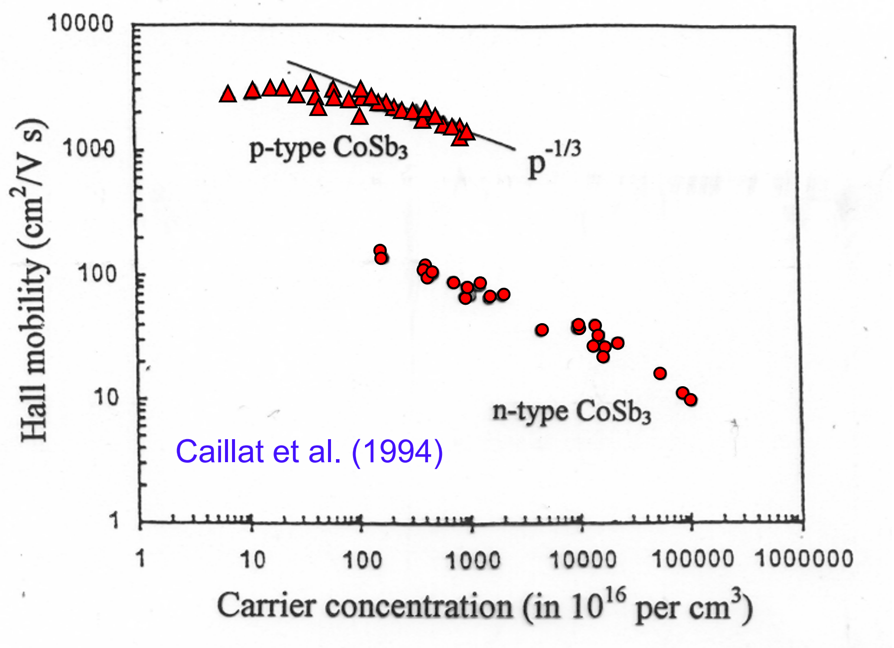

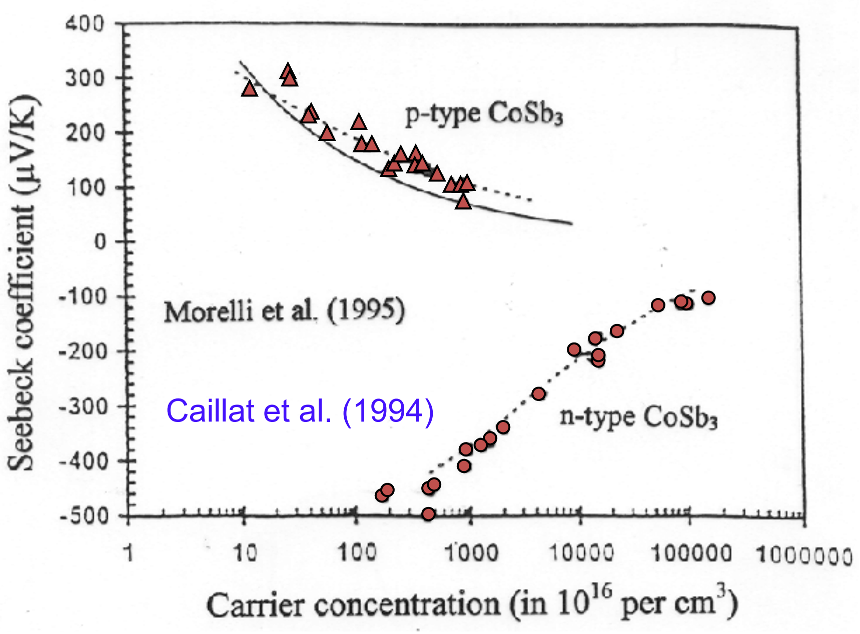

Very high mobilities, especially for the p-type material.
Large Seebeck coefficients.

Promising power factors $P \approx 20\text{-}30\ \mu W/K^2\text{-cm}$

Thermal conductivity of $CoSb_3$

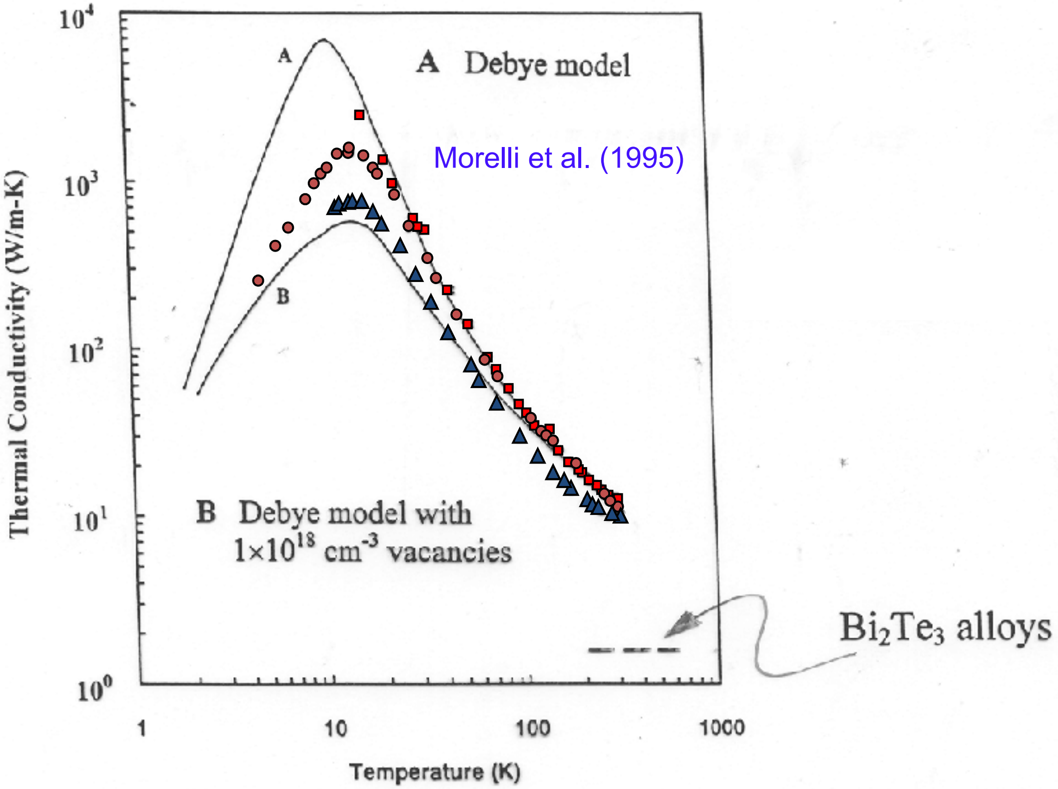

- Classic phonon heat conduction behavior.
- Very high conductivity at low temperatures.
- Essentially no electronic contribution.

Crucial to reduce lattice thermal conductivity!

Major effort to reduce thermal conductivity

Traditional ways of reducing thermal conductivity:

- Scattering by charge carriers
- Scattering by point defects
- Scattering on structural defects (grain boundaries)
- Scattering by mixed-valence ions

Effective but not quite enough for skutterudites.

1994- Slack: PGEC Paradigm

Filler ions are loosely bonded and might act as “rattlers”,

strongly scattering normal phonon modes.

Worldwide effort to identify the most effective “rattlers”.

Dependence of κ_p on the rattling amplitude

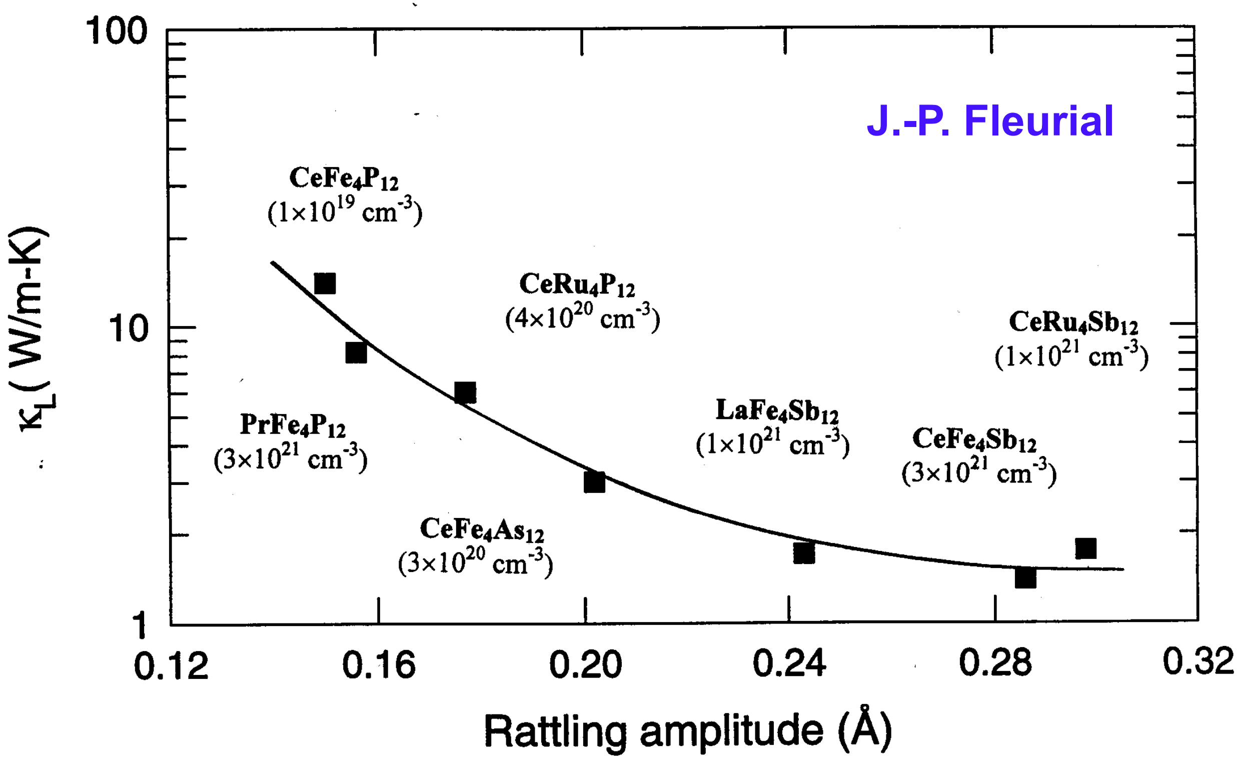

Note the trend:

Antimonides yield the lowest thermal conductivity!

Suitable filler species for skutterudites

- Rare-earths (Ce, La, Yb, …)
- Alkaline-earths (Ba, Ca, Sr)
- Actinides (U, Th)
- Elements (Tl, Sn)

Fillers enter as ions and **donate** electrons.

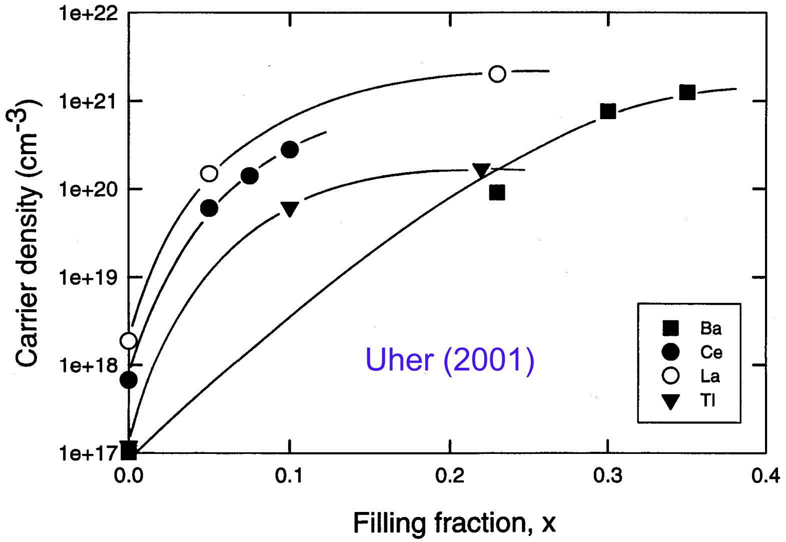

Uher (2001)

The structure is rapidly saturated with negative charge ⇒

There are limits to void occupancy!

Occupancy limits

$Ce_yCo_4Sb_{12}$	$y_{max} \approx 0.1$	(Chen et al. 1997)
$Tl_yCo_4Sb_{12}$	$y_{max} \approx 0.22$	(Sales et al. 2000)
$La_yCo_4Sb_{12}$	$y_{max} \approx 0.23$	(Nolas et al. 1998)
$Yb_yCo_4Sb_{12}$	$y_{max} \approx 0.25$	(Anno et al. 2000)
$Ba_yCo_4Sb_{12}$	$y_{max} \approx 0.45$	(Chen et al. 2001)
$Eu_yCo_4Sb_{12}$	$y_{max} \approx 0.54$	(Berger et al. 2001)

To increase void occupancy ⇔ charge compensate

Fe^{26}
2-8-14-2
$3d^6 4s^2$

Co^{27}
2-8-15-2
$3d^7 4s^2$

$Ce_yFe_{4-x}Co_xSb_{12}$

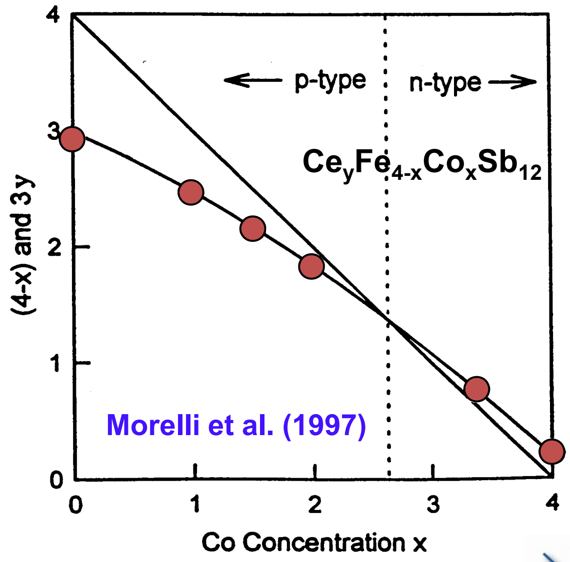

Strong charge compensation leads to p-type skutterudites

($ReFe_{4-x}Co_xSb_{12}$ with $x \le 1$)

Working with such a system, ZT ~ 1.4 reported in 1997 for p-type.

Fleurial et al. (1997)

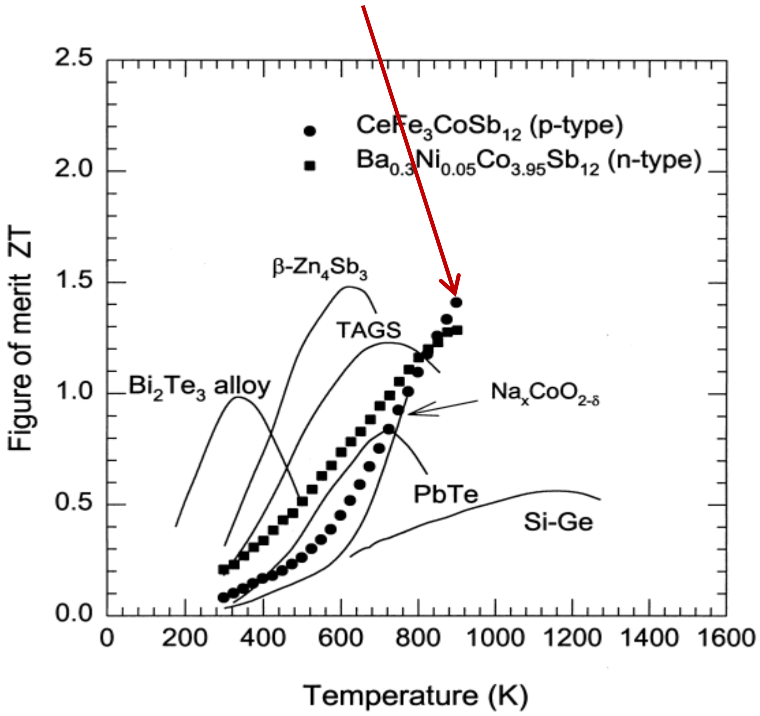

Such apparent record-high p-type ZT stimulated much interest in general and focused attention to **n-type skutterudites** that, at that time, were no better than ZT ~ 0.7.

Can high ZT be achieved with n-type skutterudites?

Difficulties:

- Compensation drives the system p-type
- Cage occupancy is limited
- Smaller and heavier rare-earths do not go in the cage

Potential Approaches:

- Fillers drive the system n-type naturally.
- Look beyond rare-earths
- Employ multiple filling
- Introduce nanometer-scale features into the matrix.
- Try modest degree of charge compensation

Alkaline-earth-filled skutterudites

$Ba_yCo_4Sb_{12}$

Collaboration of: Shanghai Institute of Ceramics
University of Michigan
Wuhan University of Technology

Tang et al. (2001a,b), Chen et al. (2001a,b)

Ba^{2+} is a strictly a **divalent** ion.
Ba^{2+} is a rather large ion.
No intermediate valence state.
Large filling limit, $y_{max} \approx 0.45$

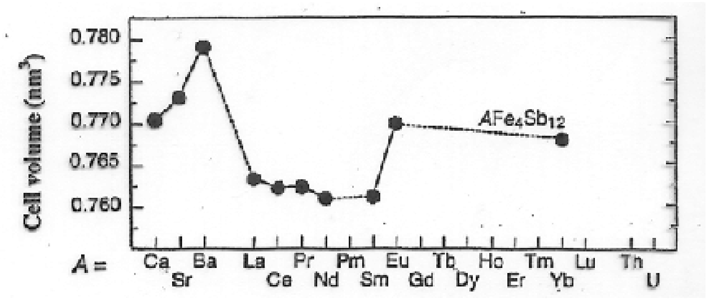

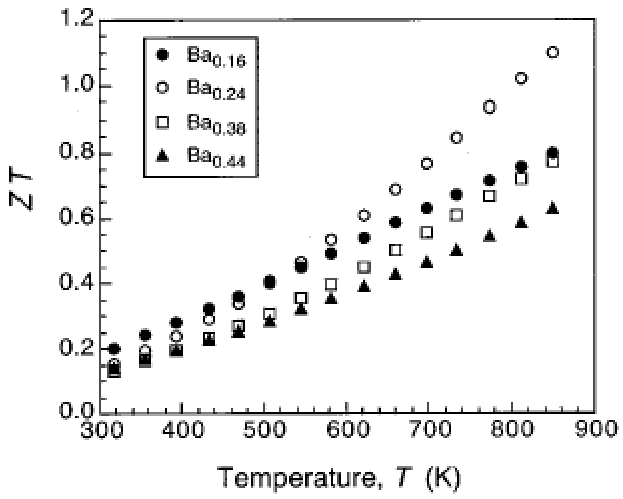

Comprehensive transport studies 2K-900K
Identified an excellent n-type skutterudite

Best ZT ≈ 1.1 at 850K near y = 0.2-0.3

Multiple filling of the voids

Different filler size, mass and bonding

⇒ different “spring constant”

⇒ different characteristic frequency

A broader spectrum of phonons affected

⇒ a larger reduction in κ_{ph} expected.

Does it work?

$Ce_yBa_{1-y}Co_4Sb_{12}$ $La_yBa_{1-y}Co_4Sb_{12}$ $Sr_yBa_{1-y}Co_4Sb_{12}$	Chen et al. (2001)	**Reduction in κ_{ph}.**
$Yb_xCe_{1-x}Fe_4Sb_{12}$	Rowe et al. (1998) Berardan et al. (2003)	**Power factor up,** **κ_{ph} not measured.**
$La_yCe_{1-y}Ru_4P_{12}$	Giri et al. (2002)	**Some reduction in κ_{ph}.**

More work needed to clarify the influence of multifilling.

Multiple filling of the voids

So far, filling limits based on experimental work.
Is there any useful theoretical input? The answer is YES!

Shi et al. PRL (2005): density functional method to determine **filling fraction limit (FFL).**
Mei et al. (2006) FFL determined by interaction between the guest and host and
Shi et al. (2007) by the formation ability of secondary phases.
Shi et al. (2008) Selection rule: for FFL > 0 , **electronegativities** must satisfy

$$x_{Sb} - x_{imp} > 0.80$$

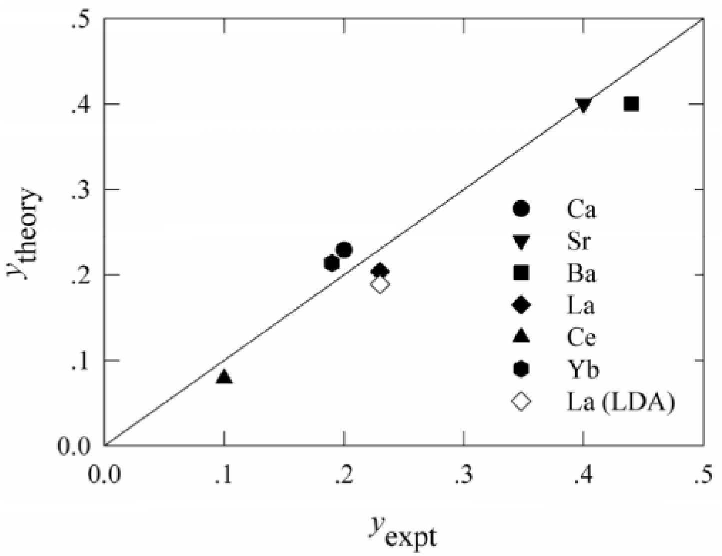

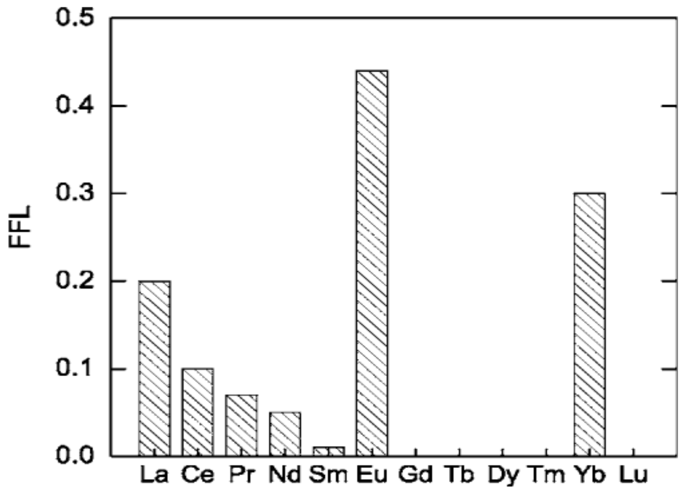

Excellent agreement with the experimental results.

Multiple filling of the voids

Yang et al. (2007): density functional theory calculations of spring constant and resonance frequencies of fillers in $CoSb_3$.

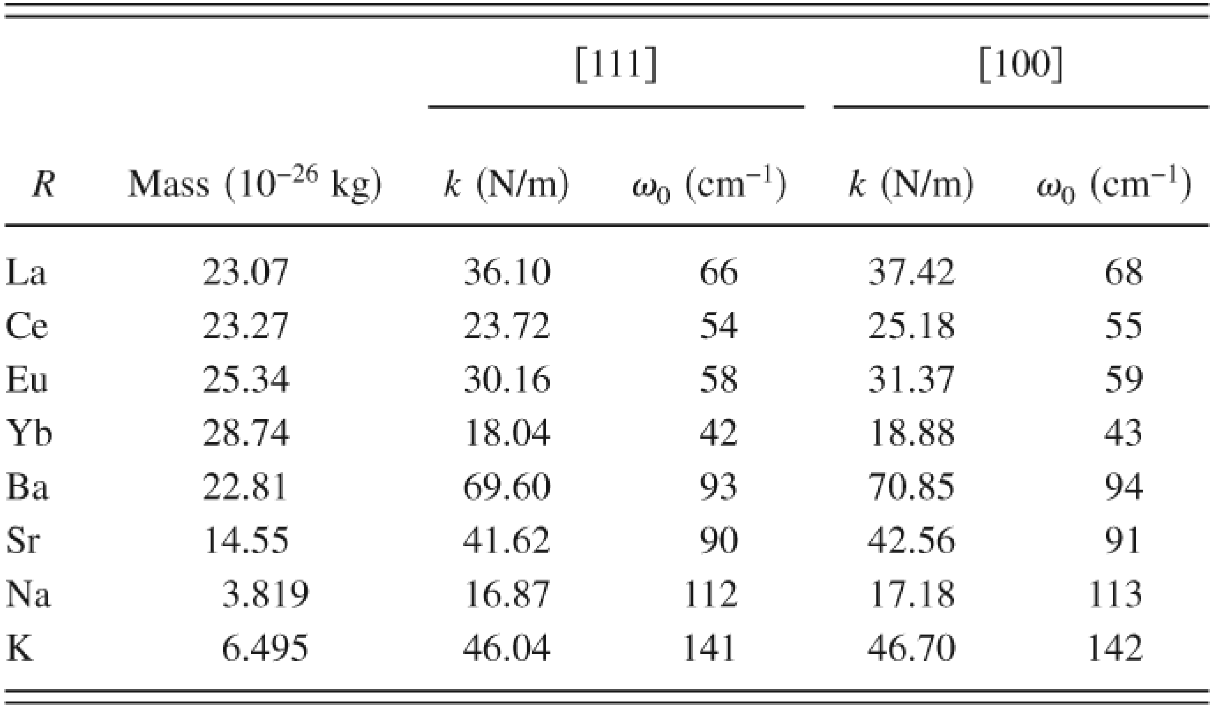

		[111]		[100]	
R	Mass (10^{-26} kg)	k (N/m)	ω_0 (cm^{-1})	k (N/m)	ω_0 (cm^{-1})
La	23.07	36.10	66	37.42	68
Ce	23.27	23.72	54	25.18	55
Eu	25.34	30.16	58	31.37	59
Yb	28.74	18.04	42	18.88	43
Ba	22.81	69.60	93	70.85	94
Sr	14.55	41.62	90	42.56	91
Na	3.819	16.87	112	17.18	113
K	6.495	46.04	141	46.70	142

To obtain the greatest reduction in thermal conductivity, select fillers that have widely different resonance frequencies!

Multiple filling of the voids

$Ba_xYb_yCo_4Sb_{12}$

Filler	k (N/m)	ω_o (cm^{-1})
Ba	69.6	93
Yb	18	42

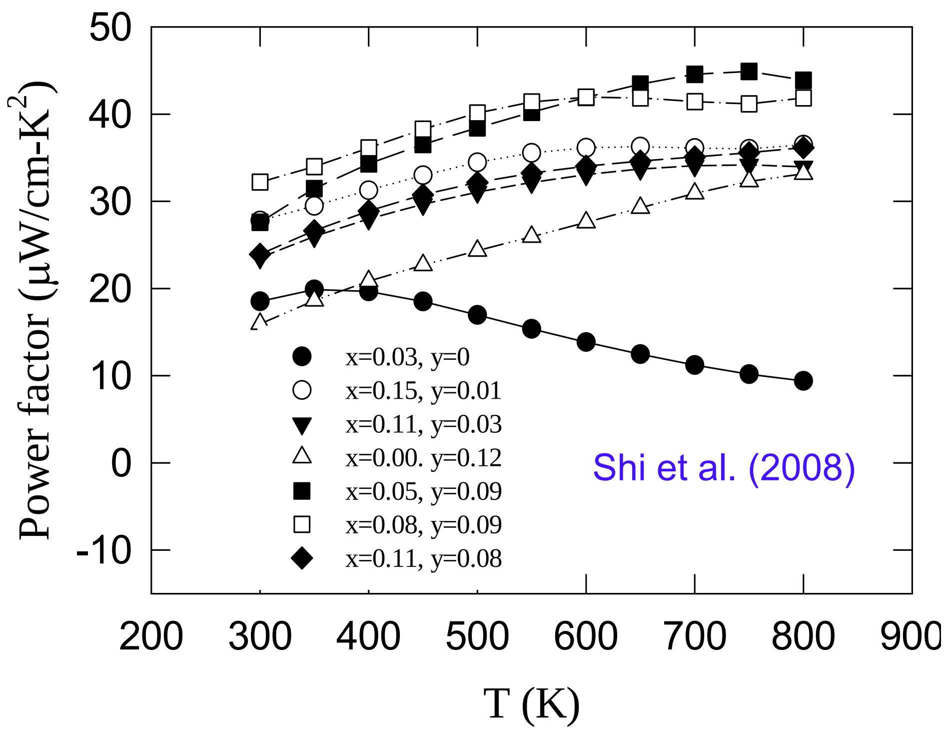

Shi et al. (2008)

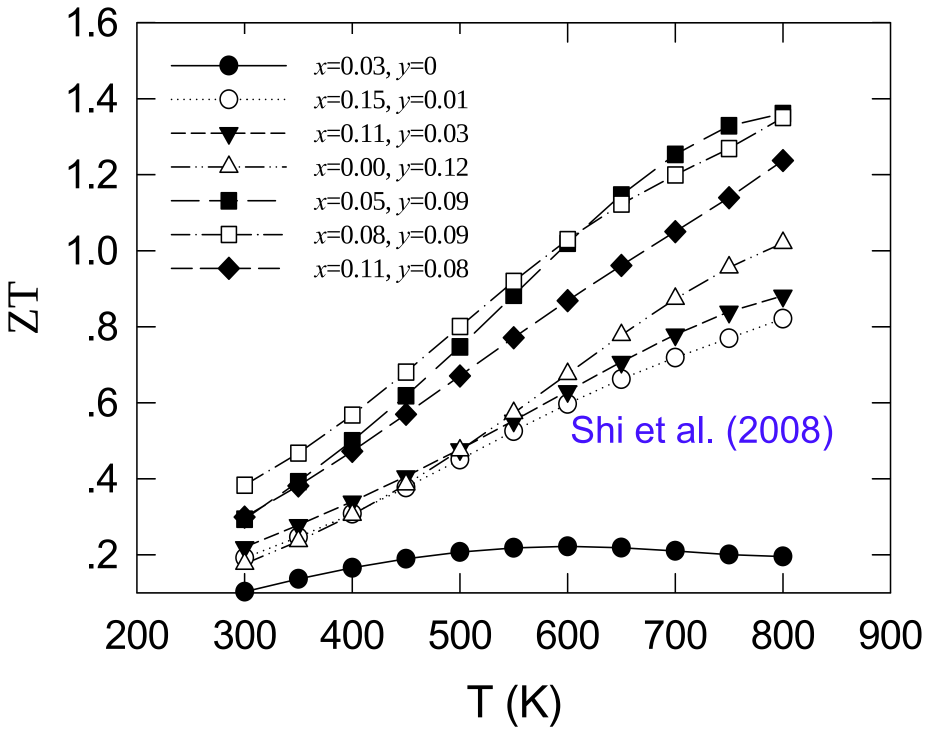

Shi et al. (2008)

- Power factor: reaches 45 μW/cm-K^2 at 750K, stays above 30 μW/cm-K^2 for T > 300K.
- ZT ≥ 1.36 at 800K, the highest ZT for n-type skutterudites by year 2008.
- Several compositions with ZT > 1.3.
- **Excellent n-type skutterudites!**

Nanostructure in Bulk Skutterudites

If charge carriers have large m* ⇒ possibility that $\ell_{ph} > \ell_e$
Enhancing phonon boundary scattering (grain size ~ phonon wavelength) may actually improve ZT by lowering the lattice thermal conductivity.

Sharp, Poon, and Goldsmid (2000)

I. **Consolidate precipitated nanopowders:** not a very effective route as the grains grow rapidly during thermal processing and any benefit is annealed out! Bertini et al. (2003)

II. **Quench-in the nanostructure by melt spinning:**

Tang et al. (2007)
H. Li et al. APL (2008)
Qiang Li et al. (2008)

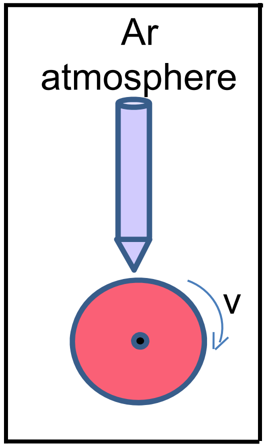

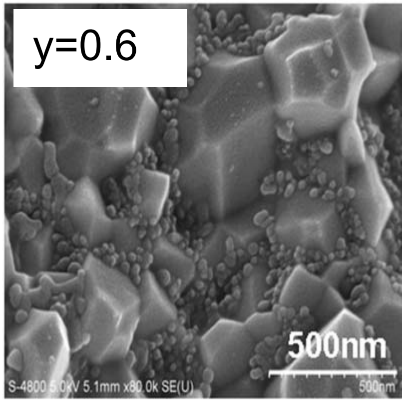

H. Li et al. APL (2008)

$Yb_{0.3}Co_4Sb_{12+y}$

Very rapid synthesis
Larger content of Yb
κ strongly reduced
ZT = 1.3 at 800K
Reproducible on cycling

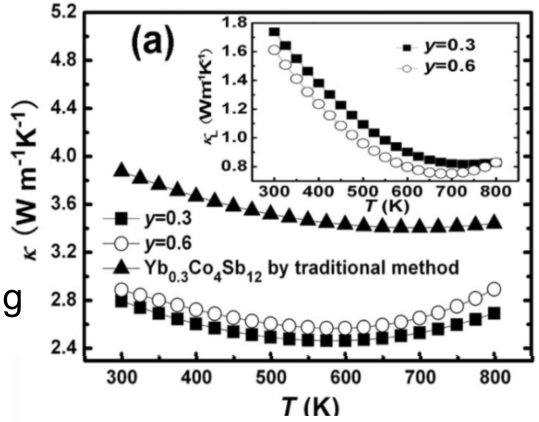

H. Li et al. APL (2008)

Nanostructure in Bulk Skutterudites

III. **In-situ formed nanostructure:** H. Li et al. APL (2009)

By attempting to double-fill $CoSb_3$ with In and Ce, (**$In_xCe_yCo_4Sb_{12}$**), we observed a finely dispersed InSb nano-phase at the boundaries.

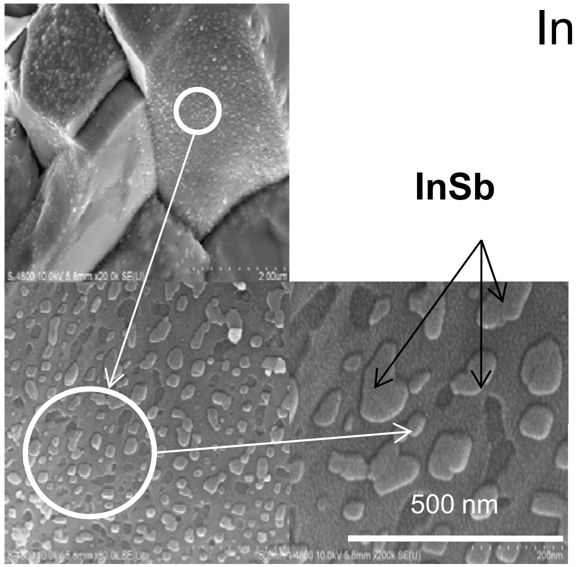

In should not go into voids

$X_{Sb} – X_{in} = 0.27 < 0.8$

↓

The presence of the InSb nanophase reduced lattice thermal conductivity.
ZT enhanced to 1.43 at 800K.

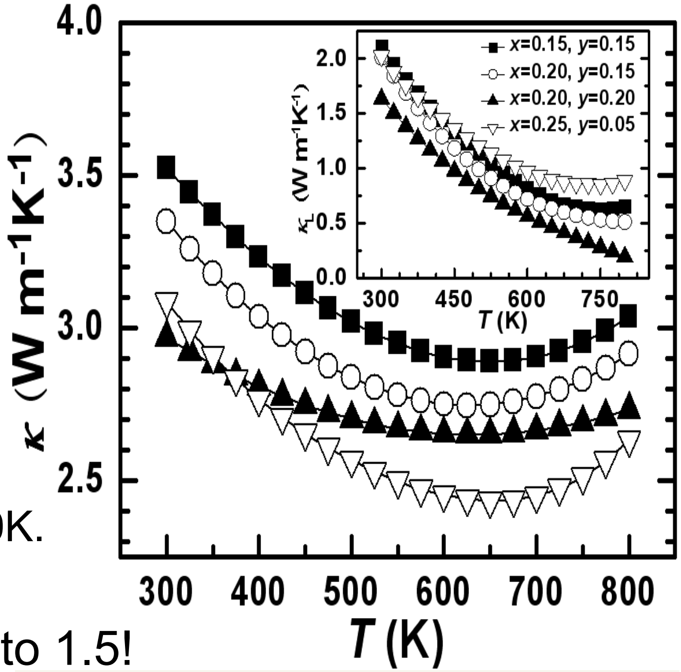

Subsequent work raised ZT to 1.5!

Excellent progress in n-type skutterudites!

Where are we today?

- N-type skutterudites with the demonstrated ZT ~ 1.5-1.7 at 800K. Shi et al. (2011)
- P-type skutterudites with the demonstrated ZT ~1.0 at 800K. More work needed!
- Operational range of filled $CoSb_3$-based skutterudites is 700K-1000K.
- Skutterudites possess **outstanding mechanical properties**. Salvador et al. (2009)
- Readily available chemicals, no reliance on tellurium.
- Perhaps the most prospective of novel TE materials for power generation.

Thermal conductivity is still **too high** and limits the value of ZT.

What can we do?

→ Create disorder on filler sites PRL **105**, 265901 (2010)

→ Form nanostructures in TE materials APL **94**, 102114 (2009)

→ Create disorder on pnicogen rings PRB **86**, 195209 (2012)

Is disorder on the filler lattice beneficial?

Kim et al. PRL 105, 265901 (2010)

Important and relevant question not considered before.
Could additional disorder further lower thermal conductivity?

Phase diagram established by *ab initio* calculations, cluster expansion and MC simulations.

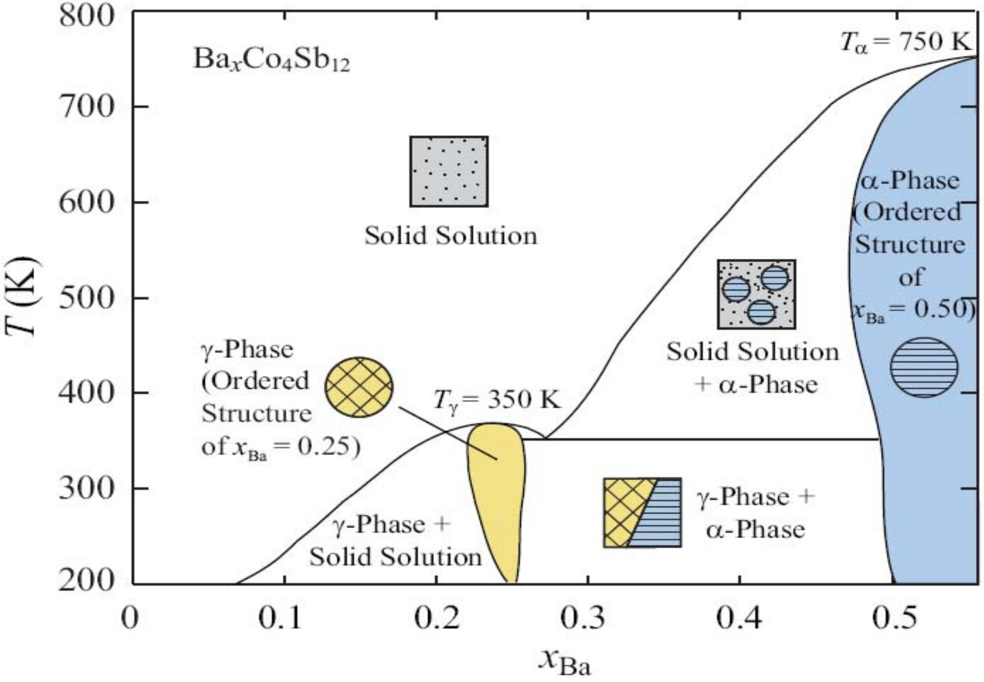

Phase diagram exhibits ordered phases of Ba below and near the FFL :

γ-phase with x = 0.25 that disorders at 350K
α-phase with x = 0.5 that disorders above 750K

The phases coexist at intermediate x and low temperature.
Coexistence of each phase with solid solution at high temperatures.

Is disorder on the filler lattice beneficial?

Kim et al. PRL 105, 265901 (2010)

After interatomic potentials are found, thermal conductivity is obtained by MD simulations and with the heat current determined by Greene-Kubo autocorrelation approach. Lattice thermal conductivity at 300K as a function of Ba content x is shown.

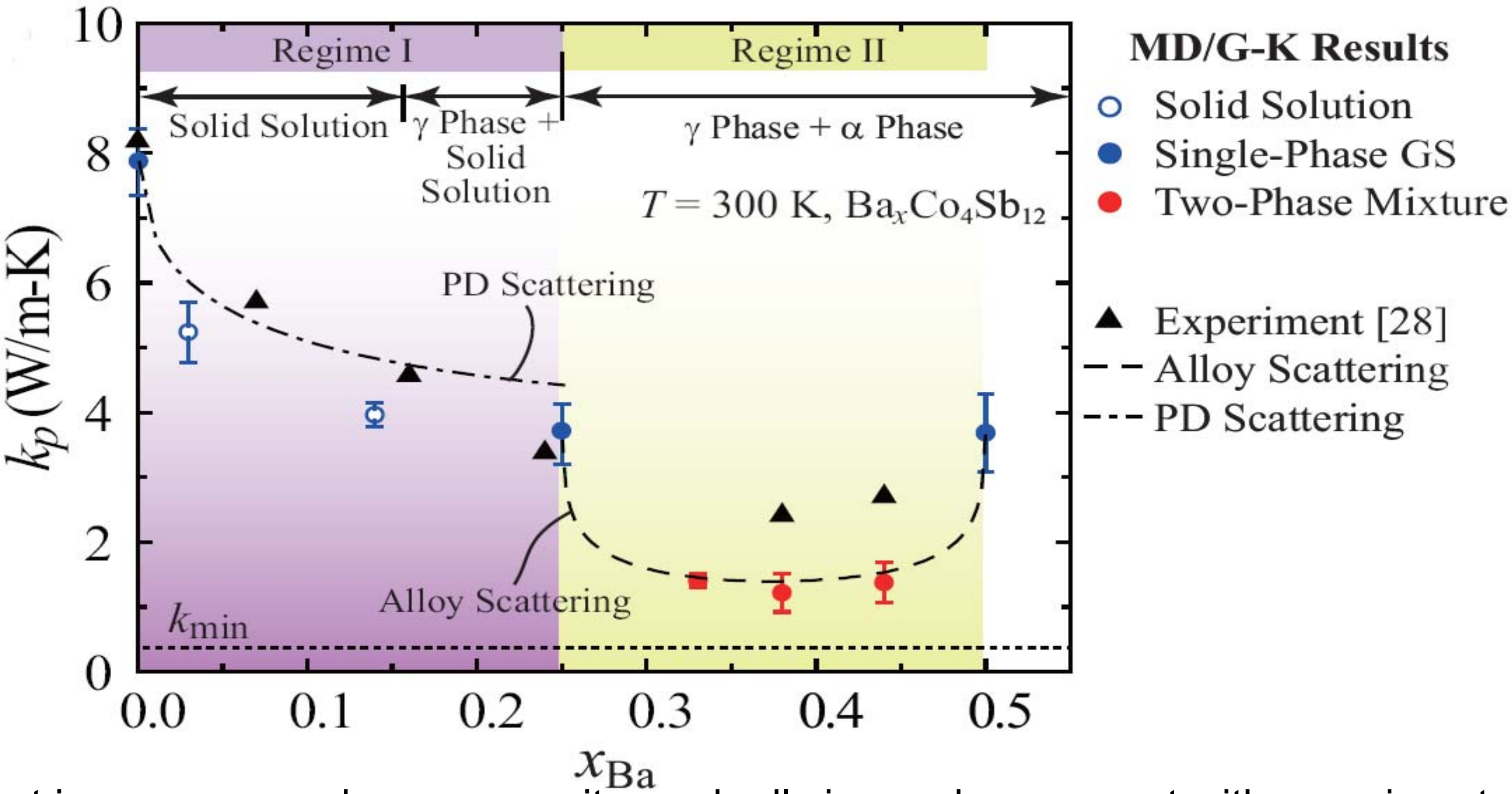

As the Ba content increases, κ_{ph} decreases quite markedly in good agreement with experiment. Within the **solid solution regime**, Ba acts as a point defect scatterer and this persists to x = 0.25. In the **two-phase regime** (0.25 < x < 0.50), strong alloy scattering sets in → κ_{ph} falls further.

The presence of order-disorder phase transformations of filler species in the voids of skutterudites is highly beneficial to improving their TE performance.

Nanostructures in skutterudites

If charge carriers have large m^* $\Rightarrow$ possibility that $\ell_{ph} > \ell_e$
Enhancing phonon boundary scattering (grain size ~ phonon wavelength) may actually improve ZT by lowering the lattice thermal conductivity.

I. Intrinsic processes during cooling of the melt

Spinodal decomposition (Androulakis et al., 2007)

Nucleation and growth (Heremans et al, 2005)

Matrix encapsulation (Sootsman et al., 2006)

Compensating double doping (Liu et al. 2008)

Compound formation (Li et al., 2009)

II. Extrinsic processes of preparing nanosized powders by

Grinding
Milling
} (Poudel et al., 2008)

Wet chemistry (Bertini et al., 2003)

followed by compacting into pellets/ingots.

While both approaches successfully form nanocomposite structures, the intrinsic routes are superior especially for power generation TE materials that will have to withstand extended exposure to high-T environment.

The stability of the nanostructure matters!

Nanostructures in skutterudites

(a) Quench-in the nanostructure by melt spinning:

H. Li et al. (2008)

Tang et al. (2007)

Qiang Li et al. (2008)

H. Li et al. APL (2008)

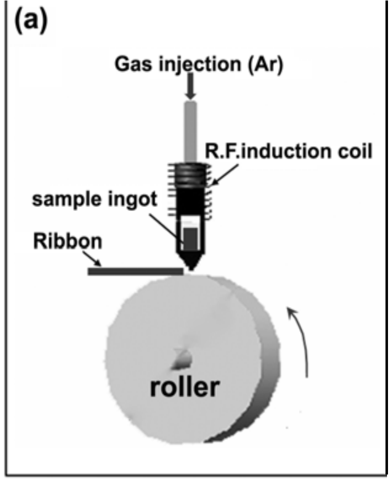

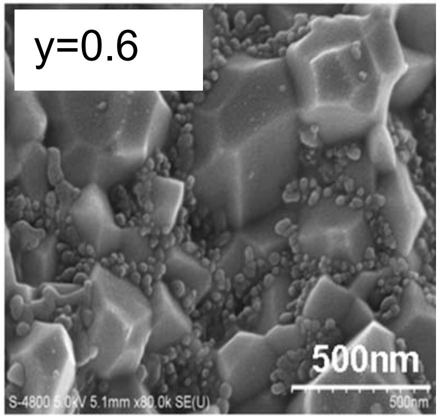

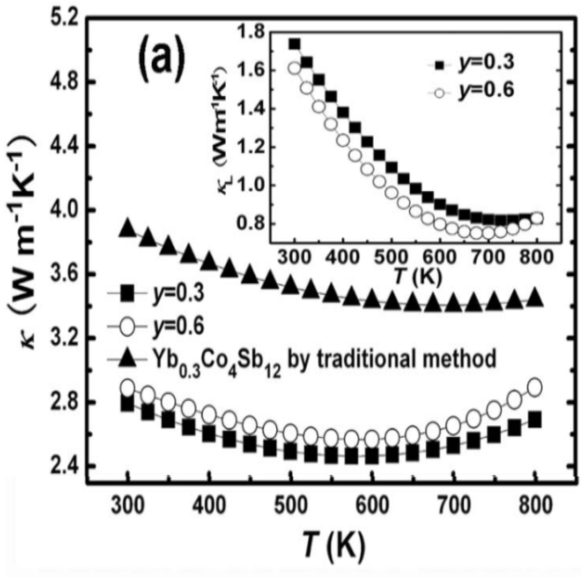

H. Li et al. APL (2008)

$Yb_{0.3}Co_4Sb_{12+y}$

Very rapid synthesis. Extremely high cooling rates.

Larger content of Yb ⟹ κ strongly reduced.

ZT = 1.3 at 800K

Reproducible on cycling

Nanostructures in skutterudites

(b) In-situ formed nanostructure: H. Li et al. (2009)

According to Shi et al. (2005), filling of cages requires

$$X_{Sb} - X_{imp} > 0.80$$

Indium clearly does not satisfy this condition since

$$X_{Sb} - X_{In} = 2.05 - 1.78 = 0.27 \,!$$

Yet, Indium-filled skutterudites have been reported on.

He et al. (2006)
Jung et al. (2008)
Peng et al. (2008)

In collaboration with WUT we were interested what happens if **melt-spinning** is used in the synthesis of double-filled skutterudites containing Indium as one of the fillers.

$In_xCe_yCo_4Sb_{12+z}$ (x = 0.15, 0.2; y = 0.15, 0.20; z = 0, 0.3) by **melt-spinning**

$In_{0.15}Ce_{0.15}Co_4Sb_{12}$ reference sample by **traditional** method for comparison

Nanostructures in skutterudites

Traditional + SPS process

Course matrix grains ~ 1-3 μm
Nanoparticles ~ 20-100 nm

Melt-spinning + SPS

Much finer matrix ~ 300 nm
Very fine nanostructure
~ 10-15 nm

Field emission scanning electron microscopy

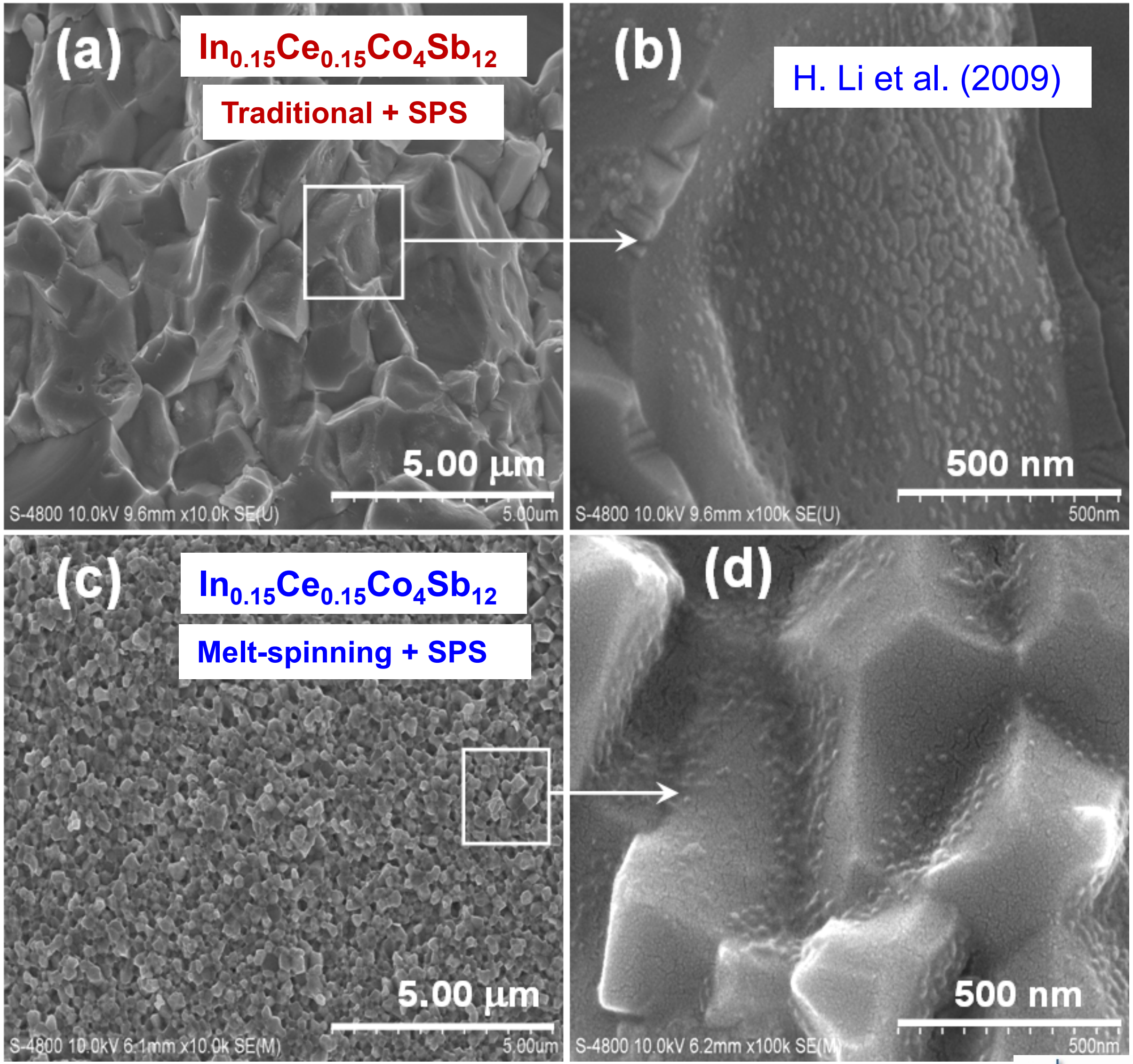

H. Li et al. (2009)

Nanostructures in skutterudites

Nanoparticles are InSb !

Domains I, II, III ↔ Ce-filled $CoSb_3$
In not detected

Domain IV ↔ InSb (200)

Interlayer distances correspond to InSb (101)

Indium forms a fine InSb nanostructure in skutterudites!

High Resolution Transmission Electron Microscopy + EDS

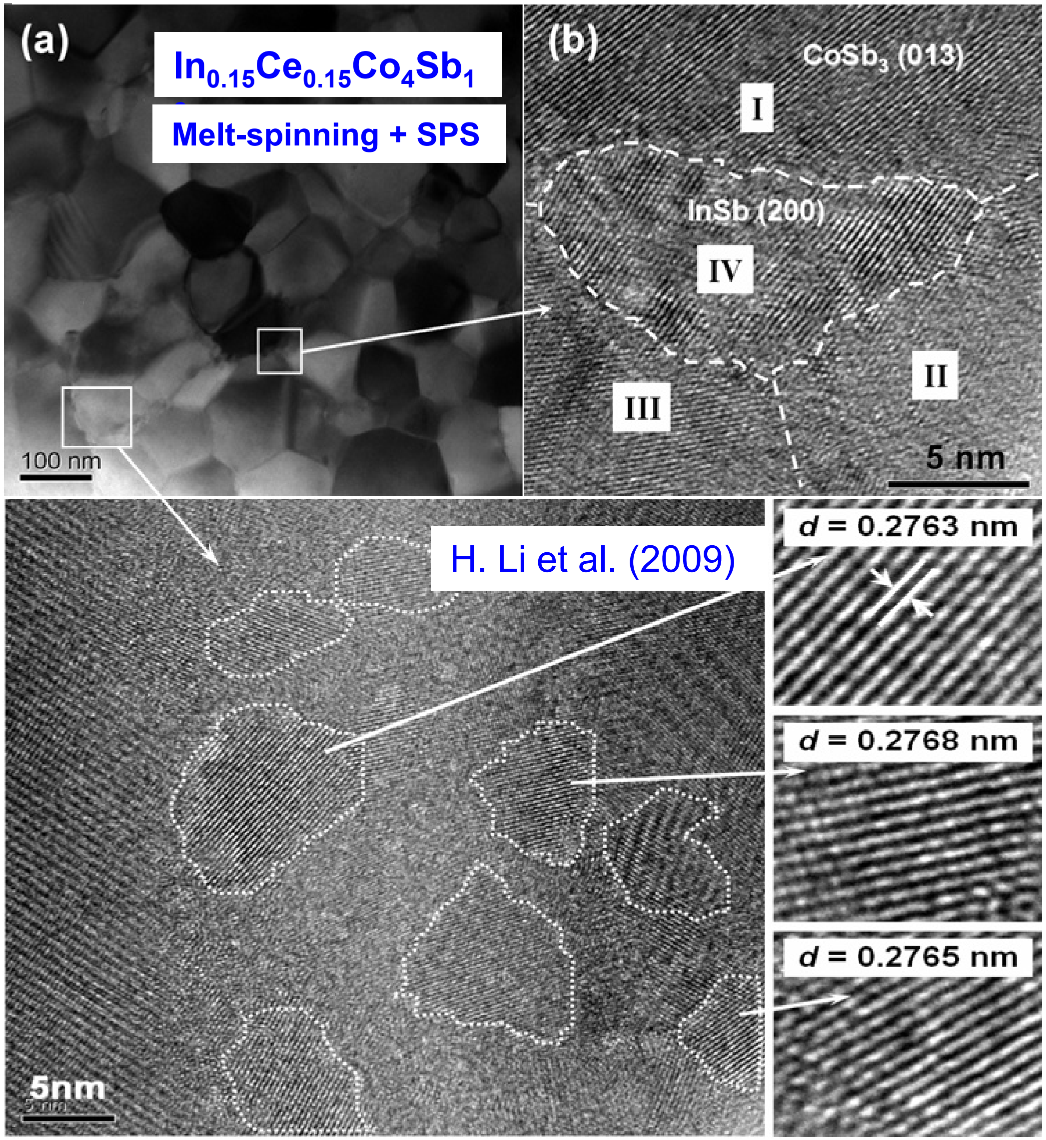

Nanostructures in skutterudites

Effect of InSb nanostructure on the electronic properties:

- Fine nanostructure of MS-SPS scatters electrons

compare $In_{0.15}Ce_{0.15}Co_4Sb_{12}$ TM
with $In_{0.15}Ce_{0.15}Co_4Sb_{12}$ MS-SPS

- With increasing x, y, and z, ⟶ σ increases

- For the same composition, Seebeck coefficient of MS-SPS higher than that of TM

- Power factor of MS-SPS smaller than for TM

↓

- Nanostructure indeed scatters charge carriers !

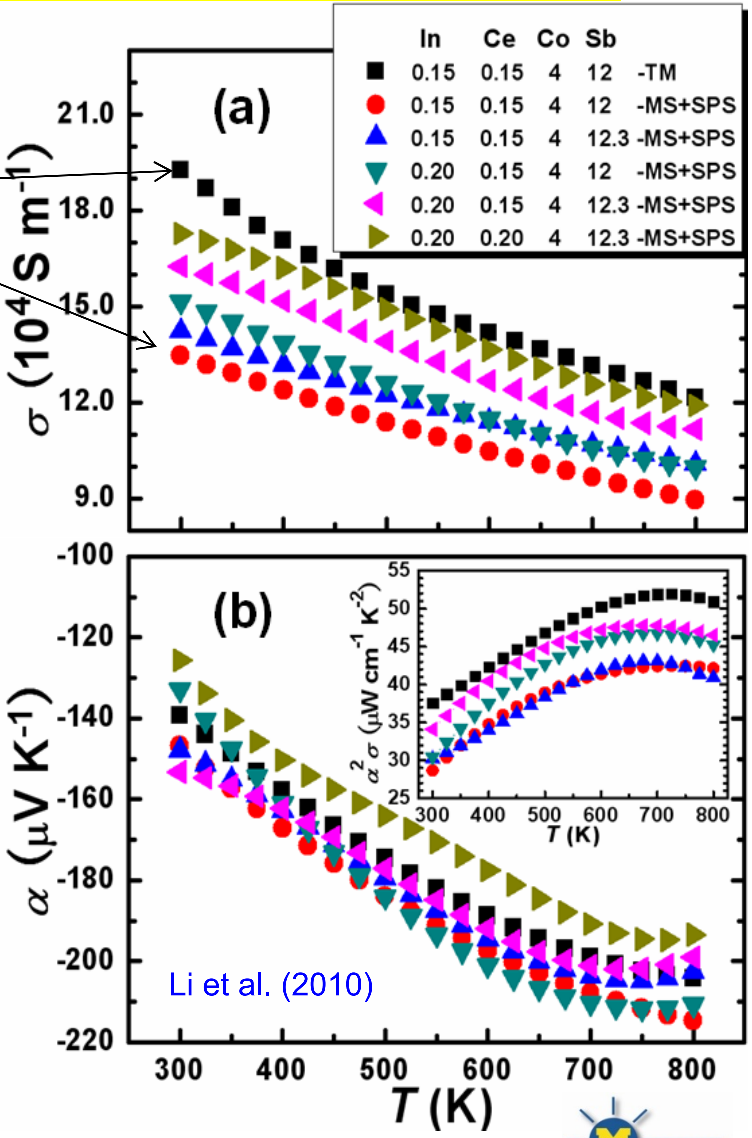

Li et al. (2010)

Nanostructures in skutterudites

Effect InSb nanostructure on thermal properties:

- Nanostructure of MS-SPS strongly scatters phonons

  compare $In_{0.15}Ce_{0.15}Co_4Sb_{12}$ TM

  with $In_{0.15}Ce_{0.15}Co_4Sb_{12}$ MS-SPS

- κ of MS-SPS some 35% lower than for TM

- Greater density of InSb (more In) → lower κ_L

- Excess of Sb increases κ_L

- Vacancies on the Sb lattice may be further reducing κ

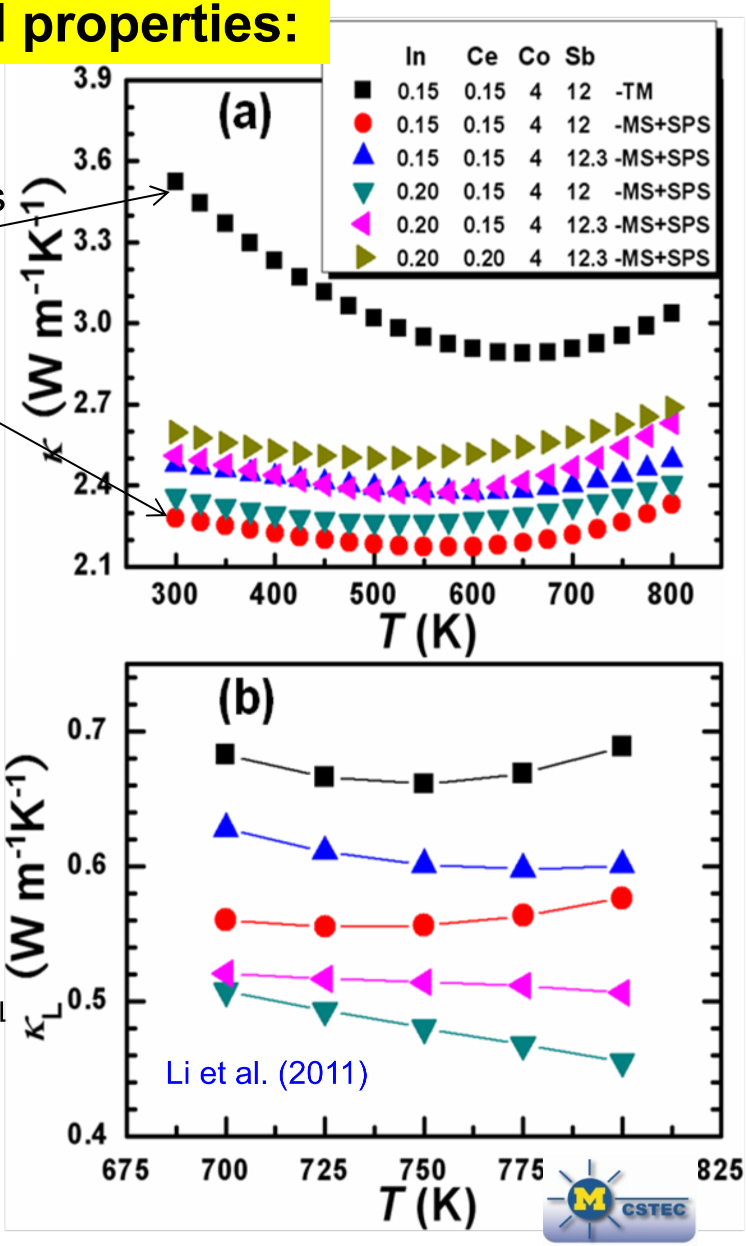

Li et al. (2011)

Nanostructures in skutterudites

Effect of InSb nanostructure on TE properties:

- ZT of MS-SPS 10% higher than TM
- Highest ZT > 1.5 at 800K
- ZT > 1 above 500K

Excellent n-type skutterudites with

ZT ~ 1.5 at 800K

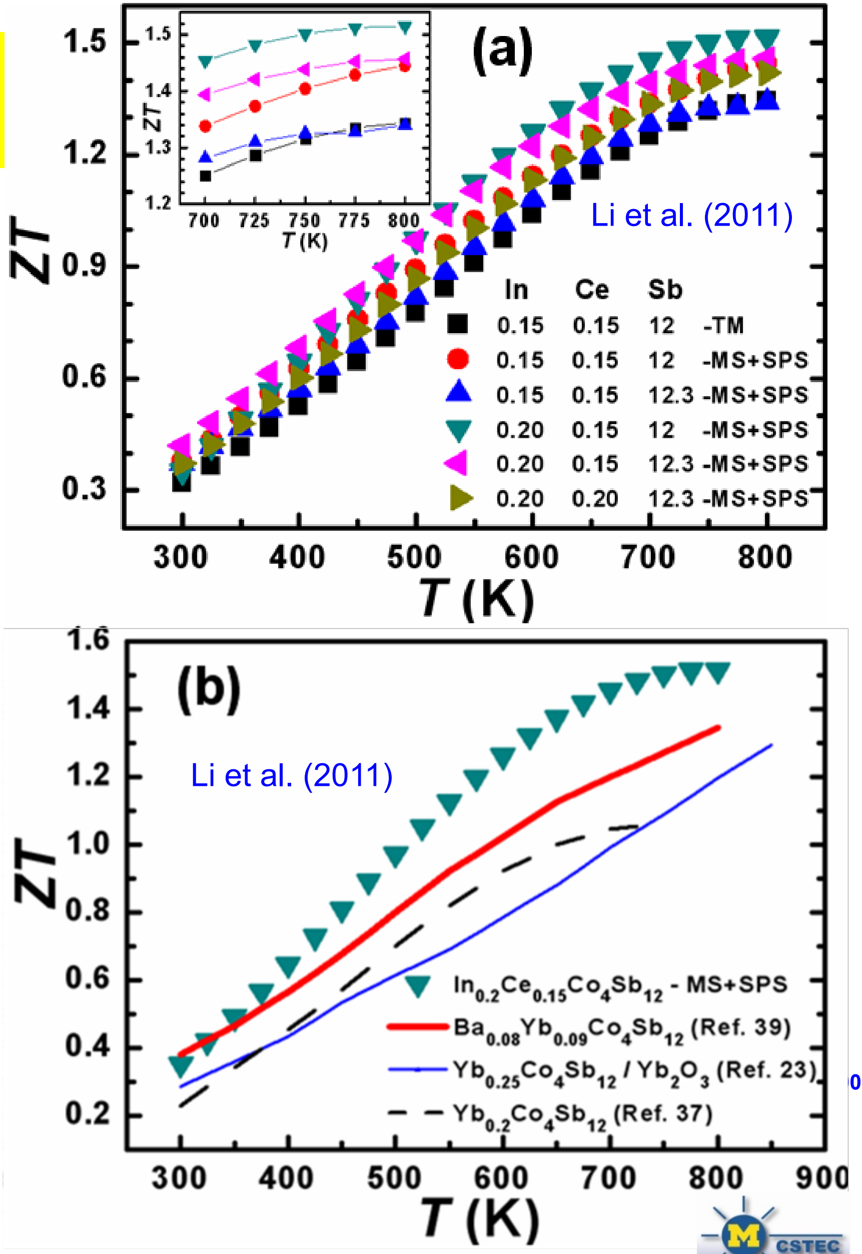

Disorder on pnicogen rings

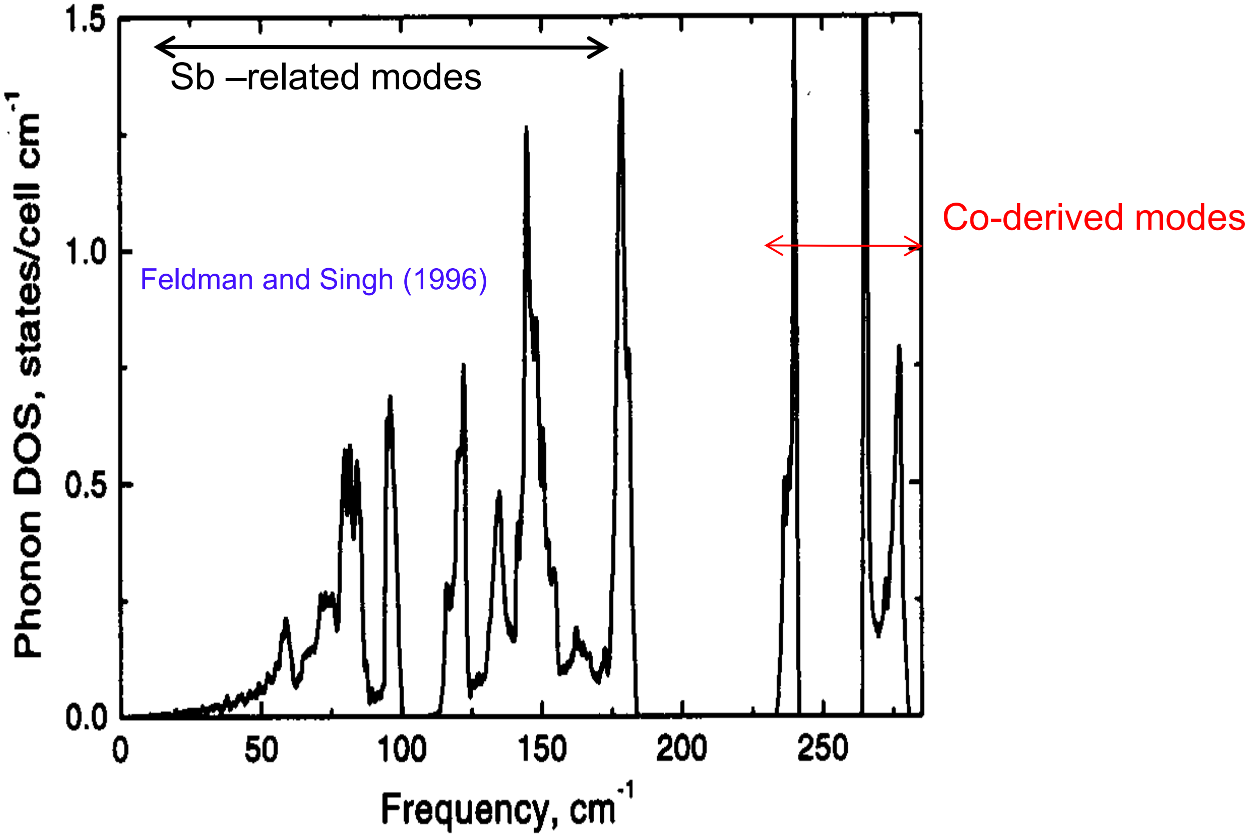

Heat in $CoSb_3$ is carried by Sb modes!

To lower thermal conductivity, must mess up the Sb ring structure!

Disorder on pnicogen rings

How can we do it?

Doping is the easiest way.

For n-type skutterudites, one uses elements such as Te to form $CoSb_{3-x}Te_x$. Each Te (valency = 6) at the site of Sb (valency = 5) brings in 1 electron.

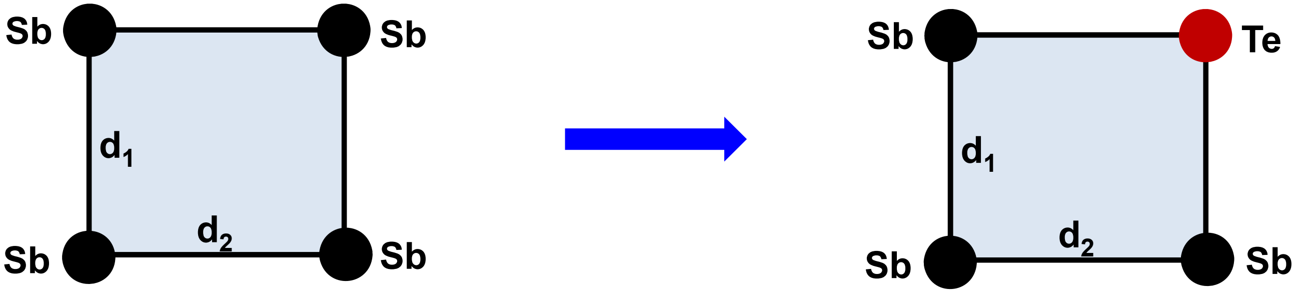

Skutterudite gets saturated with negative charge → solubility of Te limited to x~0.15.

Thermal conductivity is reduced but a **large Coulomb potential** strongly scatters charge carriers and lowers their mobility.

No good!

Disorder on pnicogen rings

How about double-doping with compensating charges?

Liu et al., (2008), Su et al. (2011, 2012)

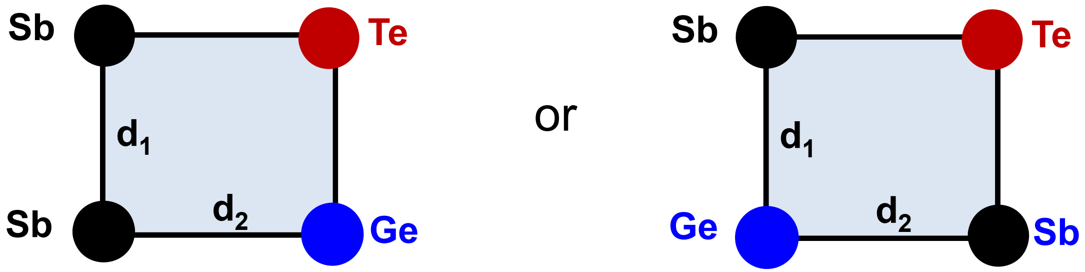

$CoSb_{3-m-n}Ge_mTe_n$

Si		S
Ge	Sb	Se
Sn		Te

- Te solubility increased to x = 0.2
- Ge partly charge compensates

ZT reaches 1.1 at 825K!

This is a binary skutterudite!

Disorder on pnicogen rings

Moreover, a nanostructure develops in the matrix

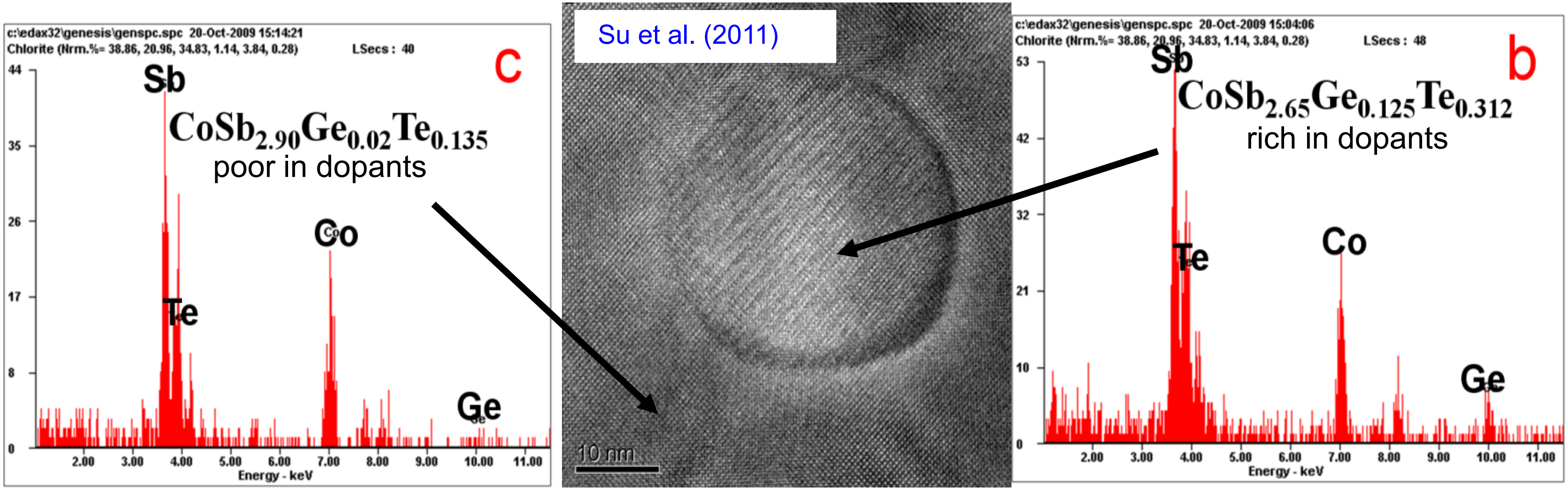

Su et al. (2011)

$CoSb_{2.90}Ge_{0.02}Te_{0.135}$ poor in dopants

$CoSb_{2.65}Ge_{0.125}Te_{0.312}$ rich in dopants

We believe the nanostructure has similar origin as in the LAST materials.

High ZT's achieved due to strong point-defect scattering and perhaps also a contribution from phonons scattering on the nanodots.

Disorder on pnicogen rings

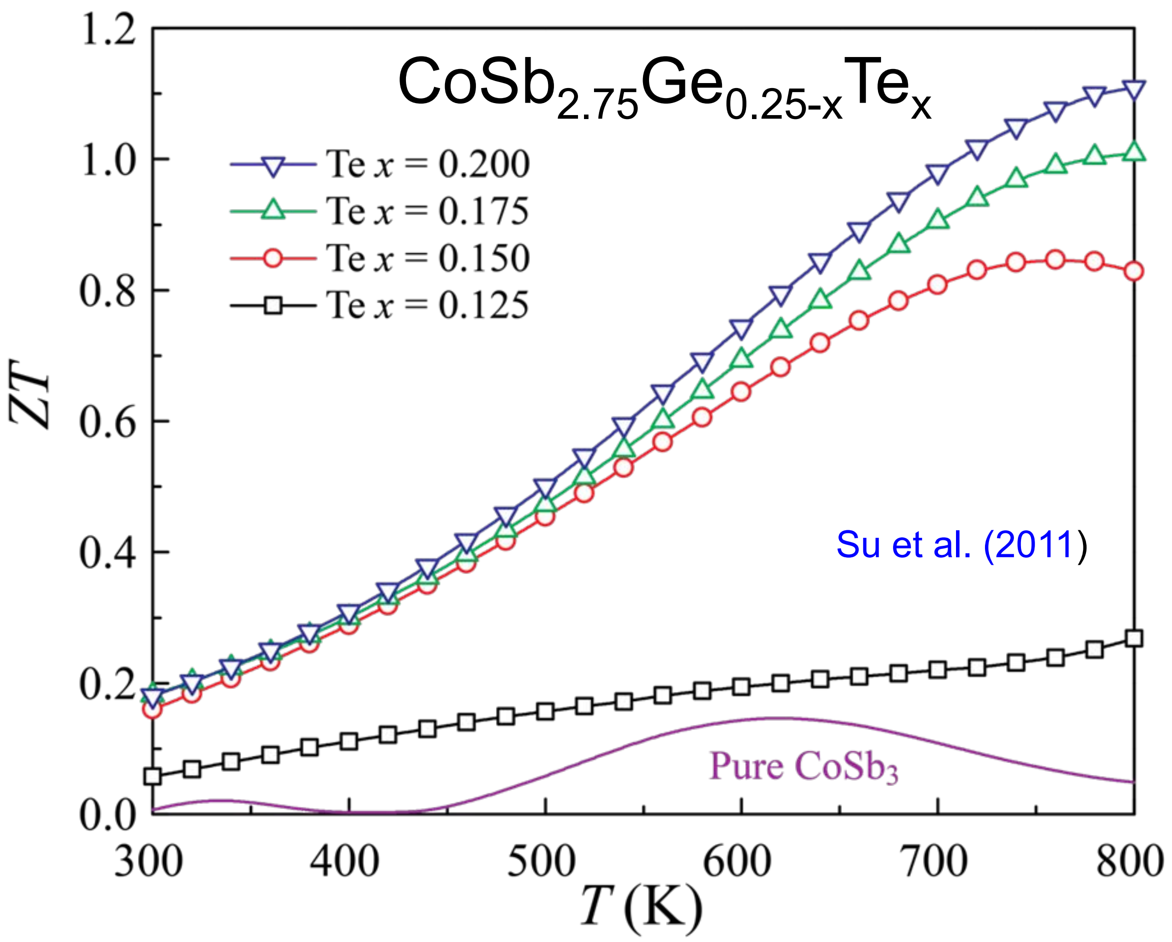

Values of ZT = 1.1 are comparable to the best <u>single-filled</u> n-type skutterudites!

Disorder on pnicogen rings

Why is ZT so high?

Are there particular ring configurations that maximize ZT?

To identify low energy configurations of pnicogen rings: used **DFT** guided by **cluster expansion**

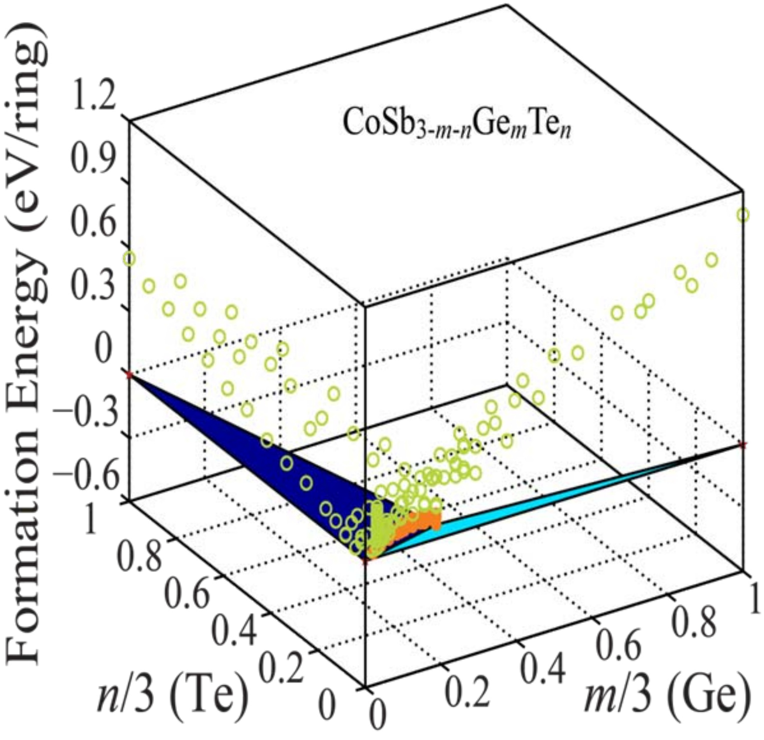

Vienna *ab initio* Simulation Package within generalized gradient approximation (GGA) for exchange and correlation, and using the projector augmented wave (PAW) method.

Explored some 340 configurations of Ge, Te, and Sb over the Sb sublattice.

"Wing" shape hull ⇒ ternary solid solutions unstable.

Only two globally stable forms of skutterudites: $CoSb_3$ and $CoGe_{1.5}Te_{1.5}$

Tendency to phase separate is minimized along the charge-compensated $CoSb_{3(1-x)}Ge_{1.5x}Te_{1.5x}$ tie-line.

Configurations with the lowest energy along the charge-compensated tie-line all contain rings with **counter-diagonal Ge_2Te_2**.

Disorder on pnicogen rings

DFT Formation Energies

High energy structure with a single element dopant

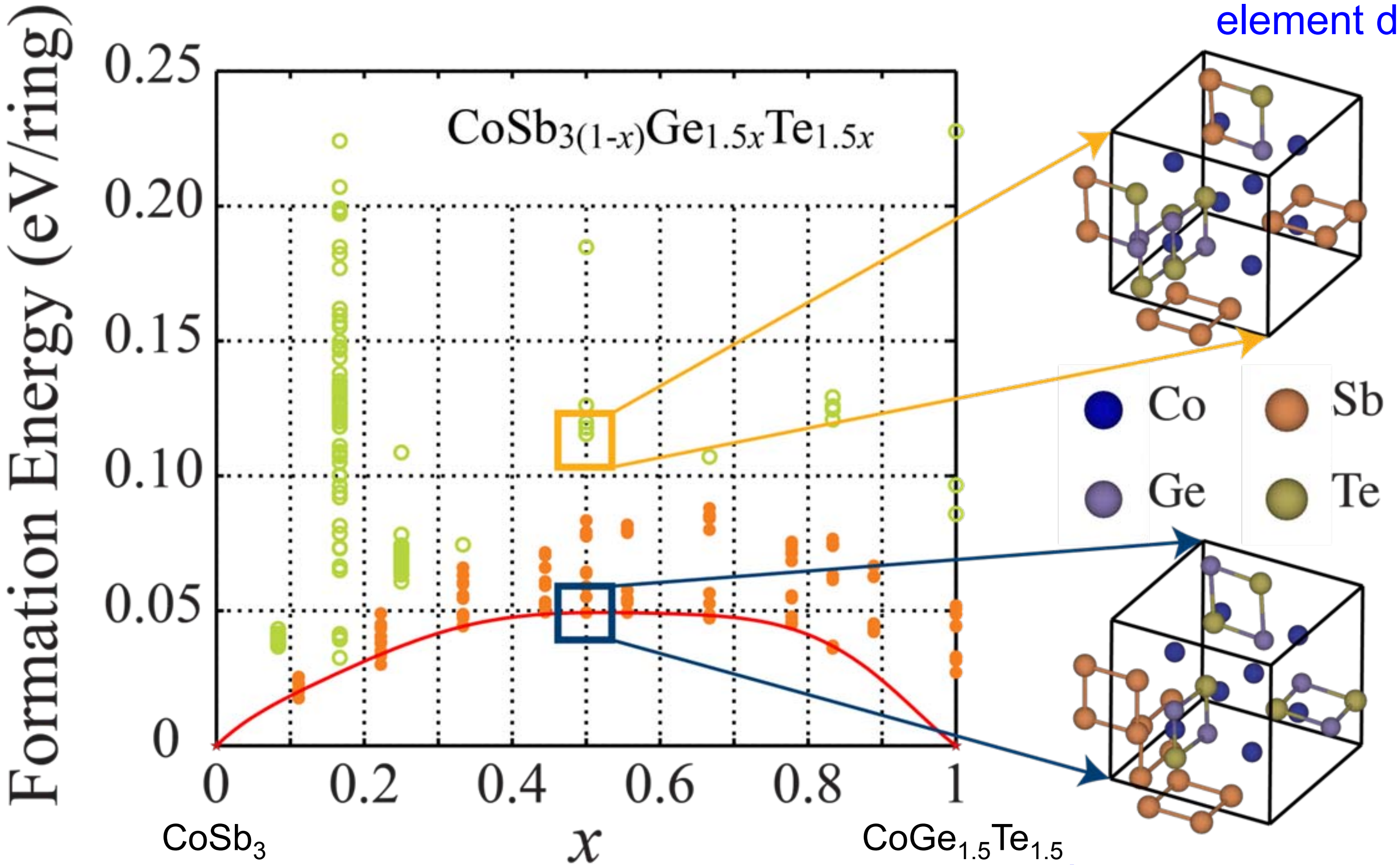

Low energy structure with counter-diagonal Ge_2Te_2 rings at x = 0.5

Red line: the fifth-order Redlich-Kister polynomial fit to the lower bound of formation energies used to model finite-T phase stability.

Disorder on pnicogen rings

Crystal structure with energetically favorable ring configurations at x = 0.5 ($CoSb_{1.5}Ge_{0.75}Te_{0.75}$)

The structure mixes Sb_4 rings with counter-diagonal Ge_2Te_2 rings.

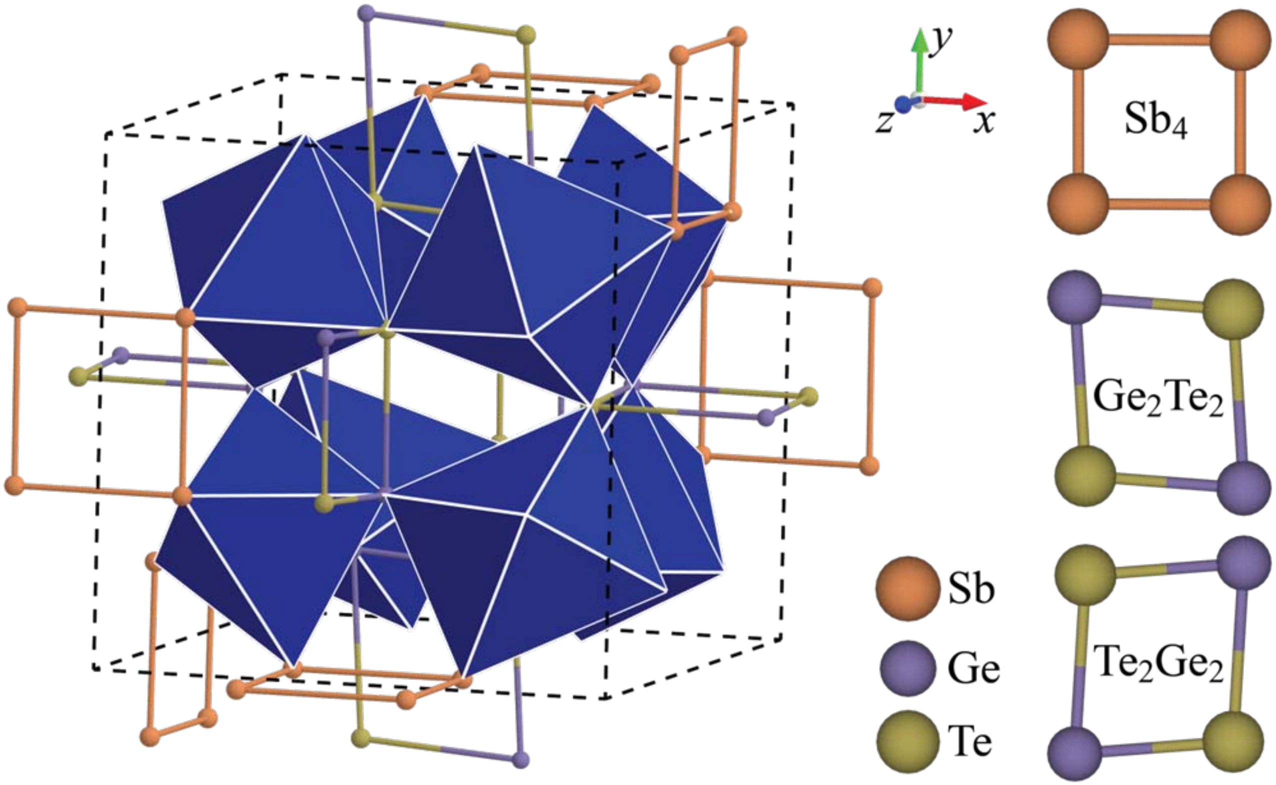

Counter Diagonal
Ge_2Te_2 Rings
Short-range Order

Disorder on pnicogen rings

Free Energy Model

Calculated with an assumption that the $CoSb_{3(1-x)}Ge_{1.5x}Te_{1.5x}$ structure can be approximated by a pseudo-binary substitutional alloy $Co_{4/3}[Sb_4]_{(1-x)}[Ge_2Te_2]_x$ where x measures the fraction of Sb_4 rings substituted by the counter-diagonal Ge_2Te_2 rings.

Enthalpy per ring Entropy per ring

Gibbs Free Energy per ring:

$$g(x) = h(x) - Ts(x)$$

$$h(x) = x(1-x)\sum_{n=0}^{5} L_n (1-2x)^n$$

5th order Redlich-Kister polynomial to the lower bound of DFT formation energy at 0K

$$s(x) = \frac{S}{N} = \frac{1}{N} k_B \ln\left\{\frac{N!}{(Nx)![N(1-x)]!} \cdot 2^{Nx}\right\} \approx -k_B \left[x \ln\left(x/2\right) + (1-x)\ln(1-x)\right]$$

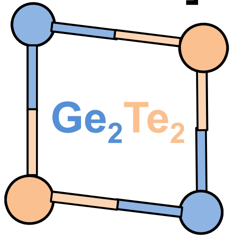

Entropy calculated for an ideal situation of non-interacting Sb_4 and Ge_2Te_2 rings, accounting for two degenerate orientations of the counter-diagonal Ge_2Te_2 rings.

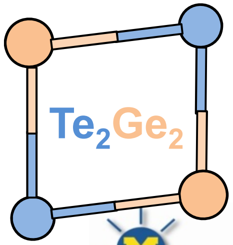

$$g(x) = x(1-x)\sum_{n=0}^{5} L_n (1-2x)^n + k_B T\left[x \ln\left(\frac{x}{2}\right) + (1-x)\ln(1-x)\right]$$

Minimization of the total free energy above, allowing for the possibility of two-phase coexistence, yields the temperature-composition phase diagram.

Disorder on pnicogen rings

Phase Diagram

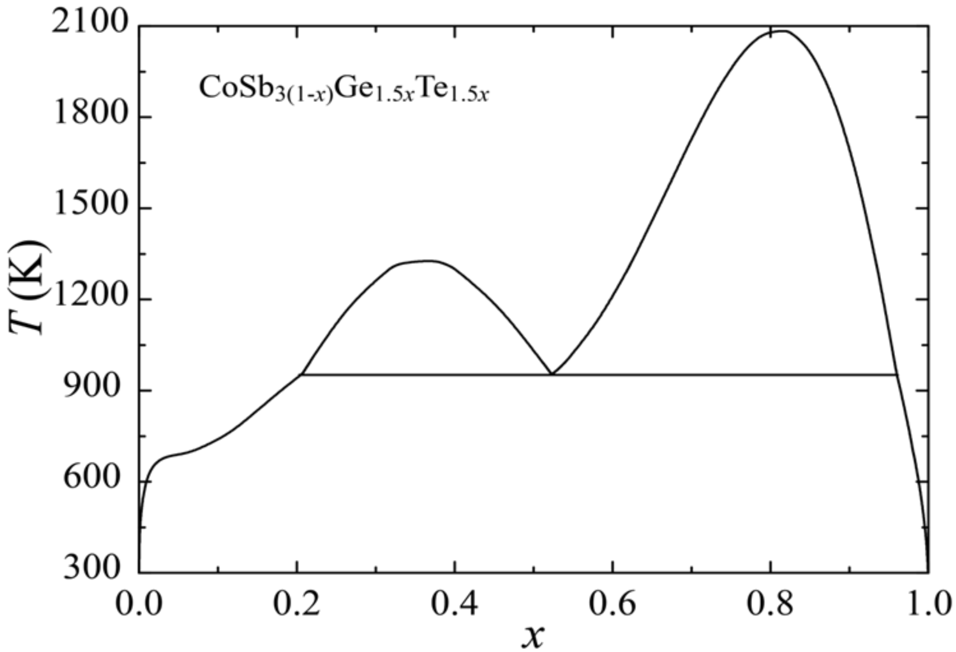

Miscibility gap develops below 600K between $CoSb_3$ and $CoGe_{1.5}Te_{1.5}$ (α- and β-phases)

Any intermediate composition results in a coexistence of the α- and β-phases in equilib. The diagram describes an **incoherent** two-phase equilibrium.

Two-phase coexistence can also occur **coherently**.

To be coherent, crystal planes across the interface must be continuous, i.e., the phase with the larger lattice parameter must be a bit compressed and the phase with the smaller lattice parameter stretched, resulting in strain energy penalty. In general, the strain energy due to coherent two-phase coexistence depends on the microstructure.

Disorder on pnicogen rings

Coherency Strain

One possible microstructure are alternating layers of phase α and phase β.

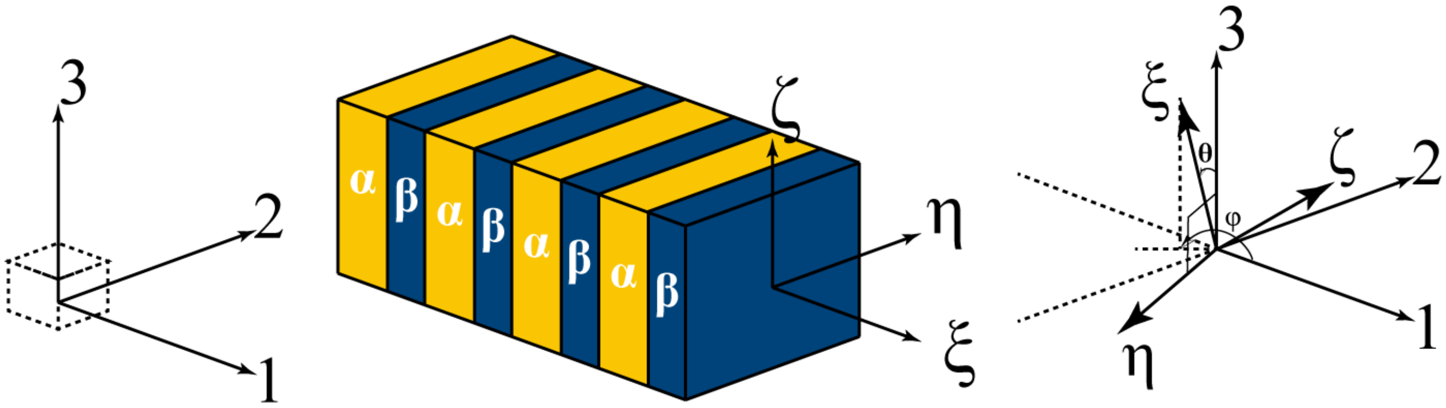

With further simplifying assumptions (e.g., elastic moduli independent of concentration, the lattice parameter obeying the Vegard's law), the analysis of coherent two-phase equilibrium becomes straightforward and reduces to the application of a common tangent construction of strain-modified homogeneous free energy.

Disorder on pnicogen rings

Phase Diagram

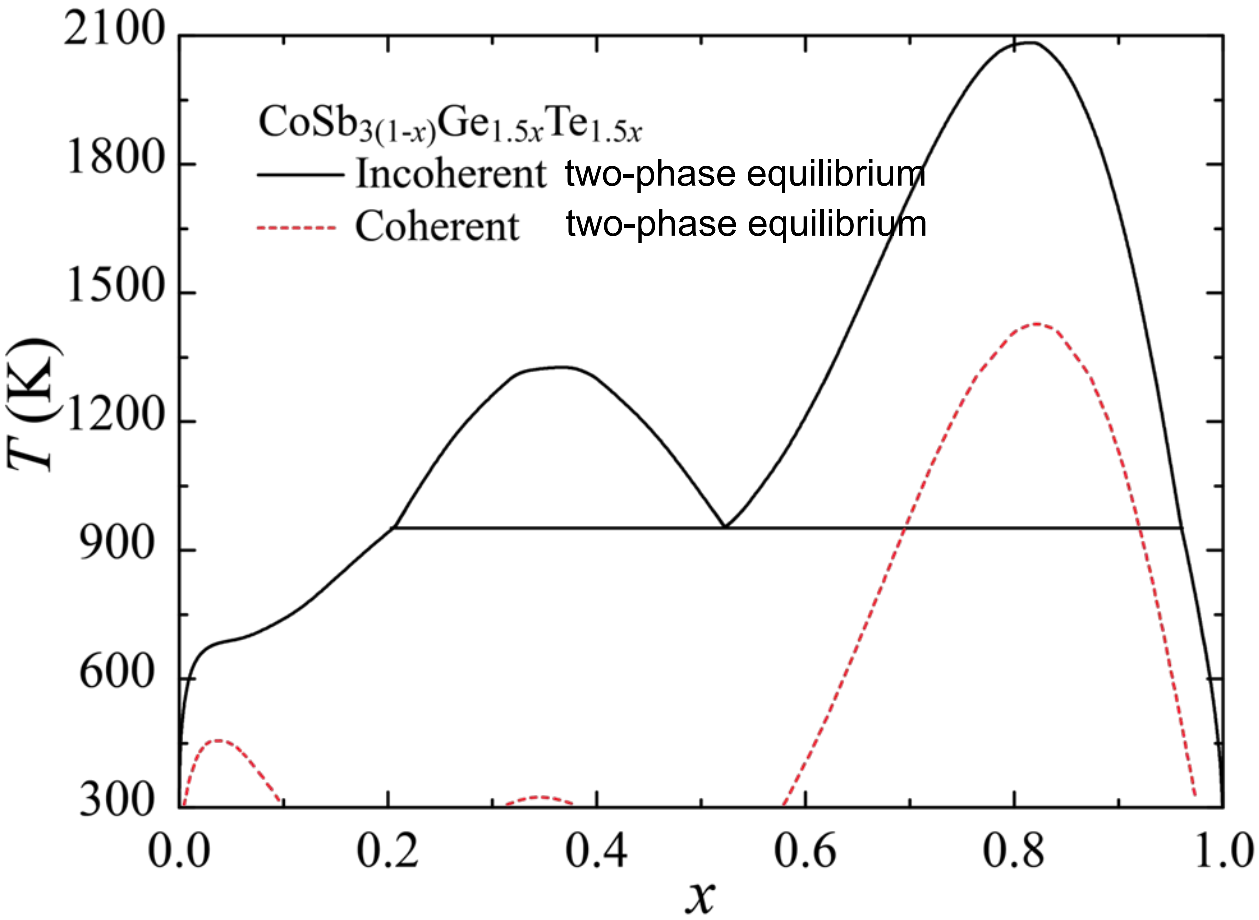

Miscibility gap dramatically suppressed by the strain energy penalty due to coherency.

Large **solid solution domain** becomes available and accessible by experiment!

Disorder on pnicogen rings

Coherency strains make charge-balanced $CoSb_{3(1-x)}Ge_{1.5x}Te_{1.5x}$ accessible.
Calculations predict pronounced short-range order of Ge and Te.

Will it work?

Prepared charge-balanced $CoSb_{3(1-x)}Ge_{1.5x}Te_{1.5x}$ with x = 0, 0.17, 0.33, 0.50, and 1 by melt quenching followed by SPS at 900 K, 40 MPa for 5 min.

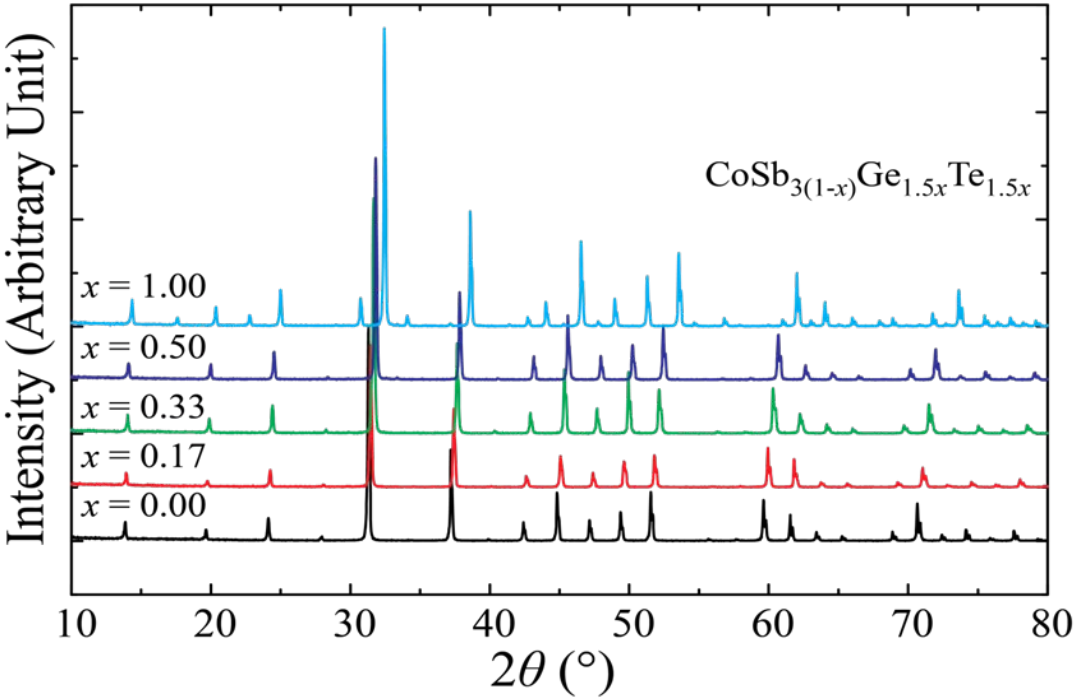

XRD confirms the existence of a solid solution for each composition.
TEM study did not reveal any nanodots. Perhaps these are observed only when Ge/Te is imbalanced as was the case of our previous study (Chem. Mater. 23, 2948 (2011)).

Disorder on pnicogen rings

Vegard's Law

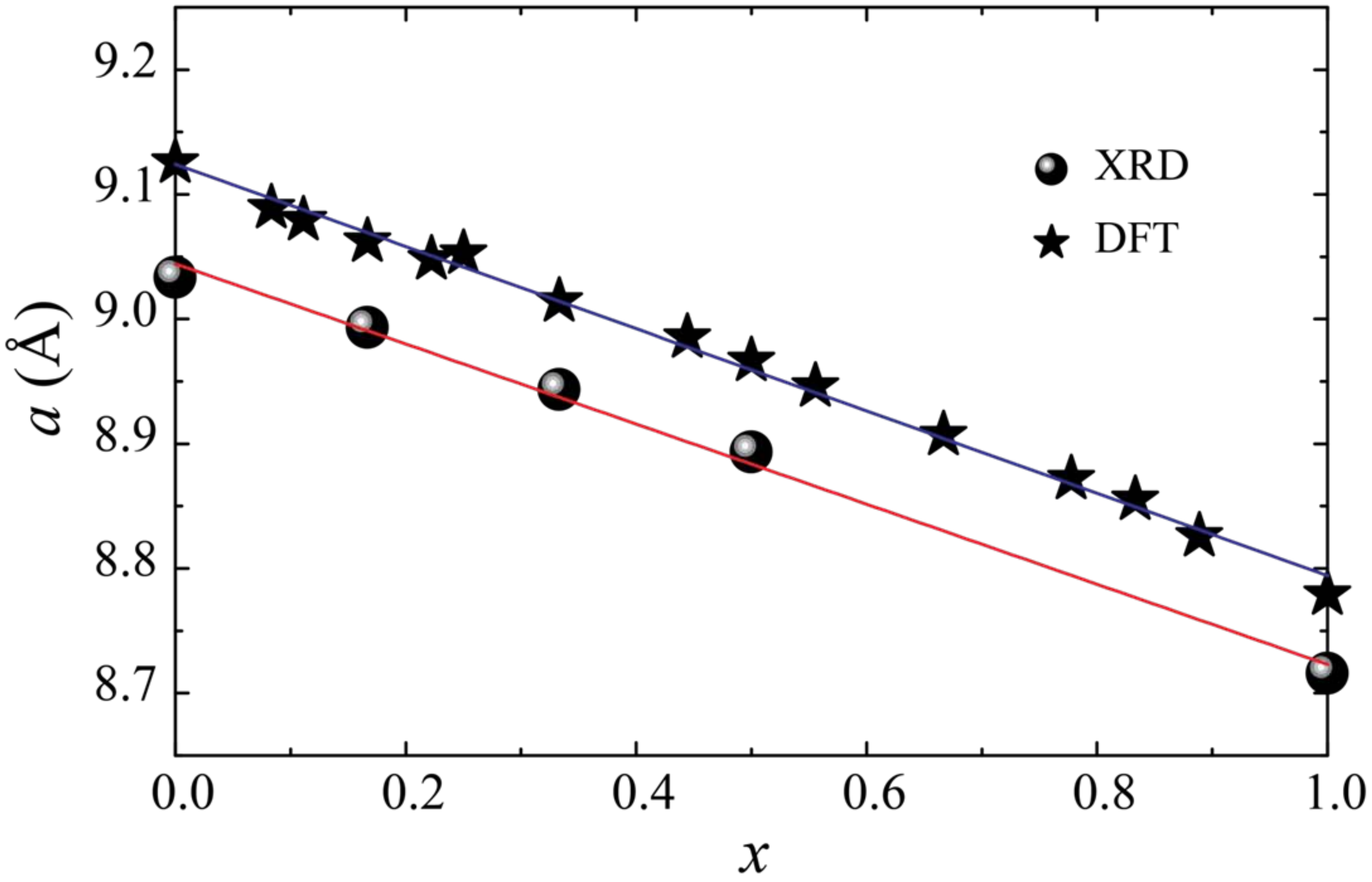

Disorder on pnicogen rings

Lattice dynamics calculations of charge-balanced skutterudite alloys

VASP and PHONON codes used for *ab in*itio phonon calculations
Total energy and Hellmann-Feynman (H-F) forces from fully relaxed configurations,
Initial ionic forces taken as less than 10^{-5} eV/Å,
Ionic displacements of 0.03Å samples for each atom along x-,y-, z-directions
Interatomic force constant tensors fit to the calculated H-F forces
Diagonalizing dynamical matrix → phonon dispersion → density of states
↘ atomic displacement tensor
Trace of diagonalized atomic displacement tensor ≡ atomic displacement parameter (ADP)

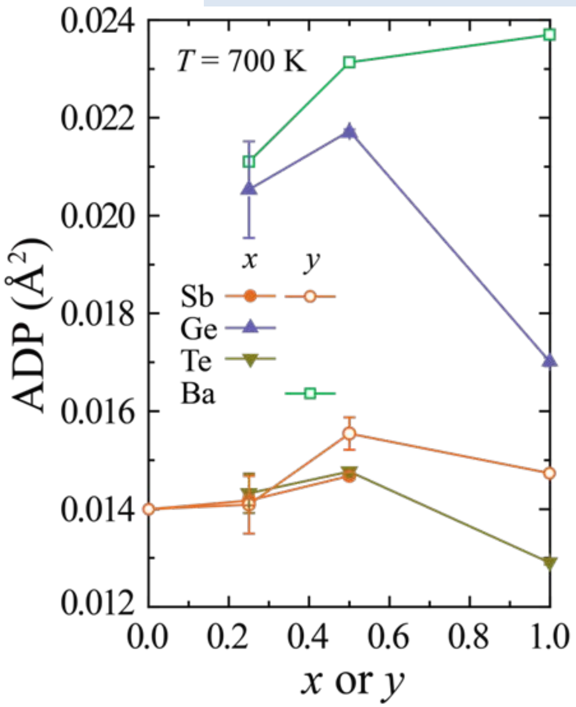

y is Ba content in $Ba_yCo_4Sb_{12}$

Due to strong covalent bonds of the rings, ADPs not expected to be large.

A major surprise

ADP of Ge is large in x =0.25, 0.5 and comparable to Ba!

Could Ge play the role of a rattler?

(a) Rattlers lower frequencies via local bond softening
(b) Give rise to independent low-frequency modes

Disorder on pnicogen rings

Displacements of Ge

Atomic configurations on a ring and octahedron for x=0.5 ($CoSb_{1.5}Ge_{0.75}Te_{0.75}$)

Red arrow → large displacements of each Ge atom.

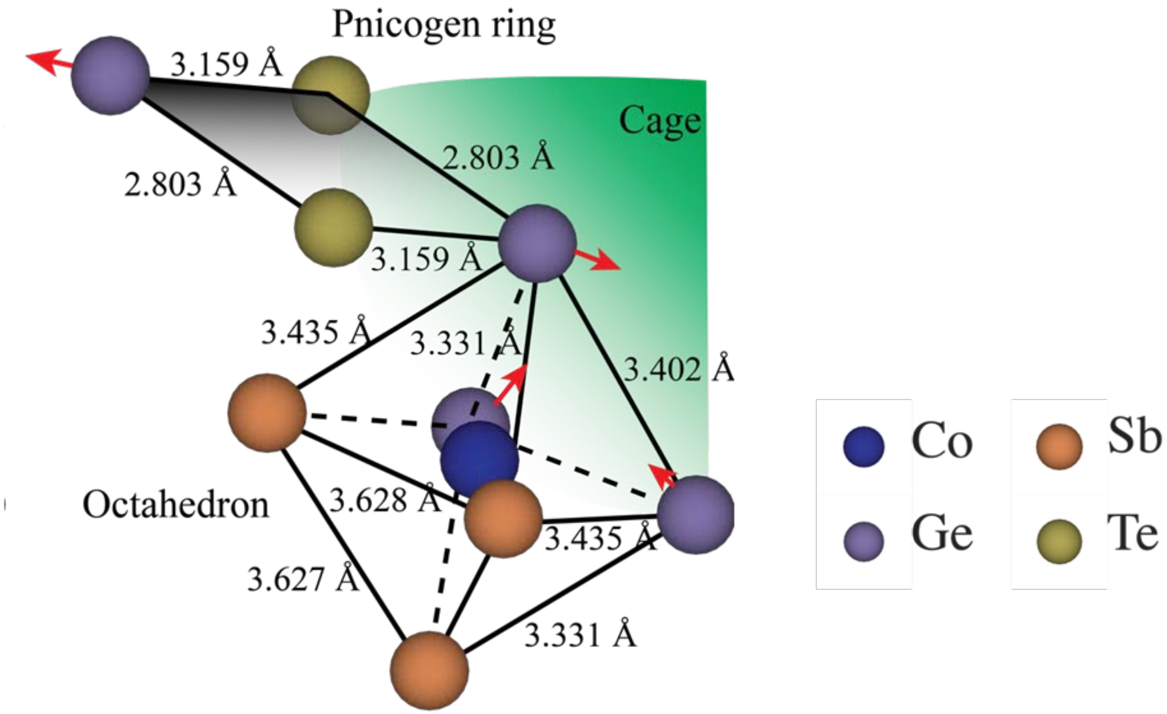

Ge distortions responsible for large ADPs are **along the diagonal** of CD Ge_2Te_2 rings!
(a breathing mode of the cage)

Disorder on pnicogen rings

Projected Phonon Dispersion

Phonon modes from either Ba fillers or Ge dopants show very little dispersion

↓

Both are local deformation modes with low group velocity.

However, in spite of similarity to Ba filler modes, collective modes of Ge deform **different segments** of the structure and have **different frequencies**!

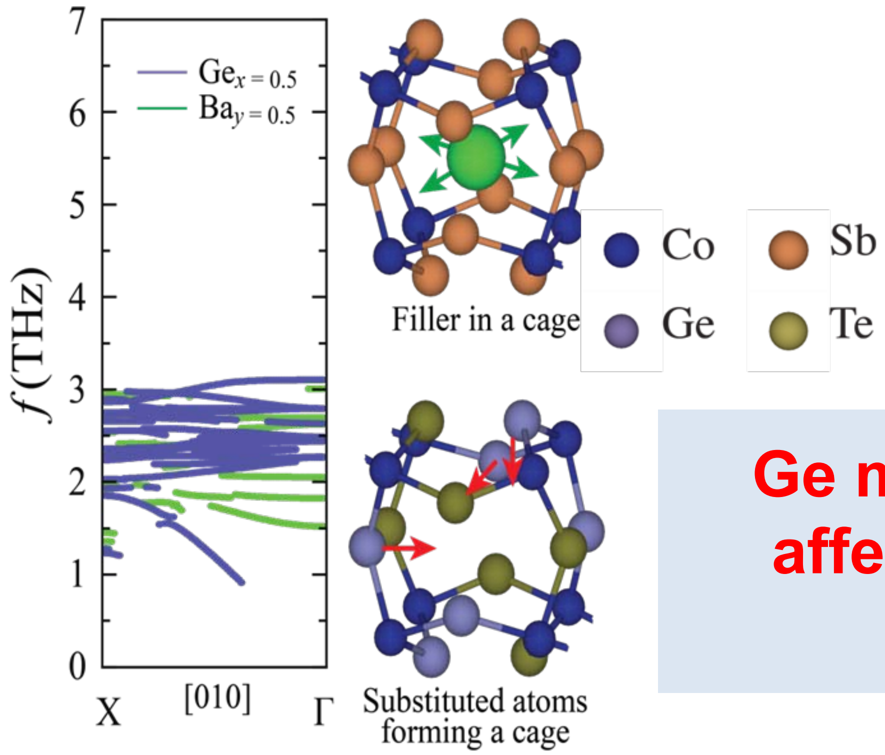

	Ge	Ba
Γ	2.27 THz	1.52 THz
X	1.24 THz	1.45 THz

Ge modes and Ba rattler modes affect different portions of the phonon spectrum!

Thermal conductivity

$$\kappa = D \times C_p \times d$$

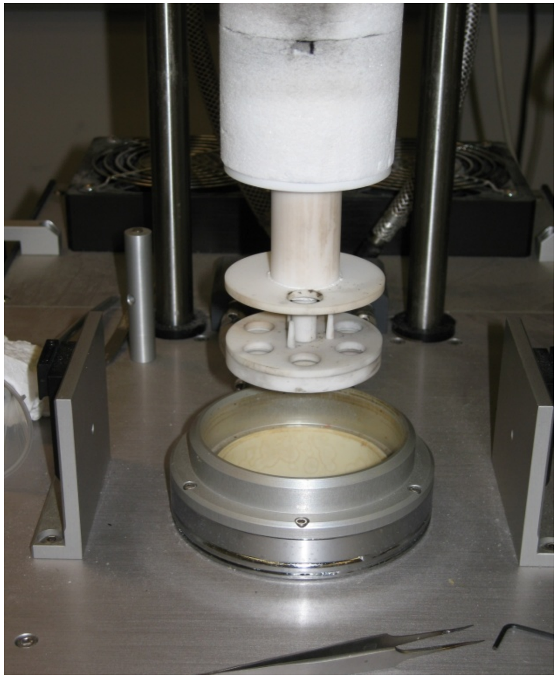

FlashLine 5000 apparatus from Anter Corp.
Temperature range 300K – 1800K
Six sample carousel
Fully automated operation

DSC 404C Pegasus® (Netzsch)
Temperature range 300K-1800K
Fully automated operation

Seebeck coefficient

University of Michigan

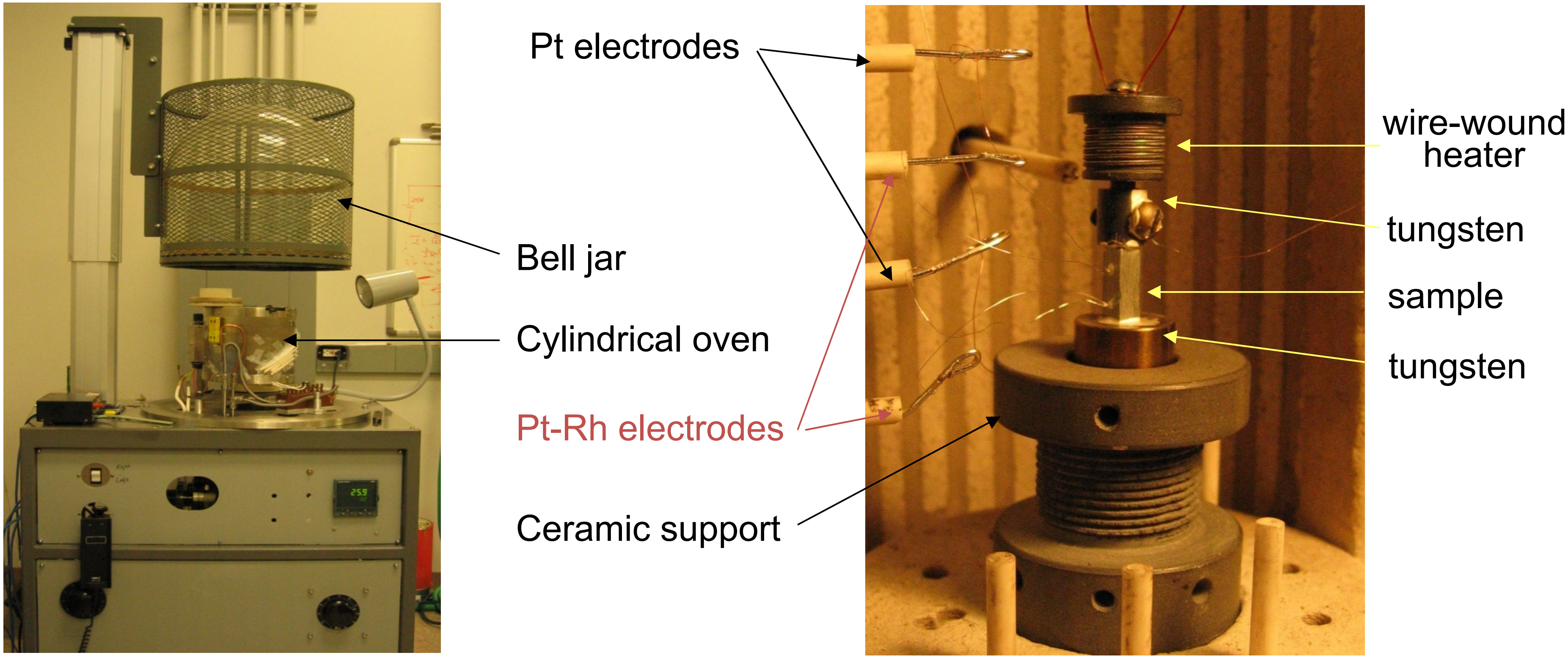

Fully computerized system operating to 1300K under vacuum or Ar gas.

Pt vs. Pt/Rh thermocouples, Pt legs used for Seebeck probes.

Probes attached with Ag paste (T<800K) or inserted in tiny holes with graphite paste.

Tungsten electrodes for current injection.

Disorder on pnicogen rings

Thermal conductivity – experimental data

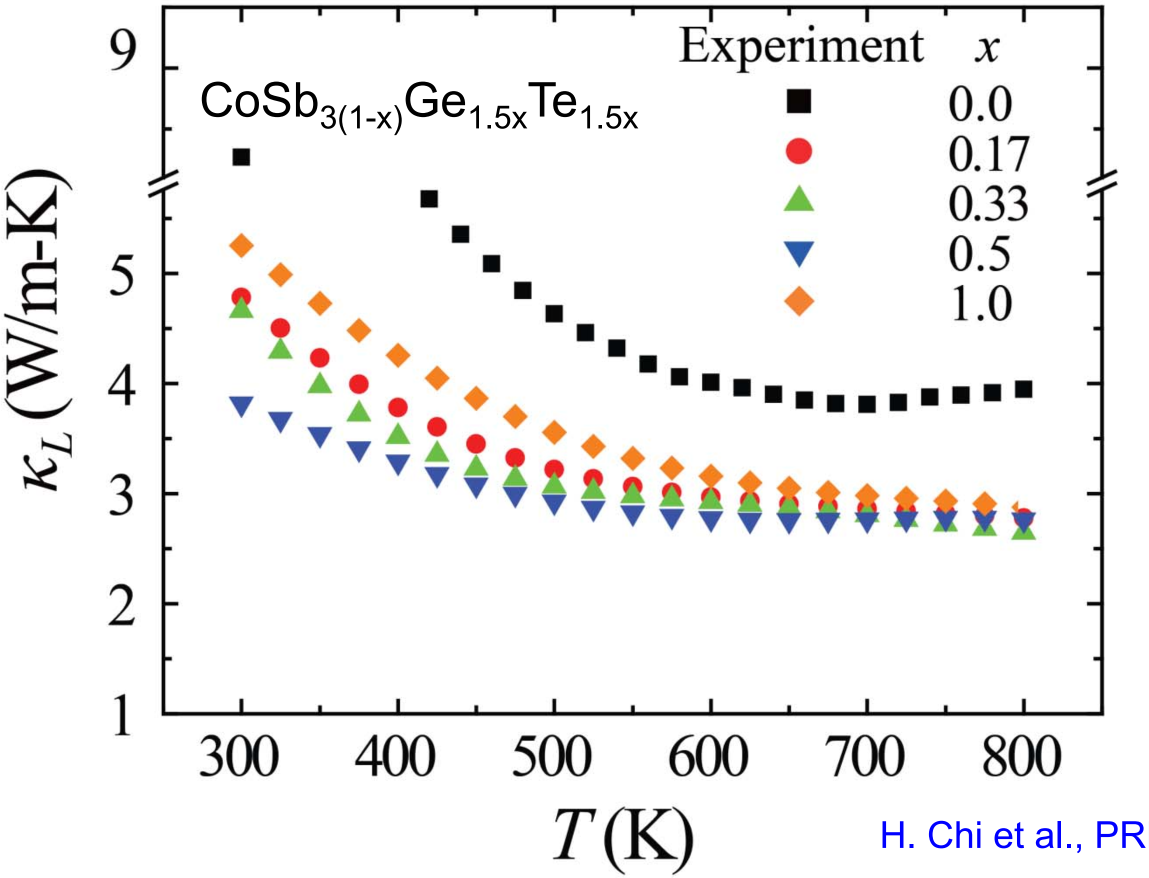

H. Chi et al., PRB **86**, 195209 (2012)

A strong decrease in thermal conductivity with increasing x.

Minimum in κ_L near x = 0.5 coincides with the calculated ADP maximum of Ge.

Disorder on pnicogen rings

Thermal conductivity – theoretical modeling

Starting with κ_L of $CoSb_3$ (x = 0) and $CoGe_{1.5}Te_{1.5}$ (x = 1), both dominated by phonon-phonon scattering, we add point-defect scattering for intermediate compositions (Matthiesen rule)

$$1/\kappa_L(x,T) = x/\kappa_L(0,T) + (1-x)/\kappa_L(1,T) + 1/\kappa_{L,d}$$

$\kappa_L(0,T)$ and $\kappa_L(1,T)$ obtained from the Slack relation

$$\kappa_L(T) = \frac{3.1\times10^4 \langle M\rangle \delta T_{D,\infty}^3}{T\langle\gamma_G^2\rangle N_c^{2/3}}$$

Point defect - limited lattice thermal conductivity given as

$$\kappa_{L,\mathrm{d}} = \frac{k_{\mathrm{B}}}{4\pi u_{p,g,A}(a_1 CT)^{1/2}}$$

The relaxation time for phonon-phonon scattering

$$CT = \frac{(6n)^{1/3} k_B}{2\pi^{4/3}\kappa_L(0)}$$

estimated from the experimental value $\kappa_L(0,300K) = 8.3$ W/m-K. *CT = 4.76×10^-16^ s.*

The Rayleigh point-defect scattering rate $a_1 = \frac{V_c\Gamma_s}{4\pi u^3_{p.g,A}}$, where $\Gamma_s = x(1-x)\left[\left(\frac{\Delta M}{M}\right)^2 + 3\gamma_G^3\left(\frac{\Delta R}{R}\right)^2\right]$

For the **hybrid case** (filler y=0.5 and various levels of substitution x) we write

$$\frac{1}{\kappa_{L,y=0.5}(x,T)} = \frac{x}{\kappa_{L,y=0.5}(0,T)} + \frac{(1-x)}{\kappa_{L,y=0.5}(1,T)} + \frac{1}{\kappa_{L,d}}$$

where $\kappa_{L,y=0.5}(0,T)$ was obtained by our previous classical MD results.

Disorder on pnicogen rings

Also used non-equilibrium *ab initio* molecular dynamics simulations (NEAIMD) to calculate the lattice thermal conductivity as the ratio of time averaged applied heat flux to the resulting temperature gradient, $\kappa_L = \frac{\langle q(t) \rangle}{\langle dT/dz \rangle}$

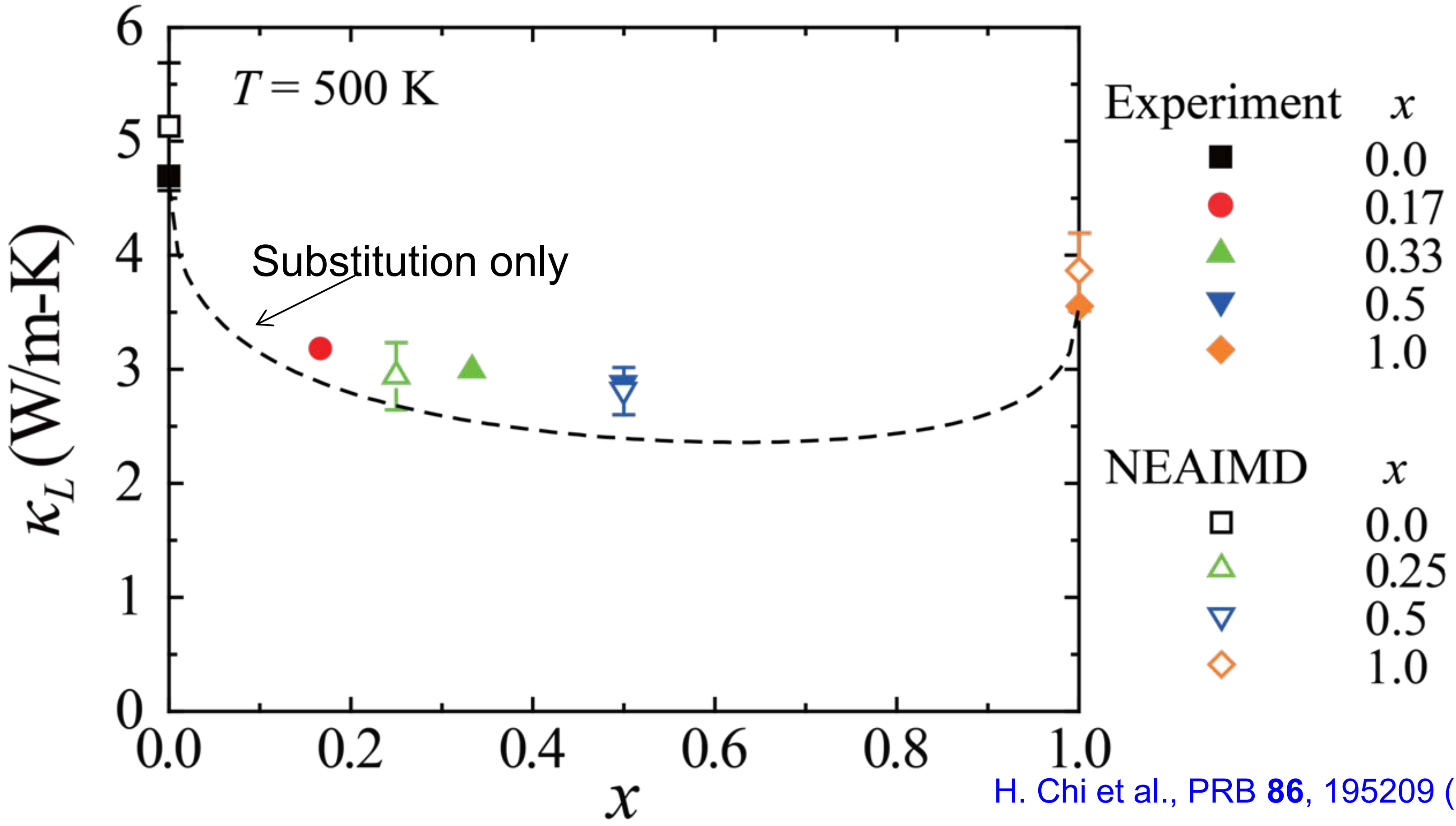

H. Chi et al., PRB **86**, 195209 (2012)

Excellent agreement with experimental data and with the point defect model.

Disorder on pnicogen rings

Phonon Conductivity Results

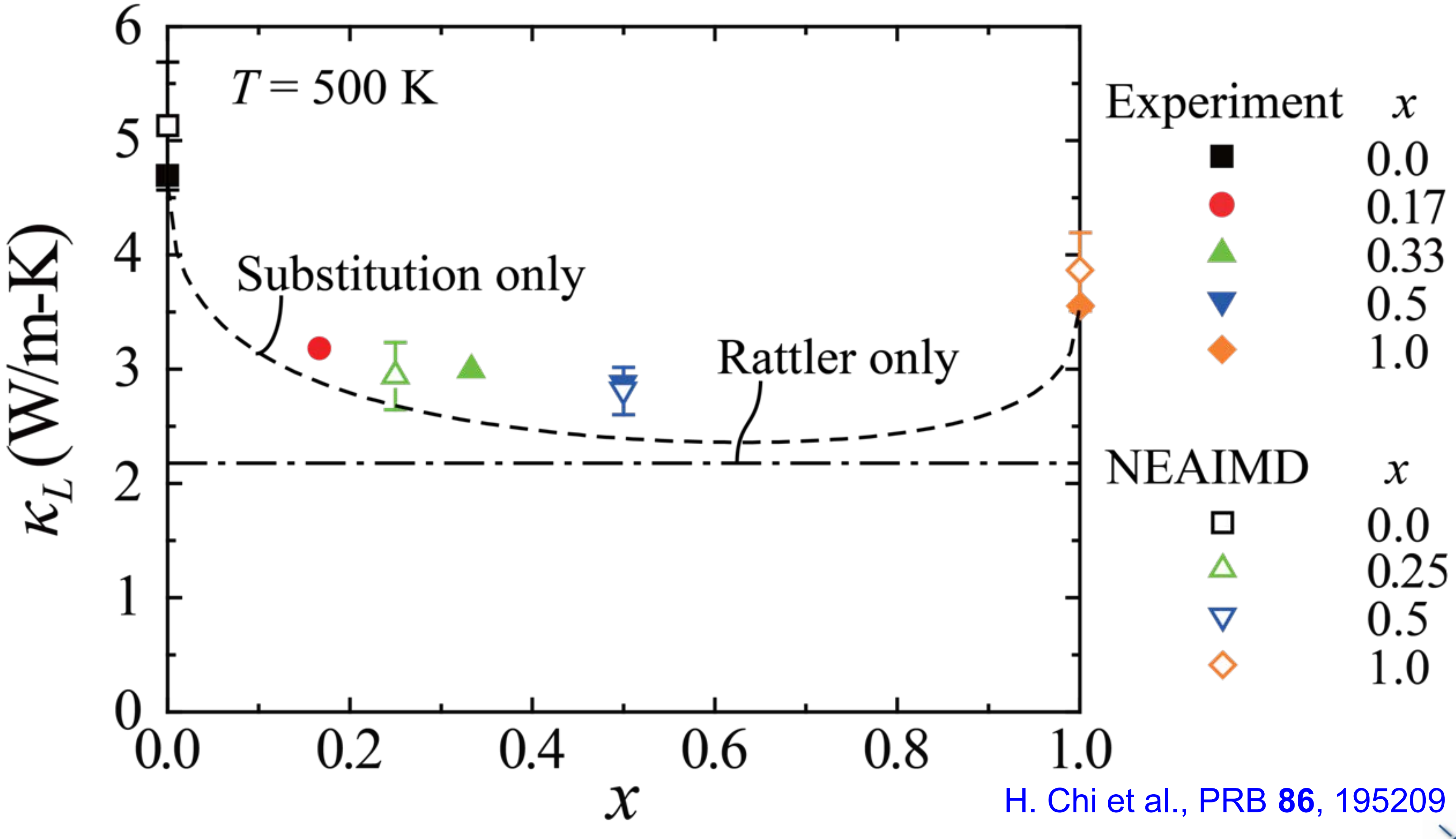

H. Chi et al., PRB **86**, 195209 (2012)

Disorder on pnicogen rings

Phonon Conductivity Results

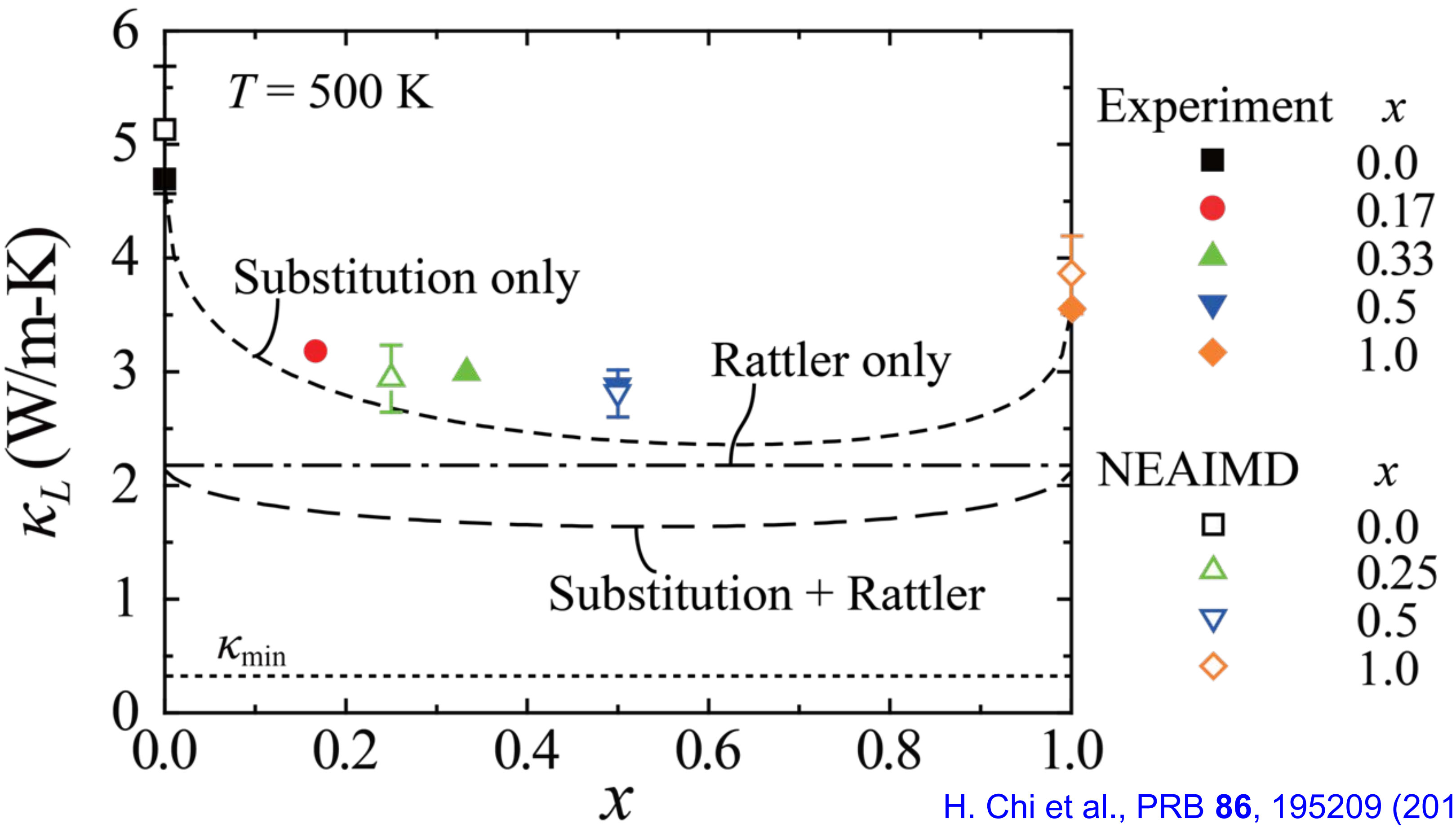

H. Chi et al., PRB **86**, 195209 (2012)

Forming skutterudites with ring substitutions as well as void filling → further 33% reduction in the thermal conductivity should result!

Future outlook/prospect

We expect a combination of filling and substitutional charge-balanced double-doping to act in a complementary manner in suppressing the lattice thermal conductivity.

Such combined strategy should lead to even lower thermal conductivity and higher ZT values of skutterudites than have been realized so far using either strategy in isolation.

Applications of thermoelectricity

Current:

- Medical cooling boxes, picnic boxes, small refrigerators.
- Spot cooling of electronic devices, especially radiation detectors.
- Climate control of car seats and the steering wheel (Amerigon).

- Small power generators for remote areas.
- Small - scale waste heat recovery.
- **POWER SOURCES FOR DEEP-SPACE MISSIONS.**

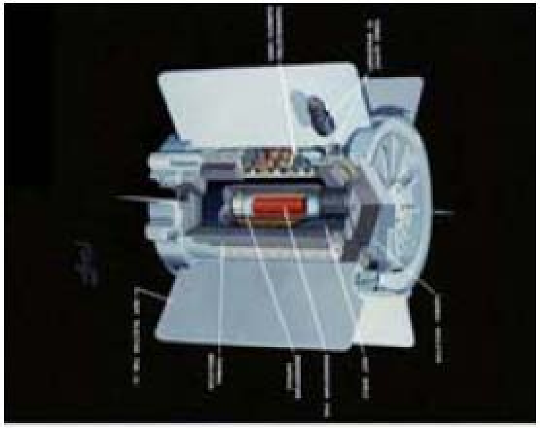

PIONEER 10 and 11

Beyond Mars, solar cells are useless.
Radioisotope thermoelectric generator (RTG)
Mostly plutonium oxide (half-life ~ 75 years).
Phenomenal success with all missions!

Applications of thermoelectricity

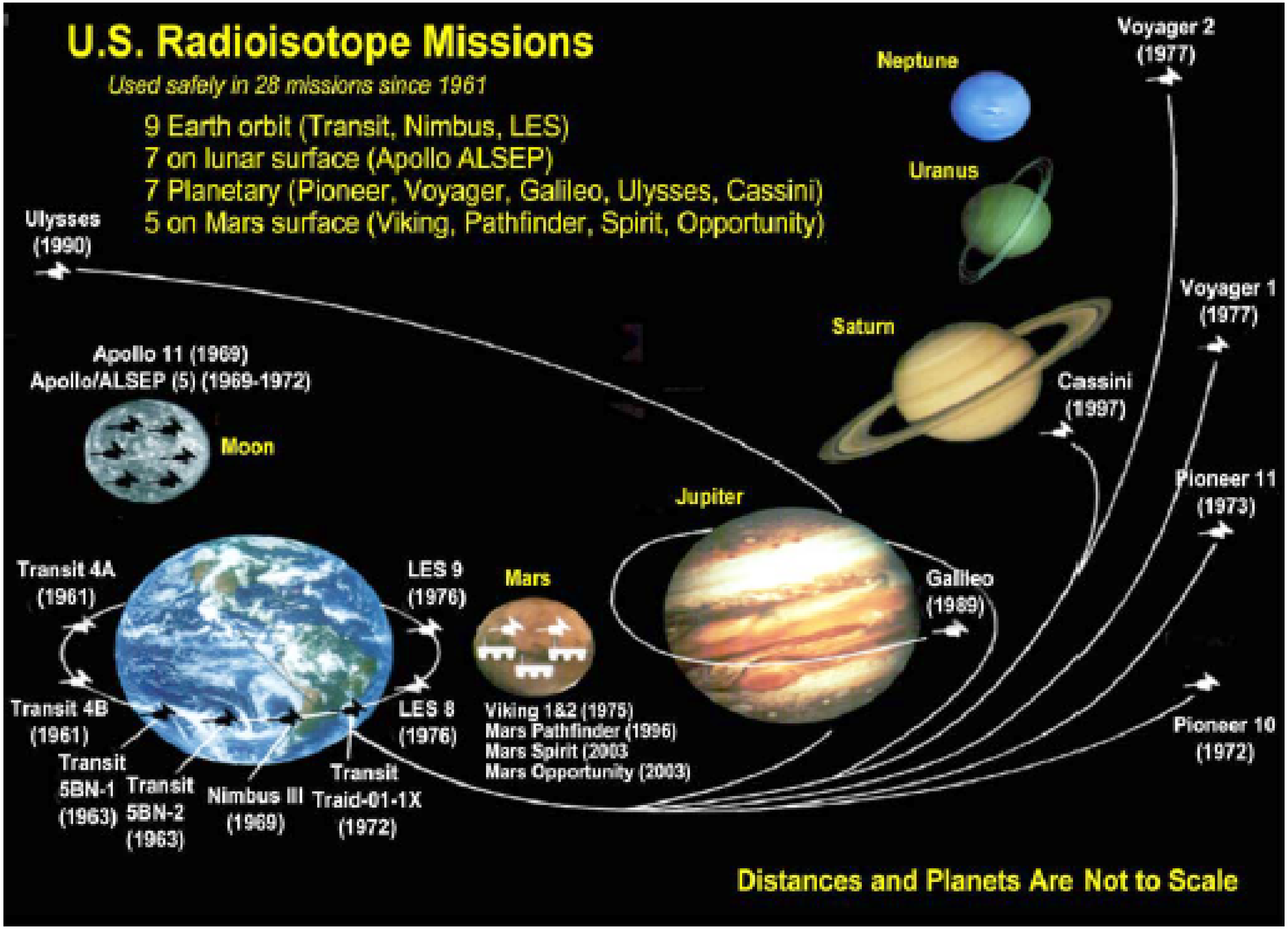

U.S. Radioisotope Missions

Used safely in 28 missions since 1961

9 Earth orbit (Transit, Nimbus, LES)
7 on lunar surface (Apollo ALSEP)
7 Planetary (Pioneer, Voyager, Galileo, Ulysses, Cassini)
5 on Mars surface (Viking, Pathfinder, Spirit, Opportunity)

Distances and Planets Are Not to Scale

Applications of thermoelectricity

Future:

- Large-scale refrigeration, heat management.
- Nuclear fuel-heated TE generators for the NASA’s Mars missions.
- Solar energy harvesting
- Large-scale waste heat recovery.

On average, 60% of energy becomes waste heat.

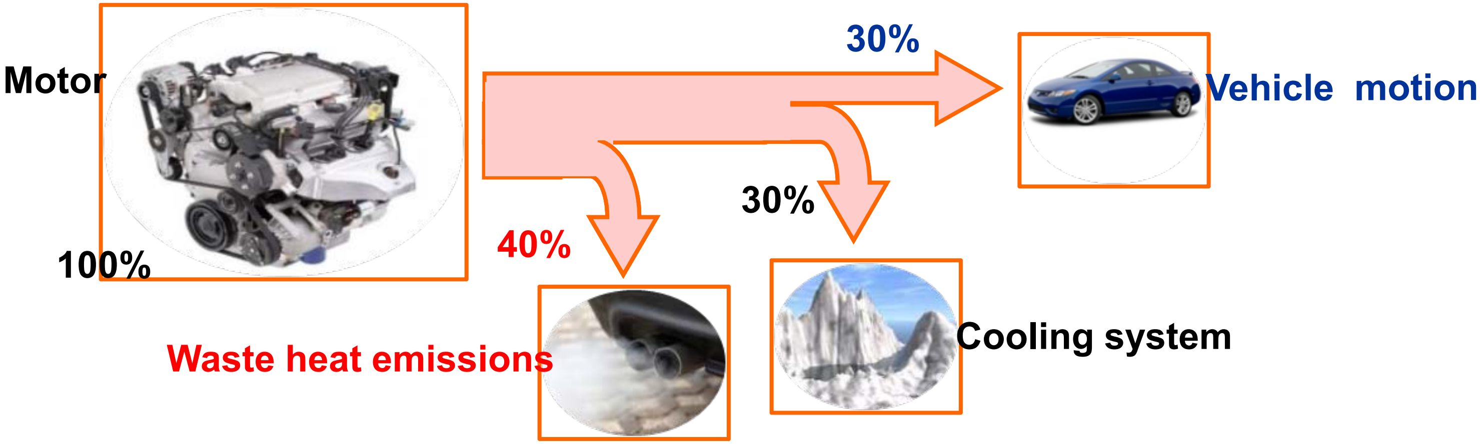

Aiming at just 10% capture and conversion to electrical energy

⇩

Huge impact on the overall energy utilization.

Waste Heat Recovery

Relationship between TE conversion efficiency η and

$$\eta = \frac{T_H - T_C}{T_H} \frac{\sqrt{1+ZT} - 1}{\sqrt{1+ZT} + \frac{T_C}{T_H}}$$

Carnot term

Material's property

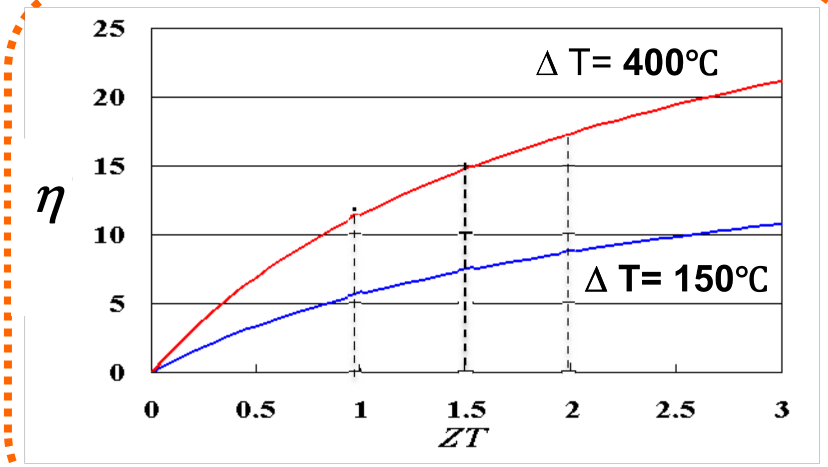

Relationship between η and *ZT* under a typical ΔT of exhaust pipe
(Cold side temperature equals to 90 °C)

	ZT=1.0	*ZT*=1.5	*ZT*=2.0
ΔT = 150 °C	**5.7%**	**7.4%**	**8.8%**
ΔT = 400 °C	**11.5%**	**14.8%**	**17.4%**

η_{max} reaches 15% when *ZT* = 1.5

Applications of thermoelectricity

TE Generators for Automotive Applications:

Two main sources of heat: **radiator** (100^{o}C – 115^{o}C)
exhaust system (300^{o}C<T<800^{o}C)

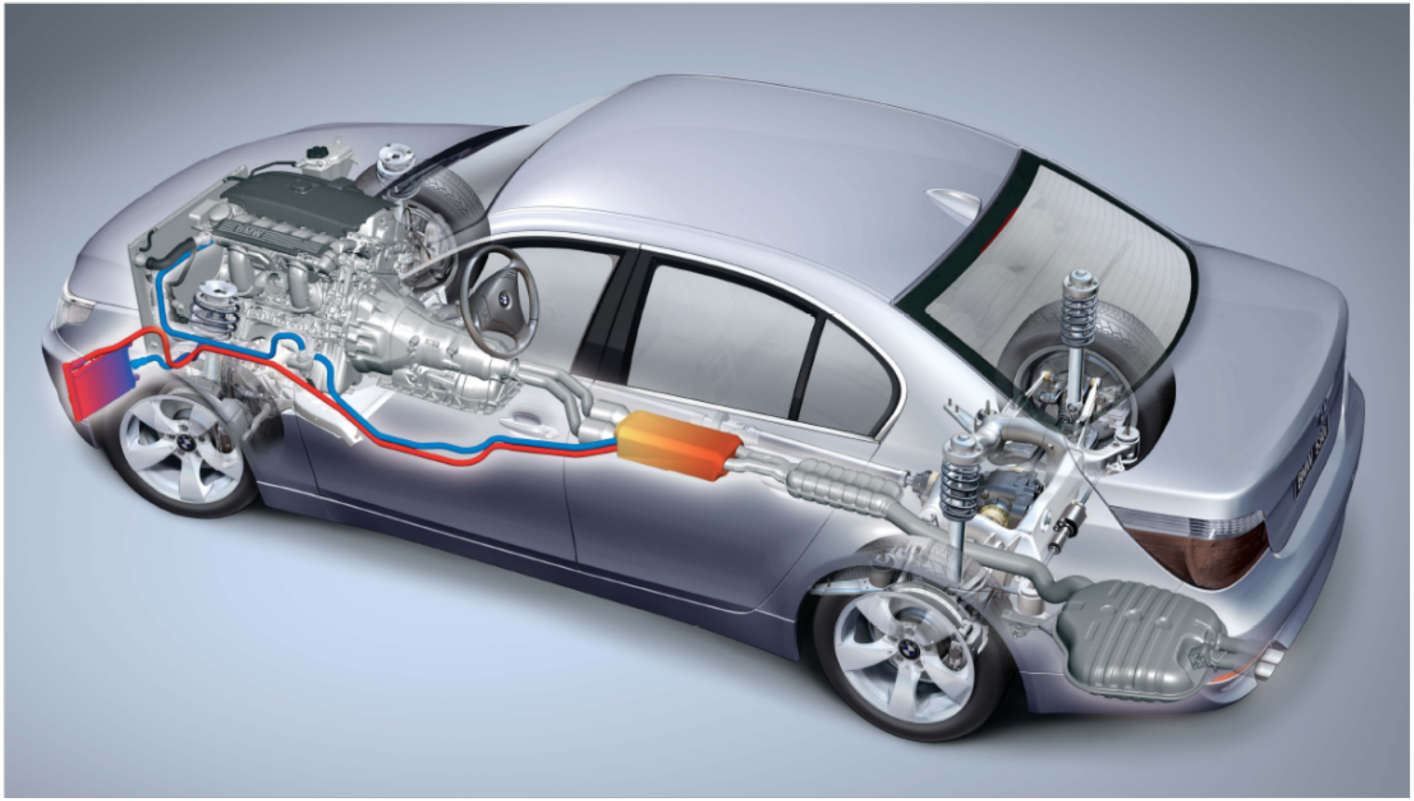

Applications of thermoelectricity

Plenty of heat available along the tail pipe

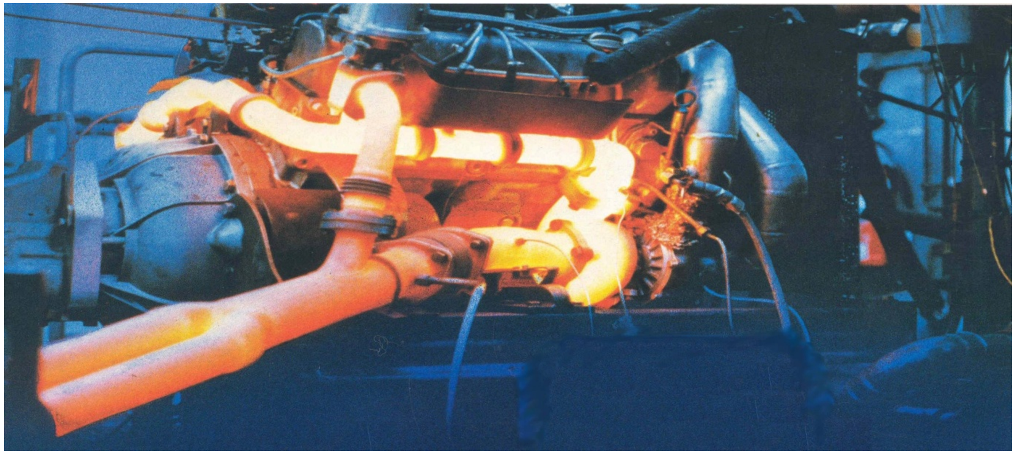

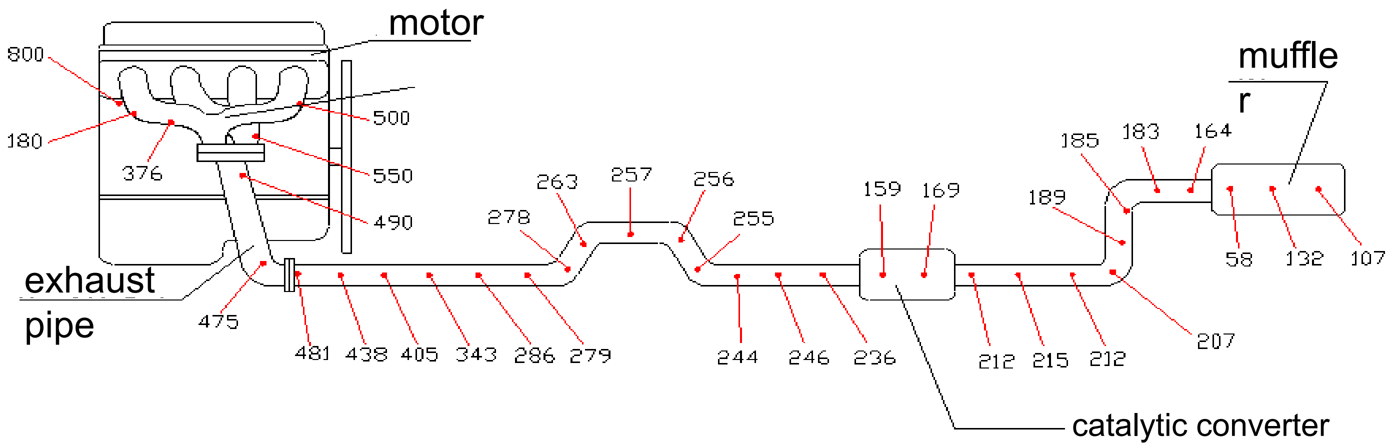

Aiming at just 10% capture and conversion to electrical energy

Huge impact on the overall energy utilization.

Applications of thermoelectricity

TE Generators for Automotive Applications:

Gen I – GM R&D (1996)

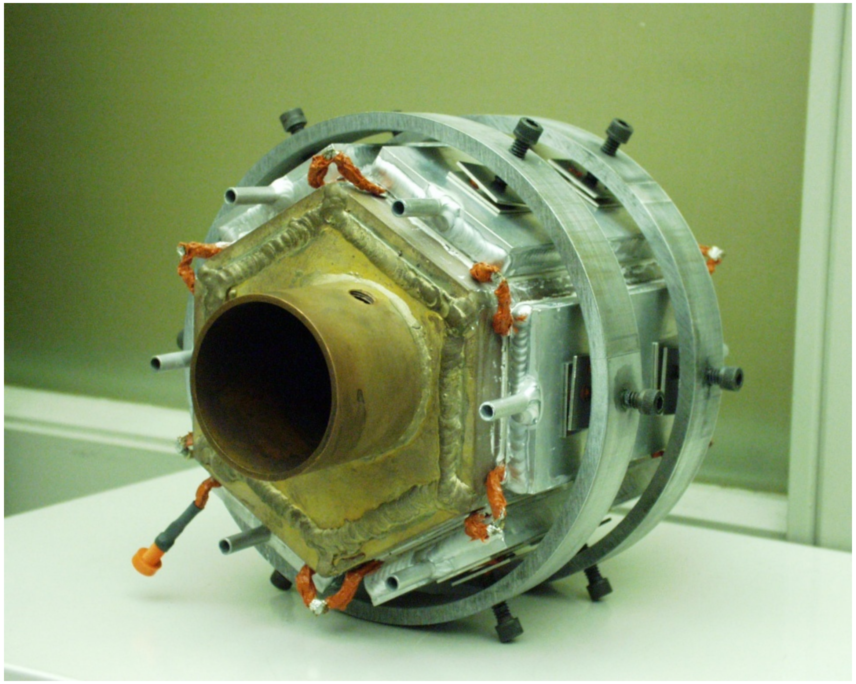

Delivers 109 Watts from the exhaust.

Gen II – GM R&D (2006)

Peak output of 290 Watts

Applications of thermoelectricity

Economic impact of the 10% solution:

- **100 million gallons of fuel savings per year**

GM scenario: 2 million cars & 2.8 million trucks
15,000 miles/vehicle/year
CAFE standards

- **1.5 million gallons of fuel savings by hybrids in 2010**

GM scenario: 50,000 hybrids (1% of GM annual fleet)

Applications of thermoelectricity

Impact of 10% solution on your pocket:

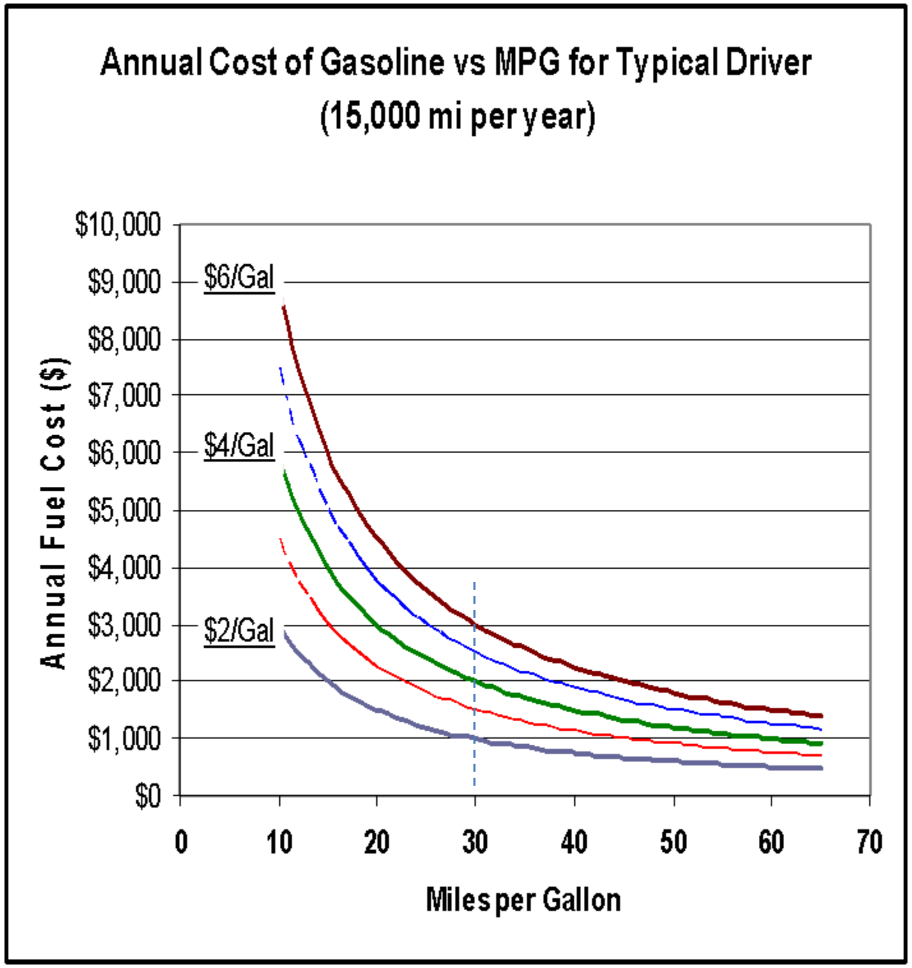

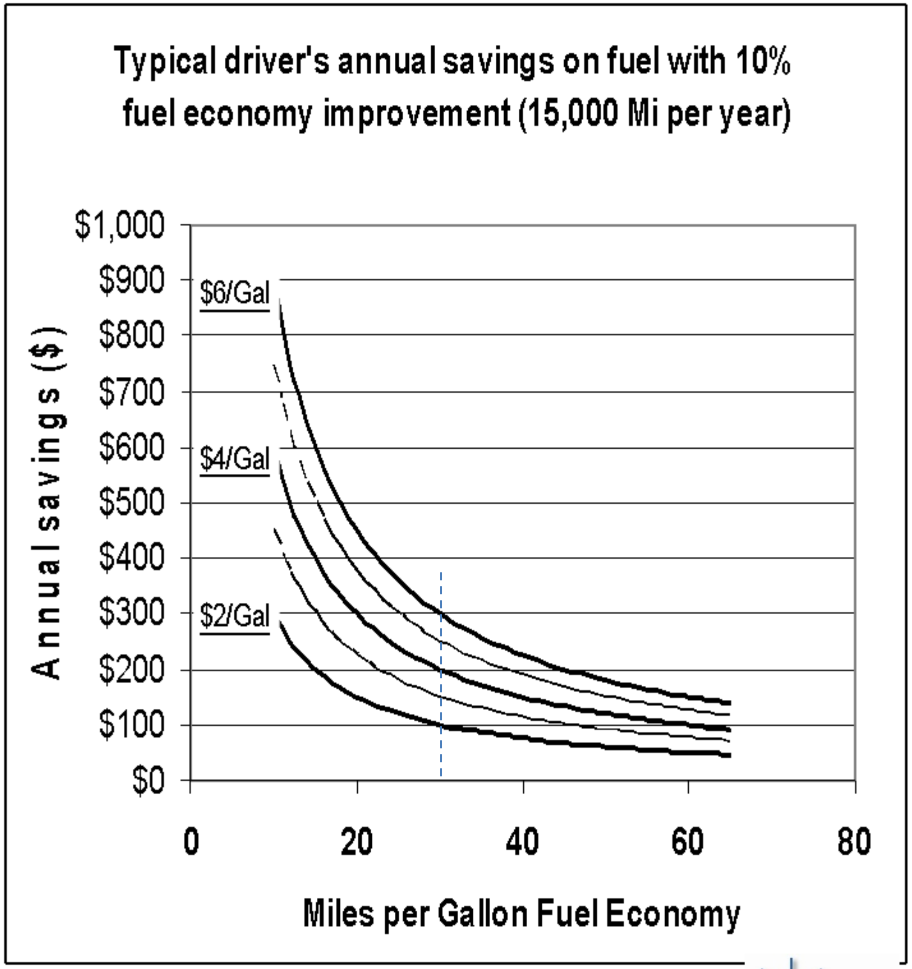

Waste Heat Recovery

Module cost

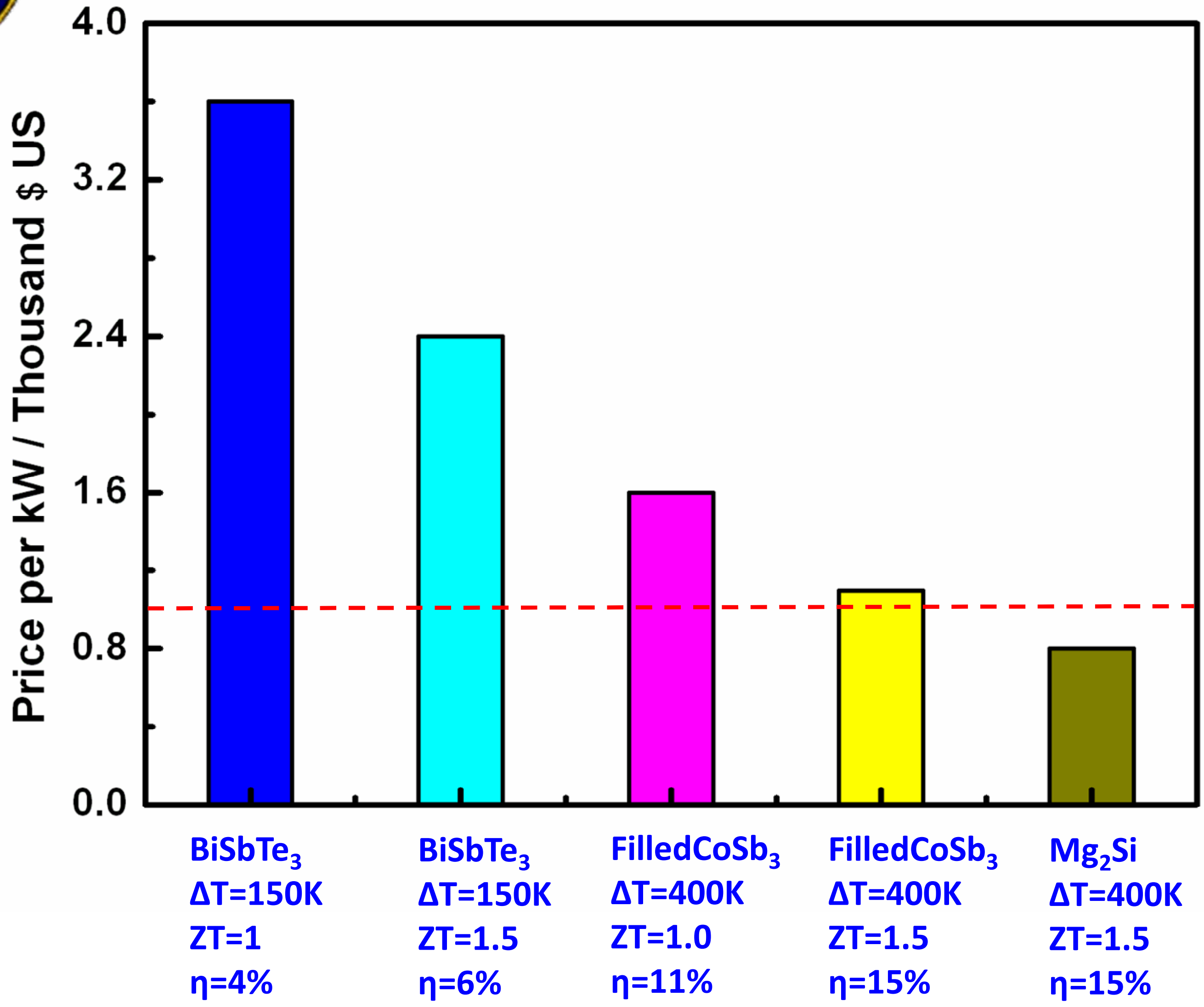

Conclusions

- Tremendous progress in the development of n-type skutterudites, ZT~1.5.
- Formation of stable, robust nanostructures a major contribution to high ZT values.
- Nanocomposites were formed by processes such as *in-situ* compound formation and compensating double-doping on the pnicogen site.
- The primary role of nanostructures in bulk matrices is to strongly enhance phonon boundary scattering while preserving good electronic properties.
- Issues to be explored further: what other kinds of nanostructures are possible? long-term stability of nanocomposite structures?
- MS + SPS processing a major advance in terms of time, energy, scale-up potential.
- Major effort needed to advance p-type skutterudites!!
- Outstanding mechanical properties bode well for applications. (Salvador et al. 2009)
- ZT values greater than unity possible without filling provided the pnicogen ring structure is effectively disturbed

Skutterudites are likely to be the first of the novel thermoelectrics in practical power generation applications.